DOTTORATO DI RICERCA IN SCIENZE CHIMICHE

CICLO XXXII

COORDINATORE Prof. PIERO BAGLIONI

Nanomateriali per il rinforzo e la deacidificazione di manufatti a base cellulosica

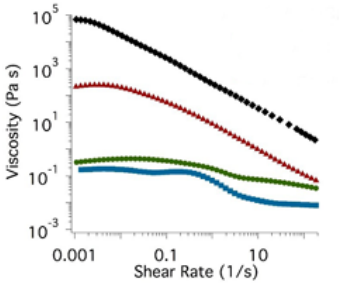

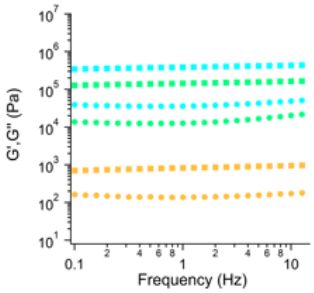

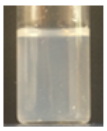

Dottorando

QINGMENG XU

Tutore

Prof. Piero Baglioni

UNIVERSITÀ
DEGLI STUDI
FIRENZE

DOTTORATO DI RICERCA IN

SCIENZE CHIMICHE

CICLO XXXII

COORDINATORE Prof. PIERO BAGLIONI

Nanomaterials for strengthening and deacidification of cellulose-based artifacts

Nanomateriali per il rinforzo e la deacidificazione di manufatti a base cellulosica

---

Settore Scientifico Disciplinare CHIM/02

Dottorando

Qingmeng Xu

_____

Tutore

Prof. Piero Baglioni

_____

Coordinatore

Prof. Piero Baglioni

_____

Anni 2016/2019

Abstract

Cellulose-based materials constitute a large part of the global patrimony of mankind. Their preservation and protection must be granted to transfer this heritage to future generations. The acid-catalyzed hydrolysis of glycosidic bonds, that is the most important degradation pathway of cellulose-based materials, results in the decrease of cellulose degrees of polymerization (DP) and in the loss of the original mechanical properties. Therefore, in the case of acidic and strongly mechanically-degraded cellulosic works of art, both a deacidification and a reinforcement treatment are required. In this regard, a single-step method can reduce risk and stress for the artifact and, at the same time, grant a reduction in terms of costs and time.

Alkaline nanoparticles, mainly calcium or magnesium hydroxide in short-chain alcohols were proposed for the deacidification of paper and canvas in 2002. Since then, several synthetic strategies and formulations of nanoparticles in different carrier solvents have been developed and excellent results in neutralizing acidity and creating an alkaline buffer have been achieved.

In the present dissertation, hybrid systems for the simultaneous strengthening and deacidification of paper are presented; these materials have been prepared using cellulose nanocrystals (CNC) and alkaline nanoparticles. Nanocelluloses are non-toxic, renewable and biodegradable. Moreover, they have excellent mechanical properties, high surface area, and form almost transparent films. The alkaline nanoparticles used for the preparation of hybrids, were obtained using a novel synthetic route based on a solvothermal process.

The mechanical response of CNC dispersions in water and water/ethanol blends were studied and related to the changes due to the addition of alkaline nanoparticles. Small-angle X-ray scattering (SAXS) measurements were used to deepen the interactions between cellulose nanocrystals in the presence of ethanol and of calcium hydroxide and calcium carbonate nanoparticles. The most promising systems were therefore tested for strengthening and deacidification of artificially aged paper.

Even if water is commonly used in conservation practice, it can solubilize original compounds and swell cellulose fibers, leading to a decrease in the mechanical properties of paper. The use of solvent blends (ethanol/water) reduces the possible detrimental effect of water, even if the use of such mixture may not be compatible with materials highly sensitive to polar blends. Therefore,

we have devoted research efforts to the modification of cellulose nanocrystals with the aim of increasing their dispersibility in pure ethanol, which offer good wetting properties without altering cellulose fibers.

Different preparation procedures for the hydrophobization of cellulose nanocrystals were tested. Cellulose nanocrystal modified with oleic acid were deemed a suitable starting material to prepare hybrid systems in ethanol featuring alkaline nanoparticles. The mechanical characterization of systems at different concentrations of nanocrystals, with and without alkaline nanoparticles, was achieved using rheological measurements. SAXS measurements were carried out on the most interesting systems so to shed light on the mechanism of gelation, so to complete the picture of the interactions between nanocellulose and alkaline nanoparticles in different environment. Finally, hybrids at high concentration of grafted cellulose were tested on artificially and naturally aged paper, showing an overall positive effect.

In conclusion, hybrid systems based on cellulose nanocrystals and alkaline nanoparticles for the simultaneous strengthening and deacidification may represent a powerful tool to extend the useful life of cellulosic artifacts, including valuable and historical objects whose preservation and protection must be granted to transfer this heritage to future generations.

Contents

Part I – Fundamentals

Chapter 1 Cellulose-based artworks: chemistry and degradation

In this chapter, the chemical composition and the degradation pathways of the most diffuse cellulosic material, i.e., paper, are reported and discussed. Paper has been widely used since ancient times as a substrate for the production of artworks; indeed, a large part of the global patrimony of mankind features cellulose-based materials.

1.1 Paper

Paper is a very complex material because not only cellulose fibers but also a multitude of different compounds are added to refine the quality and improve the properties of the final product. The history of paper-making is indeed a fascinating and interesting subject; however, a detailed discussion about the topic is out of the scope of this thesis. In this regard, it is worth noting that, up to the 18th century, old rags of linen, hemp, and cotton were mainly used as cellulose source for paper-making. These materials, mostly made of high-quality cellulose, had a remarkable chemical stability and are not particularly prone to degradation. During the Industrial Revolution the demand for paper increased considerably, while the rags were scarce. It was thus necessary to search for a new raw material. In 1840, Koller proposed the use of wood as a cellulose source for the paper making process. To this aim, prior to the formation of paper sheets, cellulose should be isolated from other wood components, such as extractives and lignin. The latter, in particular, has a fundamental role in the degradation of paper (Ek et al. 2009), as it will be shown later. More in general, several chemical and mechanical process were used to isolate cellulose during the years, and most of them resulted in a final product more prone to degradation. Similarly, several additives used in the paper making process, trigger the hydrolysis and/or oxidation of cellulose. Therefore, the conservation status of paper mainly depends on the conservation status of cellulose, which is greatly influenced by the way paper sheets are obtained and persevered. In the following sections, we

are going to list the main properties of paper components and discuss about cellulose degradation and the way it is affected by internal and external factors.

1.1.1 Paper components

As stated above, the chemical composition of paper mainly depends on the origin and chemical treatment of raw material and on the additives used during the paper-making process. The main component of paper is cellulose, whose structure, properties and degradation will be described in section 1.1.1.1. Lignin is discussed in section 1.1.1.2, while sizing agents and other paper additives will be described in section 1.1.1.3.

1.1.1.1 Cellulose

Cellulose was first discovered and isolated by Anselme Payen in 1838 (Klemm et al. 2005). It is the most abundant natural polymer available on the earth and it is an important structural component of the cell wall of various plants. In addition, there are also non-plant sources of cellulose, such as algae, fungi, bacteria, and even some sea animals such as tunicates (Klemm et al. 2005). The characteristics of cellulose are variable and depends upon the origin. Cellulose obtained from cotton fibers is always relatively pure compared to the one extracted from wood, as above indicated. Bacterial cellulose (BC) is produced by the gram-negative bacteria Acetobacter xylinum (or Gluconacetobacter xylinum). Under special culturing conditions, BC develops some particular features that makes it suitable for niche applications (Bodin et al. 2007).

In the next section, the structure and molecular properties of cellulose will be described. The degradation pathways of cellulose in acidic and alkaline medium, listed after, are important for developing conservation strategies.

Structure and molecular properties

Regardless of its sources, cellulose always has the same structure. It is formed by condensation of anhydroglucose monomers linked through β-(1,4)-glycosidic bonds. In each monomer, as a result of the bonding at each carbon atom, the carbohydrate rings are bent up at one end and down at the other, creating the so-called chair conformation. The smaller substituents, hydrogen atoms on the ring extend either above or below the ring in the axial

position. The bulkier hydroxyl groups and -CH_2OH point toward the sides of the ring. This equatorial position minimizes the interactions between these bulky substituents on the ring, stabilizing the chair structure (Mcmurry et al. 2010). Every monomer unit is corkscrewed at 180° with respect to its neighbors, forming the repeating unit, a dimer of glucose, known as cellobiose (Habibi et al. 2010), and, each cellulose chain has two different terminations: the nonreducing end contains a hydroxyl moiety and the reducing end has a chemically reducing group, as is shown in Figure 1.1.

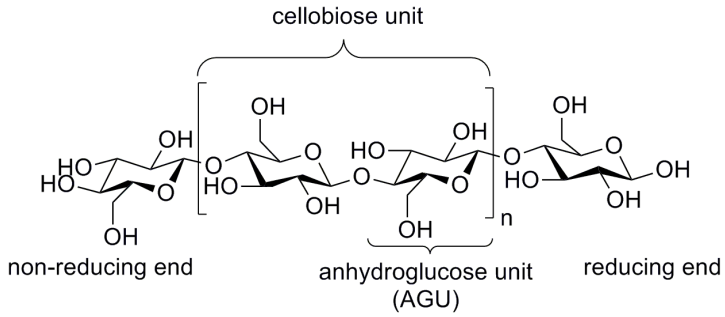

Figure 1.1 The structure of cellulose (Olsson and Westman 2013).

Cellulose is a polymer with high molecular weight. The ratio between the molecular weight of the cellulose molecule and the weight of a glucose unit, i.e. the number of units in a chain, is the degree of polymerization (DP). It varies depending on the source: for example, it is approximately 10,000 glucose units for wood-derived cellulose and 15,000 units for cotton-derived cellulose (Sjöström 1993). Higher DP values usually correspond to fibers that have higher mechanical resistance.

A great number of hydrogen bonds is established between different chains (intermolecular bonds), contributing to the rigidity and toughness of cellulose fibers. The same type of bonds can connect different locations on the same chain (intramolecular bonds). Water can interact with cellulose through the same type of bonds; as a matter of fact, cellulose can absorb about 7% of moisture at ambient condition. Despite its high hygroscopicity, cellulose can be swelled in water, without being solubilized. The reactivity of hydroxyl groups is also important for chemical modification (see Chapter 5).

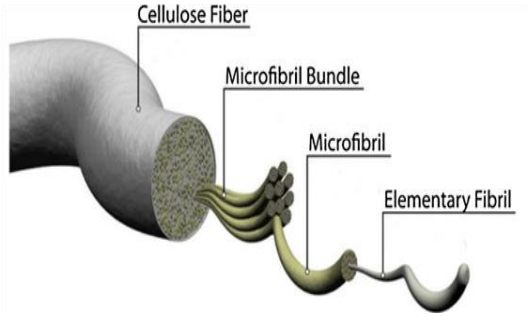

Figure 1.2 A schematic representation of the hierarchical structure of cellulose fiber (Zhu et al. 2014)

Differences in cellulose's supramolecular structure determine different physical and chemical properties: defect-free and rod-like crystalline regions, known as crystallites, are more resistant to degradation because they are tightly packed by a strong and very complex intra- and intermolecular hydrogen-bond network; amorphous zones are weaker and they can easily be degraded by chemical reagents. Crystallites can be used for the strengthening of paper, as will be discussed in Chapter 4 and 5. Typically, the crystalline regions of a cotton fiber, represent about 80% of the cellulose, whereas the remaining part has an amorphous structure. The basic fibrillar element, which is called elementary fibril, has a 2-4 nm cross-section and a 100 nm length. Elementary fibrils feature both crystalline and amorphous zones. Micro-fibrils are made of a bound of elementary fibrils and form microfibrils bundle and, finally, fibers as shown in Figure 1.2.

Degradation pathways: reactions in acidic medium

The acid-catalyzed hydrolysis is one of the key reactions responsible for cellulose degradation. The acid hydrolysis occurs randomly at the "glycosidic oxygen", resulting in the formation of a carbonium cation. The type of carbonium ion (non-cyclic or cyclic) which is most likely to be formed during the reaction is still under investigation (Sarip et al. 2016). Nevertheless, here we are going to describe the mechanism of links scission as the three steps process proposed by Harris in 1975 (Harris 1975), which is outlined in Figure 1.3. In the first step, the catalyzing hydrogen ion interacts with the oxygen linking two carbon atoms, forming a conjugate acid. The second step is relatively slow compared to the previous one; the flip of the electron pair from the carbon to the oxygen results in the cleavage of the covalent bond and the subsequent

formation of a carbocation. In the last step, the carbocation is pre-associated with water. The electron pair of the pre-associated water molecule is transferred to the carbocation and a proton is regenerated. All the three steps make the acidic hydrolysis an auto-catalytic, or self-accelerating, reaction (Timell 1964).

The extent of depolymerization following acid-catalyzed hydrolysis is affected by several factors, such as the starting DP of cellulose, the acid concentration, the temperature and the duration of the reaction. Due to the fact that crystalline regions are tightly packed, as mentioned above, they are more resistant to degradation (Lin et al. 2009). It is worth noting that acid catalyzed depolymerization does not require high temperature to take place; it readily occurs even at room temperature.

Almost every organic matter is prone to oxidation that is initiated by atmospheric oxygen. The causes and influencing factors are manifold: condition of the cellulose, the temperature, light and irradiation, humidity changes, the presence of catalysts and pollutants. The oxidation of cellulose is a 'heterogeneous reaction', which is limited initially to the amorphous regions spreading slowly to the well-organized crystalline regions. In an acidic medium, all hydroxyl groups and the reducing end groups increased by acidic hydrolysis are oxidized to aldehyde, keto or carboxyl groups. As a result, rings opening may occur but not necessary chain cleavage takes place. Carbonyl groups (ketone and aldehyde groups) are responsible for color changes. They are well-known chromophores which, as part of conjugated systems, cause the yellow, yellowish brown or brown color of oxidized cellulose. On further oxidation the carbonyl groups turn into acidic carboxyl groups which can promote acid hydrolysis of cellulose, creating a mechanism which is called spiraling effect (Shahani and Harrison 2002). Figure 1.4 depicts the most important final products of oxidation reactions in acidic medium: uronic, glucuronic, aldaric and glucaric acids. In addition, the oxidized cellulose is more prone by alkaline degradation which will be discussed in the following section. These bonds which are more sensitive to hydrolysis are called “weak linkages” or “weak links” (Sharples 1954a, b).

Degradation pathways: reactions in alkaline medium

The β-alkoxy elimination is the most important degradation mechanism of cellulose that takes place in an alkaline environment (Agnes Timar-Balazsy 1998; Hosoya et al. 2018); this mechanism can eventually lead to the so-called peeling reaction, as explained below. Oxidized cellulose is more susceptible to alkaline

solutions than native cellulose due to the presence of many carbonyl groups distributed on the oxycellulose polymer chain, as previously discussed. Alkaline

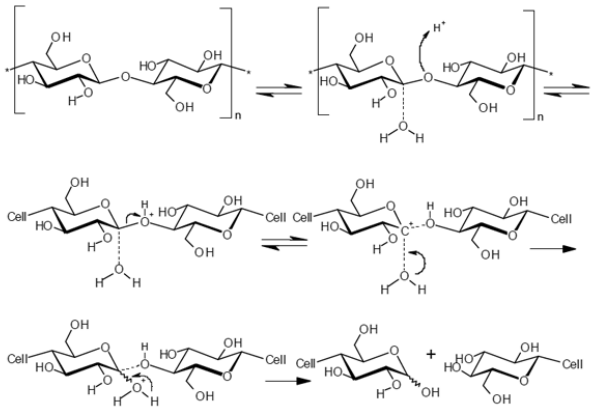

Figure 1.3. Three steps acidic hydrolysis of glycosidic bonds.

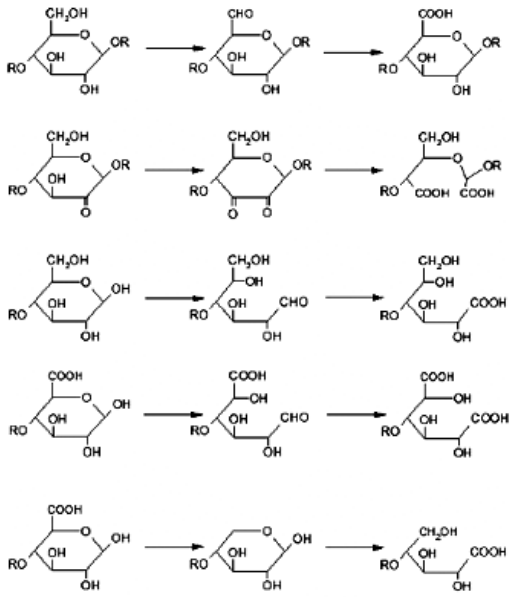

Figure 1.4. Oxidation products in acidic medium.

degradation is not random. At slightly-above neutral pH values of 8–9, alkali attack carbonyl (C=O) moiety (Hosoya et al. 2018), resulting in the production of water and a carbocation and the cleavage of the adjacent glycosidic bond in β position as depicted in Figure 1.5. It should be noted that any carbonyl (C=O) moiety, no matter whether it is located at C-2, C-3, or C-6, can be preferred, as

shown in Figure 1.6. On the other hand, at higher pH (pH>10), an isomerization of the reducing end occurs, resulting in the migration of the carbonyl group and the subsequent random cleavage of the cellulose chain.

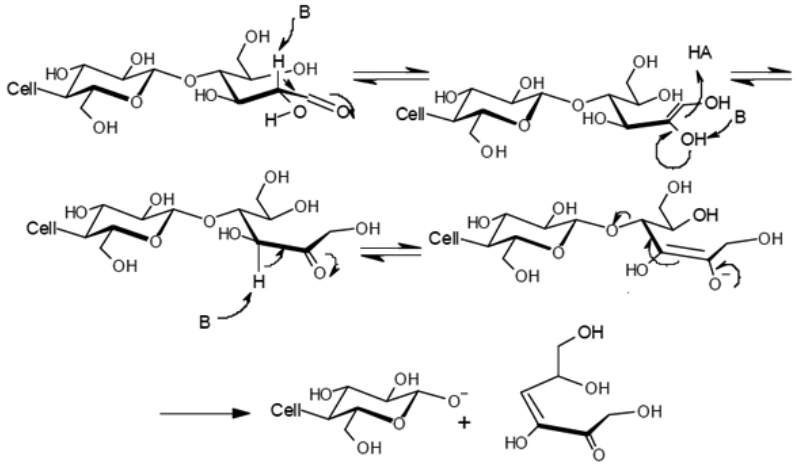

Figure 1.5. β-alkoxy elimination mechanism.

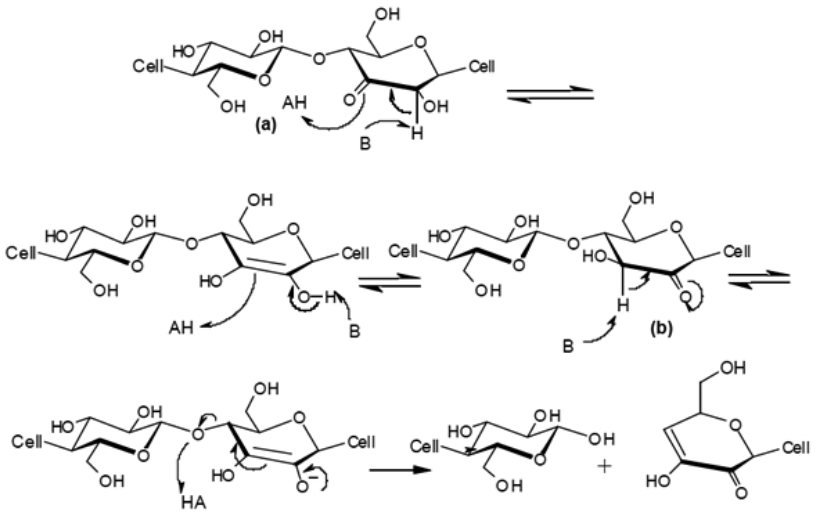

Figure 1.6. Cellulose chain scission resulting from oxidation: either oxidation of the C3 hydroxyl to a carbonyl (a) or the same process on the C2 hydroxyl (b) can result in chain scission.

Some scientists concluded that alkaline condition can accelerate the oxidation of cellulose, but no precise explanation was indicated (Whitmore and

Bogaard 1994; Sequeira et al. 2006). On the other hand, Kolar hypothesized that alkaline species promote radical formation that initiates the degradation of cellulose (Kolar 1997). However, it is well-known that neutral pH represents the better environment for the conservation of cellulose.

1.1.1.2 Lignin

Lignin was introduced into paper when wood was started to be used as cellulose source for the paper making. It is a rigid and thermoplastic polymer, constituted by a three dimensional network of phenilpropane derivatives (coniferyl, sinapyl and paracoumaryl alcohol). The chemical composition of lignin is variable depending on wood sources, such as softwoods and hardwoods, and its structure is still not completely known. It has been suggested that lignin forms a single amorphous macromolecule (see Figure 1.7). The presence of ester bonds may interact with hemicellulose that embeds wood cells forming a more complex structure, which still remains an issue of conflicting claims (Giummarella et al. 2019).

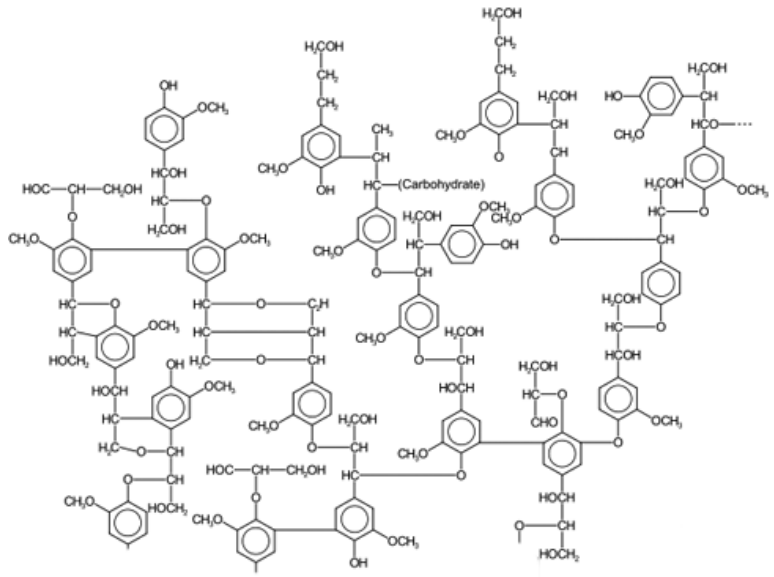

Figure 1.7. An example of possible structure of a portion of lignin molecule.

Lignin is insoluble in water due to the few hydrophilic groups; in addition to its structural importance for wood, it also protects tree from the attack of microorganisms.

Concerning the degradation of paper, lignin has a fundamental role because it is capable of absorbing UV/VIS light that induces the oxidation by photochemical reactions. Therefore, lignin must be isolated from cellulose before the formation of the sheets. Several methods were used to isolate cellulose, but no satisfying results were obtained. Treatments of wood with concentrated mineral acids do not cause dissolution of lignin but its condensation; in the presence of hydrochloric acid, solvolysis of lignin can be carried out with alcohol. On the contrary, lignin was still dissolved in an alkaline medium under widely used Kraft (sulfate) and soda pulping. Acidic and alkaline pulping processes may reduce the total amount of lignin in paper sheets but surely lower life expectancy of cellulose by inducing some degradation reaction. As a matter of fact, during the production of pulp for some short-time readings, such as newspaper or cartoon books, delignification is not achieved; this kind of paper shows significant discoloring phenomena after few years.

1.1.1.3 Sizing agents and other paper additives

The presence of additives in paper sheets is particularly important, because they greatly refine the quality and improve the properties of the paper. Sizing agents, one of the additives, were used to increase the hydrophobicity of cellulose and retard the penetration rate of aqueous fluids. Initially, it was achieved by starch in older Arabian tradition. Later, in the European Middle Ages, animal glue was used. At the beginning of the 19th century, rosin-alum sizing, which create a hydrophobic layer on paper surface, was introduced. This sizing procedure brought great economic advantages. At the beginning of the 20th century it was found that resin acids are the main causes of acid-catalyzed hydrolysis of paper produced in that period. Therefore, in modern papers, alkaline sizing, such as alkyl ketene dimer (AKD) and alkenyl succinic anhydride (ASA), are used.

Other compounds are added during the papermaking to improve paper properties, such as brightness and smoothness. Clay, calcium carbonate, talc and titanium dioxide are commonly used. Even if some additives are very stable and do not cause any cellulose degradation, their presence must be considered, in particular when a conservation intervention is needed.

1.1.2 Factors affecting paper stability

Paper stability is affected by many environmental factors, such as oxygen, light exposition, air pollutants, relative humidity, temperature radiation and microorganisms. The interaction between light and cellulose, at the microscopic scope, triggers the oxidation of hydroxyl groups and the formation of oxidized compounds, as described above. At the macroscopic scale, cellulose exhibit discoloration. Internal factors and chemical composition also affect the stability and durability of paper.

Internal factors include condition of cellulose (type, length, and crystallinity of fibers), presence of fillers (e.g. sizing agents), presence of metal ion impurities (e.g. inks). Paper produced by using wood as the raw material may contain lignin which discolors in sunlight. In addition, it was proved that lignin has the tendency to absorb SO_2 from polluted atmosphere (Begin et al. 1998; Tse et al. 2014). Alum-rosin, one of the used sizing agents, was added in pulp during paper production. Both of the two main components, alum and rosin, are acidic. In particular, aluminum sulfate not only acts as a major source of acidity in paper, but it also trigger the Al(III) electrophile-catalyzed hydrolysis of cellulose (Baty and Sinnott 2005; Chamberlain 2007). Iron and metal gall ink, obtained from the reaction between gallic acid and ferrous sulfate, are responsible for the oxidation and acid hydrolysis of paper catalyzed by transition metal ions (Neevel 1995; Kolar et al. 2003, 2006).

As an organic product, paper is susceptible to irreversible physical and chemical changes due to environmental and internal factors. Effective conservation treatments can slow down the degradation rate of cellulose-based materials. It is worth noting, though, that the developments of effective conservation strategies are not an easy task, considering the multiple influencing factors of cellulose degradation.

Chapter 2 Conservation of paper

As above explained, paper is mainly subjected to the hydrolysis of the glycosidic bonds. The degradation of paper leads to changes in the ultrastructure and, at the macroscopic scale, to a lower mechanical resistance of the material. The most common developed conservation strategies for cellulose-based materials can be divided in two main categories: deacidification (section 2.1) and reinforcement (section 2.2). In the following sections, several widely used conservation strategies will be presented.

2.1 Deacidification

Conservation scientists have been worked on deacidification since decades ago. The target of deacidification is not only the neutralization of the acids, but also the deposition of an alkaline reserve that will act as a protection for reoccurring acids. Hydroxides are commonly used to withdraw protons from the substrate; if hydroxides are in excess in respect to protons, the so-called alkaline buffer, i.e., carbonates salts, is formed by the reaction with atmospheric carbon dioxide. Sometimes, carbonates, that are less reactive, are used as neutralizing agents when paper is slightly degraded. The following three equations (2.1, 2.2 and 2.3) represent the typical reactions involved in a deacidification process:

$$H^+_{(l)} + OH^-_{(l)} \rightarrow H_2O_{(l)} \quad (2.1)$$

$$M(OH)_{2(l,s)} + CO_{2(g)} \rightarrow MCO_{3(s)} + H_2O_{(l)} \quad (2.2)$$

$$CO^{2-}_{3(s)} + 2H^+_{(aq)} \rightarrow CO_{2(g)} + H_2O_{(l)} \quad (2.3)$$

It is agreed that an effective deacidification method should have the following characteristics: the deacidification agents should fully neutralize all the acidic content and deposit an alkaline reserve to prevent further degradation;

the solvents should not be hazardous to the operator and be inert to the deacidified objects (paper, leather, ink, dyes etc.). Before deacidification, solubility tests must be carried out to check the compatibility between the neutralizing agents and the solvent with the object to be deacidified. In general, due to compatibility reason, methods with non-aqueous solvents show some advantages when compared with water-based treatment.

When millions of books are in the need of deacidification, such is as in the case of entire libraries' collections printed on bad quality paper, the cost of the treatment can be particularly crucial. In this situation, the deacidification of each single paper sheet is simply unfeasible. Therefore, mass deacidification methodologies, which are dispersed in non-aqueous solvents, have been developed. On the contrary, for the deacidification of precious and unique objects, single-sheets methods, that allows for higher control during the intervention are preferred.

In the next paragraphs several widely used deacidification methodologies, including mass deacidification and single-sheet methods, commonly used in conservation practice, will be presented.

2.1.1 Aqueous treatments

The aqueous deacidification system is generally based on the use of alkaline earth hydroxides and bicarbonates. Magnesium compounds generally lead to a higher pH (pH>9) in paper after deacidification in respect to a treatment based on calcium compounds. The solvent, water, poses no health risks for operators during the application. Moreover, it improves the visual appearance of treated papers, by removing a large amount of hydro-soluble dirt, soluble metal salts as well as sizing agents partly responsible for the yellowing of paper (Sequeira et al. 2006). Additionally, the swelling of paper facilitates better penetration of the deacidification agent into the paper matrix.

Nonetheless, aqueous treatments also show severe disadvantages. Permanent changes in the mechanical strength of paper due to swelling effects have been observed, as well as the bleeding of inks and dyes and the removal of water-soluble paper components (Kolar 1997; ZAPPALÄ 1997; Stefanis and Panayiotou 2007). Resizing is usually necessary because aqueous treatments partially remove the original sizing (Giorgi et al. 2005c). Furthermore, high pH induced by aqueous saturated calcium or magnesium hydroxide solutions can

lead to alkaline-catalyzed degradation of the oxidized cellulose (Malesic et al. 2002).

Despite these side effects, aqueous treatments are frequently used by conservators, but are usually discouraged by the scientific community that recommend the usage of non-aqueous treatments.

2.1.2 Non-aqueous treatments

Deacidification methods with apolar or less polar than water solvents can overcome some drawbacks of aqueous deacidification mentioned above. These solvents are compatible with paper components and can be generally carried out without previous verification of the water solubility of the inks or sizing. Furthermore, the evolution of non-aqueous treatments led to mass deacidification, because they are inert to the water sensitive book's bindings (Sequeira et al. 2006). Unfortunately, most of the organic solvents are flammable or toxic; for this reason, a non-aqueous treatment requires acquainted operators and equipped laboratories.

In the following sections, three selected methods, i.e., the Bookkeeper, the Battelle and alkaline nanoparticles dispersions processes, will be discussed in detail. Both Bookkeeper and Battelle methods are commercially available mass deacidification method. The Bookkeeper technology can also be used on single paper sheet. The deacidification using alkaline nanoparticles has been developed in CSGI and Chemistry Department laboratories of the University of Florence and applied on paper since 2002.

2.1.2.1 Battelle process

The Battelle process, developed by Battelle Ingenieurtechnik GmbH, was tested and approved by the National German Library in 1994. The method was based on magnesium ethoxide and titanium alkoxides in hexadimethyl disiloxane (HMDO). The combination of magnesium ethoxide and titanium alkoxides is also known as METE, magnesium ethoxide titanium ethoxide. The ratio between magnesium and titanium is approximately 1:1. The METE reacts with moisture to form magnesium hydroxide that works as deacidification agents, and the excess is converted, by reacting with carbon dioxide, into carbonate, which acts as the alkaline reserve. HMDO, a colorless organic silicon compound, is said to have lower eco-toxicological impact (Wittekind 1994).

However, it is highly flammable. This method is also known as Papersave that is the name chosen by ZFB, the company that is currently selling and developing the Battelle products. Since 2003, an interesting treatment specially designed for inhibiting ink corrosion, including both neutralizing agents and antioxidants, is available (Kolar et al. 2003; Kolar et al. 2006b; Lichtblau et al. 2006; Reissland et al. 2006; Kolar et al. 2008): calcium and magnesium alkoxides in conjunction with quaternary ammonium halides constitute the so-called Inksave process. Both apolar and polar solution variation of this treatment are being developing.

The Battelle process can fulfil stringent rules of efficient and reliable conservation methods, i.e., costs, ecotoxicology issues, chemical and physical inertness. Additionally, it is the most efficient in the adequate deposition of alkaline reserve (Ahn et al. 2012).

2.1.2.2 Bookkeeper

The Bookkeeper method (Preservation Technologies, L.P.) features insoluble magnesium oxide microparticles working as deacidification agents and fluorinated solvents (mainly perfluoroheptane). Magnesium oxide reacts with moisture in paper forming magnesium hydroxide which then neutralizes cellulose acidity. By reacting with carbon dioxide, the excess of magnesium hydroxide is transformed into magnesium carbonate, which acts as the alkaline reserve. Fluorinated solvents are apolar and completely inert to paper components and modern inks, which increase the flexibility of conservation practice.

The Bookkeeper is available for single sheet deacidification and mass deacidification. As mass deacidification method, it has been used in the National Congress Library of Washington, D.C. since its development in 1992. The use of Bookkeeper process also implied some possible drawbacks. A white veiling effect usually occurs on low porous paper, since the limit penetration of the micron-sized particles of magnesium oxide (Buchanan et al. 1994). Moreover, high concentrations of fluorinated surfactants are usually used to stabilize MgO particles in highly apolar solvents, bringing unknown effects in the long term (Zumbühl and Wuelfert 2013). Despite these drawbacks, Bookkeeper is still widely used and known as one of the best non-aqueous mass deacidification treatments available.

2.1.2.3 Nanoparticles dispersion

The use of alkaline nanoparticles, mainly calcium or magnesium hydroxide, in short-chain alcohols for the deacidification of paper and canvas was proposed in the early 2000s (Giorgi et al. 2002b, a, 2005a) by CSGI and Chemistry Department of the University of Florence researchers. Since then, several synthetic strategies and formulations of nanoparticles in different carrier solvents were developed and tested. Alkaline nanoparticles were successfully used on waterlogged wood (Giorgi et al. 2005c, 2006; Poggi et al. 2016a), on wood from organ pipes (Giorgi et al. 2009), on paper and canvas (Giorgi et al. 2002a, 2005a, Poggi et al. 2010, 2011, 2014a, 2017), and underwent extensive assessment with positive results (Sequeira et al. 2006; Stefanis and Panayiotou 2007, 2008; Bastone et al. 2017).

The synthetic procedure of alkaline nanoparticles has been improved in the last 20 years (Ambrosi et al. 2001; Salvadori and Dei 2001; Nanni and Luigi 2003; Giorgi et al. 2010; Poggi et al. 2014c, 2016b). Compared with traditional methods, the used of nanoparticles (80-400nm) has several advantages. Firstly, nanoparticles possess higher reactivity with respect to micron-sized particles. The neutralization and the carbonation processes occur rapidly, therefore, providing a stable neutral and less aggressive environment. Secondly, the penetration of nanoparticles dispersed in alcohols can be easier even when the natural porosity of paper is lowered by sizing or ink. Finally, thanks to the nano-dimensions and compatibility, the distribution of particles within the fibers is highly homogeneous.

In the next section, the synthetic procedures of nanoparticles, particularly the ones designed for the conservation of artworks, will be discussed.

A review on synthetic procedures of nanoparticles

The synthesis of nanoparticles is deepened in some excellent reviews (Baglioni and Chelazzi 2013; Kharissova et al. 2013; Hasan 2015). Herein, we will focus on the synthesis of hydroxides of alkaline earth metals specifically addressed for conservation applications.

Inorganic nanoparticles can be obtained by using two fundamental processes: the “break-down” and the “bottom-up” processes. The “break-down”

process starts from a bulk material and breaks it into small pieces until the desired shape is achieved, using mechanical, chemical or other forms of energy. Bottom-up methods deal with atoms, molecules or ions, that are assembled through appropriate experimental conditions into particles of defined size. Bottom-up procedures are much better suited to provide control of the size, shape and structure of the generated nanoparticles.

Milling is the best known "break-down" method for the manufacture of powders (Sternitzke 1997). Particles are treated through repeated high-energy impacts, producing particles with smaller size and eventual structural changes. However, milling approach is limited because particles smaller than few microns are rarely obtained. And systems resulting from milling are generally polydisperse and often tend to reaggregate. Despite this, it is still being considered for the production of nanomaterials aimed at the preservation of cultural heritage, such as, SrCO3/propanol dispersion for deacidification of wood samples (Schofield et al. 2011) and lime/alcohol dispersion for reinforcement of wall paintings (Giorgi et al. 2000).

On the contrary, the precipitation of solid particles from the liquid phase (homogeneous–phase reaction) is probably the most reliable and efficient process to obtain nanostructures; the size and the shape of the particles could be tuned by proper selection of some reaction parameters, as the temperature, the concentration of the reactants and their mole ratio and the solvent. (Arai 1996).

For example, hydroxide nanoparticles of alkaline earth metal ions can be synthesized in water (Ambrosi et al. 2001; Giorgi et al. 2005b; Poggi et al. 2010, 2011) or in organic solvents, i.e. diols (Salvadori et al. 2001).

The synthetic pathways of hydroxide nanoparticles in water to be applied on artworks is the following: aqueous solutions of calcium and magnesium chloride (or nitrate and sulfate) are heated up to 90°C and then mixed with a solution of sodium hydroxide, kept at the same temperature. The mixture must be left under vigorous stirring for about one hour; the precipitate, calcium or magnesium hydroxide, is then recovered by centrifuge. Nanoparticles must be purified from sodium chloride (or nitrate and sulfate) that is a by-product of the reaction. In the case of calcium hydroxide, whose solubility product (Ksp) is 4.8x10-5, lime water is used; magnesium hydroxide is a less soluble salt (Kps=1.5×10-11) and can be purified by using distilled water. At least five washing cycles are needed; this process does not cause significant change in particles size or shape. After drying particles are dispersed in low-chain alcohols. Particles with average size in the range of 100-400 nm are thus obtained

(Ambrosi et al. 2001; Giorgi et al. 2005a). A modified procedure, based on the use of larger amount of magnesium with respect to the coprecipitating ions, was proposed in 2010 (Poggi et al. 2010, 2011) and it resulted in the production of magnesium hydroxide nanoparticles having smaller size and higher stability.

Another approach to decrease the average particles size is the homogeneous-phase reaction in diols; the advantage arising from the usage of organic solvents is that higher temperature can be reached during the synthesis and, consequently, smaller particles can be obtained (Yura et al. 1990). Calcium chloride, solubilized in 1,2 ethanediol or 1,2 propanediol, reacts with an aqueous solution of sodium hydroxide; the precipitate is separated from the supernatant dispersion by hot filtration. Particles tend to form micro-aggregates and need to be peptized (Perez-Maqueda et al. 1998) by washing with 2-propanol in an ultrasonic bath. The peptization must be repeated at least five times to obtain particles with an average size of 30-60 nm. This synthetic procedure is, though, time-consuming and these particles are rarely applied for conservation purpose (Salvadori et al. 2001).

Calcium hydroxide nanoparticles synthesis starting from microemulsion has been developed by Nanni and Dei (Nanni et al. 2003); particles obtained with this procedure have an average diameter of 5 nm, but these characteristics are unusually required in common conservation practice.

A completely different approach is based on a solvothermal reaction in two-steps (Poggi et al. 2014a, 2016b): during the first step of the reaction, ethanol oxidizes metal calcium to the corresponding alkoxide, i.e., calcium ethoxide, which is soluble in ethanol. To hydrolyze the alkoxide and favor its conversion to calcium carbonate, water is added inside the reaction chamber. Water triggers the conversion of calcium ethoxide into calcium hydroxide. Calcium carbonate nanoparticles can be also synthesized using a similar approach. The synthesis will be discussed in Chapter 4.

2.2 Reinforcement

Reinforcement is crucial for mechanically-degraded works of art. A good strengthening method must share the following common attributes: sufficient bonding strength, chemical inertness towards the substrate, color stability, and reversibility. Different methods have been developed for the reinforcement of paper and cellulose-based materials, such as lamination (Wilson and Parks 1983;

M and J 1997), paper splitting (Brückle and Dambrogio 2000; Galinsky and Haberditzl 2004), leaf casting machine (Letnar and Vodopivec 2004) and impregnation (Kolbe 2004). In the next sections, we will focus on the impregnating materials such as natural and synthetic polymers.

2.2.1 Traditional natural polymers

Polysaccharides and gelatin are the main natural polymers used as consolidates in paper conservation. Funori, a water-soluble polysaccharide, is a natural product used for many centuries by Asian paper conservators for certain gilding techniques. The reinforcement results were very satisfying (Kolbe 2004). Chitosan (poly 2-aminodeoxy-1,4 glucoside) is a natural polysaccharide prepared from chitin, the only polysaccharide in the animal world. It contains hydroxyl groups that give them ability to from hydrogen bond. Basta (Basta 2003) obtained good strengthening results with applying chitosan on paper. Chitosan-based additives (chitosan, carboxymethyl chitosan) are more efficient in the preservation of the mechanical strength of paper after thermal ageing as compared to cellulose ethers (CMC, MC) which will be discussed in the following section (Ardelean et al. 2011). Gelatin is produced from hydrolytic decomposition bones or hides. Even if it results in a water-repelling effect, paper strength was significantly increased after its application. In addition, heavily gelatine-sized papers are more durable than those with weak sizing (Kolbe 2004).

Natural polymer was also used mixed with synthetic polymer, such as cationic starch (AC), alkyl ketene dimmers (AKD) and chitosan (CH), to obtain a double effect, i.e., resizing and reinforcement.

In ancient times, natural polymers were widely used for the reinforcement of paper. However, due to their low biostability, versatility, synthetic polymers are often currently preferred in conservation practice.

2.2.2 Synthetic polymers

Various synthetic polymers, usually in aqueous dispersions, have been used as reinforcement agents in paper conservation. In the following section, some commonly used synthetic polymers will be discussed.

2.2.2.1 Cellulose derivatives

In terms of composition, structure and properties, cellulose derivatives are compatible with cellulosic artworks. For this reason, they are often employed in the conservation and restoration of cellulose-based artworks.

Cellulose ether

Cellulose ethers are frequently used for the strengthening of paper. During the production process of cellulose ethers cellulose is firstly transformed to alkali cellulose, using sodium hydroxide, and then into the final cellulose derivative by reacting with alkylating agents, i.e., alkyl, hydroxyalkyl and carboxyalkyl groups. Table 1 summarizes the industrially and commercially important cellulose derivatives used in paper conservation.

Strnadova (Strnadova and Durovic 1994) stated that MC, HPC and MHEC exhibit good biostability, are quite stable against accelerated ageing, and very effective as consolidating agents, since they substantially increase the strength of the paper they were applied to. However, CMC was not recommended due to its considerably decreased strengthening effect after accelerated aging.

Table 1. Representative cellulose ethers in paper reinforcement.

Cellulose derivatives	Abbreviation	Substituents
Methylcellulose	MC	$-CH_3$
Carboxymethyl cellulose	CMC	$-CH_2COO^-Na^+$
Hydroxyethyl cellulose	HEC	$-C_2H_4OH$
Ethyl hydroxyethyl cellulose	EHEC	$-C_2H_5$ $-C_2H_4OH$
Hydroxypropyl cellulose	HPC	$-C_3H_7OH$

Even if cellulose ethers are widely used, they show some drawbacks. All the cellulose ethers are hygroscopic and tend to degrade. Oxidation occurs both in bulk storage and in situ, especially if there is light exposure. Moreover, in acidic environments, they may be cross-linked through the hydroxyl groups by means of aldehydes and acids.

Cellulose ester

Cellulose esters are also a broadly used as reinforcing agents in paper. Various esters of cellulose have been manufactured but only cellulose nitrate and cellulose acetate have been extensively used in conservation practice.

Cellulose nitrate (CN) is prepared by soaking cellulose pulp in a mixture of concentrated nitric and (usually) sulfuric acids. CN degrades at room temperature by a combination of oxidation and hydrolysis, which are catalyzed by the presence of acid impurities and accelerated by light. Plasticized cellulose nitrate was first used for the conservation of objects during the late nineteenth century (Horie CV 2010).

Cellulose acetate (CA) is manufactured by heating cellulose with acetic anhydride and sulphuric acid. The greatest quantity of CA was used in the lamination of paper, starting around 1934 .The heat-lamination process involves heating and pressing the paper between two sheets of CA so that the polymer flows into the paper (Horie CV 2010). It is worth noting that niether CA nor CN are anymore used in conservation practice.

2.2.2.2 Other synthetic polymers

Other synthetic polymers were used in conservation practice: these includes nylon, paralyne, polyethylene glycol and polyvinyl alcohol (Marina and Barbara 1996; Nada et al. 2000).

It has been reported that soluble nylon is not feasible to be used for the reinforcement of paper, because it is insufficiently reversible (Baer, Norbert S., Norman Indictor 1972). Paralyne, deposited by means of gas-phase deposition, can penetrate inside the paper and encapsulate each individual cellulose fiber to a uniform distribution. With this technique, durable coating with low or high thickness can be obtained. However, a heavy coating may render certain paper brittle (Humphrey 2015). Unfortunately, the method is not commonly used due to its high cost and technical requirements. Nada et al. (Nada et al. 2000) tested polyethylene glycol and polyvinyl alcohol for the strengthening of paper and

concluded that the treatment of paper with a mixture of them improved both mechanical strength and brightness stability.

In conclusion, synthetic polymers are widely used as consolidating agents due to their good mechanical property and good interactions with substrates. But they might result in irreversible changes over natural aging. More specifically, it is difficult to remove deteriorated synthetic polymers without damaging the treated surfaces.

2.2.3 Nanocellulose

Nanocellulose have been used as reinforcing agents for several different polymers (Kargarzadeh et al. 2017). Here, we are going to highlight their used in paper reinforcement.

Nanocelluloses are preferred for the reinforcement of cellulosic supports over synthetic polymers not only because of their biodegradability but also because of other unique properties, such as non-toxicity, renewability, biodegradability and the compatibility with cellulosic support.

Nanocellulose can be divided into at least three main categories: (i) cellulose nanocrystals (CNC)(Habibi et al. 2010); (ii) cellulose nanofibrils (CNF) (Nechyporchuk et al. 2016a) and (iii) bacterial nanocellulose (BC). CNC and CNF can be generated by a break–down process, i.e. acid hydrolysis of cellulose from plants into nanomaterial. BC is produced by bottom–up process, primary by metabolites of bacteria (Castro et al. 2011). Since BC is defect-free, it shows higher crystallinity and mechanical strength, compared with CNC and CNF.

Nanocellulose have been used as paper coatings (Nathalie LavoineIsabelle DeslogesBertine KhelifiJulien Bras 2014; Gicquel et al. 2017) or added to paper pulp before sheet formation (Sun et al. 2015; Vallejos et al. 2016). More recently, cellulose nanofibrils (CNF), carboxymethylated cellulose nanofibrils (CCNF) and cellulose nanocrystals (CNC), were tested in terms of structural reinforcement of degraded canvases (Kolman et al. 2018; Nechyporchuk et al. 2018). All the tested nanocelluloses provided reinforcement in the adequate elongation regime of degraded canvases.

Thanks to its uniqueness, bacterial cellulose has a wide field of applications as potential consolidates in paper. Bacterial cellulose layers (Santos et al. 2015) were cultivated and purified by in situ or ex situ to be used on the surface of the document. In both cases bacterial cellulose improved the physical properties of the damaged paper and remained stable over time. Bacterial cellulose was also

used on lining with Japanese paper, which resulted in a reduction of air permeability and wettability (Santos et al. 2016a). Moreover, BC rebuilt and improved deteriorated paper quality, without altering the information contained therein (Santos et al. 2016b). However, due to the cost of BC, its use in conservation practice is not likely to become common.

2.3 Combined deacidification and reinforcement

As discussed in Chapter 1, when cellulosic artworks are in contact with acidic compounds, hydrolysis takes place and the materials becomes brittle, so that it cannot be handled. Therefore, in the case of acidic and strongly mechanically-degraded cellulosic works of art, both a deacidification and a reinforcement treatment is required. In this regard, a single-step method can grant a reduction in terms of costs and time. In addition to that, it can also reduce risk and stress for the artifact.

The first report about deacidification and reinforcement based on alkaline particles and cellulose ether was reported by the Austrian National Library in Vienna (Bluher et al. 2001). Calcium hydroxide was used as the neutralizing agent and methylcellulose was added to the aqueous solution for reinforcement purposes. Since this first test, different one-step approaches have been reported, all based on alkaline dispersions and cellulose ether.

Guerra et al. (Guerra et al. 1995) demonstrated that simultaneous deacidification and reinforcement with mixed solutions of calcium hydroxide and methylcellulose result in a more homogeneous distribution of particles than the separate single treatments. Sundholm (Sundholm and Tahvanainen 2003, 2004) showed that the preparation methodologies of treatment solutions have a significant effect on the alkaline reserve deposited on paper. More specifically, the mixing of $Ca(OH)_2$ powder with methyl cellulose solution results in a higher alkaline reserve if compared to a system obtained by mixing a $Ca(OH)_2$ solution with a methyl cellulose solution. Seki et al. (Seki et al. 2005, 2010) developed a water/organic based method combining of strengthening with cellulose ethers (methylcellulose, carboxymethylcellulose, hydroxypropyl cellulose and ethyl cellulose) and deacidification with magnesium carbonate. Jančovičová (Jančovičová et al. 2012) proposed a single-step treatment for triple effects, i.e., the improvement of the tested mechanical, optical and chemical parameters. It

involves the used of magnesium and calcium bicarbonates, antioxidant potassium iodide and cationic starch Empresol N.

Some other polymers were applied in combined treatment. Based on amino alkyl alkoxy silanes (AAAS), a combined treatment for reinforcement and inhibition of fungus was developed (Cheradame et al. 2003; Rousset et al. 2004; IPERT et al. 2005). The chemical and physical interactions were also comprehended (Souguir et al. 2011). Lunjakorn (Lunjakorn et al. 2015, 2018) proposed a deposition method that can simultaneously create an alkaline reserve and improve the mechanical properties of historic wood pulp (HWP) paper by treatment with an organic solvent hexamethyldisiloxane suspension of Mg(OH)2 nanoparticles stabilized by trimethylsilyl cellulose.

It is worth noting that several of the above listed treatments are water-based methods. Therefore, they present several disadvantages and are, nowadays, discouraged (see section 2.1.1).

Summary: Deacidification and reinforcement are the two main conservation interventions that can be carried out for the preservation of cellulose-based artworks. Deacidification treatments are based on the usage of alkaline compounds that neutralize paper acidity. The neutralizing agents can be dispersed in water, short chain alcohol and low-polar and inert solvents. The most interesting systems are those based on organic solvents and nanoparticles. For the reinforcement treatments, the compounds that can be used include natural polymer, synthetic polymer and, more recently, nanocellulose. Nanocellulose is newly developed and it is probably the most interesting material due to the unique mechanical properties and high compatibility with cellulosic material.

Part II – Experimental Section

Chapter 3 Characterization techniques

The purpose of this study is to develop hybrid materials for concomitant neutralization of acidity and improvement of the mechanical resistance of cellulose based-artifacts. Therefore, alkaline nanoparticles, i.e., calcium hydroxide and calcium carbonate, for deacidification and cellulose nanocrystals for reinforcement were prepared. The properties of materials (particle size, stability and rheological properties) help us in understanding whether they are qualified as conservation material and how they can be applied during conservation.

Calcium hydroxide nanoparticles were prepared according to a previously reported procedure (Poggi et al. 2014b, 2017). Calcium carbonate nanoparticles were obtained using a new procedure, based on a solvothermal process, that will be discussed in Chapter 4. The formation of calcium carbonate was evaluated by Attenuated Total Reflection Fourier Transform InfraRed spectroscopy (ATR-FTIR). TGA (Thermal Gravimetric Analysis) was used to show changes in weight of the dried sample during a thermal ramp and the conversion of calcium hydroxide into calcium carbonate. Particles were characterized by (Transmission Electron Microscopy) TEM. Size and distribution were also assessed with Dynamic Light Scattering (DLS).

In order to increase hydrophobicity of CNC and disperse them well in ethanol, CNC were modified by grafting hydrophobic chains on the position of hydroxy groups. The successfully modified CNC was characterized by FTIR, DTG and AFM.

The two kinds of materials for deacidification and reinforcement were mixed physically. Rheological measurements were performed to test the mechanical responses. SAXS were used to explore the microscopic interaction between particles.

After characterizing materials, they are applied on papers with the aim of evaluating the effectiveness. In the field of cultural heritage conservation, innovative materials are usually firstly applied on mockups, before being tested on real samples. For the present study, filter paper was acidified and hydrothermally aged so to have a starting material in need of both a deacidification and a reinforcement material. Before and after the application of

hybrid systems, acidity, mechanical strength and visual appearance of the paper were measured.

Below, some general information about the way these properties measured are briefly discussed.

3.1 Characterization of hybrid systems

3.1.1 Attenuated Total Reflection Fourier Transform InfraRed spectroscopy (ATR-FTIR)

Attenuated Total Reflection (ATR) is based on the multiple internal reflection of the beam incident on the sample. When an IR beam travels from a medium of high refractive index (e.g. crystal) to a medium of low refractive index (sample), the light is partly refracted into the low refractive index medium. At a particular angle of incidence, i.e., the critical angle, all of the light waves are reflected back to the medium of high refractive index. This phenomenon is called total internal reflection. In this condition, part of the light energy extends beyond the surface of the crystal into the sample held in contact with the crystal. This invisible wave is called an evanescent wave. The attenuated beam returns to the crystal, then exits the opposite end of the crystal and is directed to the detector in the IR spectrometer. The detector records the attenuated IR beam as an interferogram signal, which can then be used to generate an IR spectrum (Sun 2009). A clean, empty crystal is normally used for collection of background spectrum. The crystal can be made of diamond, ZnSe, Ge, Si, KRS-5, etc. The main difference is refractive index.

This technique is useful for studying the surface of the materials (penetration depth of 0.5–5 μm). It is usually applied to determine the composition of the surface. There are several advantages, e.g., minimal sample preparation, fast and easy cleanup and analysis of samples in their natural states.

It is necessary to obtain good optical contact between the surface of the sample and the crystal of the accessory. Increasing the pressure of the material on the crystal is the usual solution for some rough and hard materials to obtain good surface contact (Lindon et al. 2010).

Attenuated Total Reflection Fourier-Transform Infrared Spectroscopy (ATR-FTIR) was used to determine chemical composition of the dried calcium

hydroxide nanoparticles, calcium carbonate nanoparticles, grafted CNC, CNC, oleic acid and DMSO. The measurements were carried out with a Thermo-Nicolet Nexus 870 spectrometer equipped with a liquid nitrogen-cooled Mercury Cadmium Telluride detector and a single reflection diamond crystal ATR unit. The spectra were obtained from 128 scans with 2 cm^{-1} of optical resolution, in the 4000–650 cm^{-1} range. A background spectrum of air was scanned under the same instrumental conditions before each series of measurements.

3.1.2 Transmission Electron Microscope (TEM)

Transmission electron microscope (TEM) consist of three essential systems: an electron gun for producing the electron beam and the condenser system for focusing the beam onto the object; the image-producing system; the image-recording system converting the electron image into some form perceptible to the human eye.

It is a microscopy technique in which a beam of electrons is transmitted through an ultrathin specimen, interacting with the specimen as it passes through it and utilizing energetic electrons to visualize microstructure of materials at the nanometer level.

The organization and basic principles of the transmission electron microscope (TEM) are similar to that of the light microscope. TEM has the added advantage of greater resolution. Electron beam has a much shorter wavelength than the wavelength of visible light so that it forms the image in a light microscope resolving much greater detail.

In this research, Transmission electron microscopy (TEM) images of alkaline nanoparticles were acquired with a STEM CM12 Philips electron microscope, having a point-to-point resolution of 0.3 nm. The nanoparticle samples dispersed in ethanol (1 g/L) were cast onto a carbon-coated copper grid sample holder, followed by evaporation of the solvent at room temperature.

3.1.3 Atomic Force Microscope (AFM)

The Atomic Force Microscope (AFM) is a scanning-probe microscope that measures various material properties by using a cantilever with a sharp probe that scans the surface of the specimen. It has two modes of operation, namely

contact mode and non-contact mode depending on whether the cantilever vibrates during the operation.

In contact mode, the cantilever drags across the sample surface and the deflection of the cantilever and tip is measured by a laser beam. In non-contact mode, the tip vibrates slightly above its resonance frequency and does not contact the surface of the sample. A feedback loop adjusts the height of the cantilever so that the force is kept constant. Recording the distance between the tip and sample at each point allows the software to construct a topographic image of the sample surface.

Atomic force microscopy (AFM) images were collected on CNC and GC particles with a XE7 system (Park System Corp., Korea). The images were acquired in non-contact mode using SSS-NCHR 10M AFM tips with a guaranteed radius of curvature <5 nm, a nominal force constant of 42 N m^{-1}, and a resonance frequency of 272 kHz (drive = 66%). Samples were prepared by placing about 10μL of CNC in water and GC in ethanol (about 3 mg/L) over a freshly cleaved mica sheet.

3.1.3 Thermal Gravimetric Analysis (TGA)

TGA usually records mass loss over increasing temperature of the sample (or time). A precision balance, a programmable furnace and a recorder are the basic instrumental requirements. Usually, analysis was done under dynamic nitrogen atmosphere. The measured weight loss curve gives information about changes in sample composition, thermal stability and kinetic parameters for chemical reactions in the sample. Mass loss can be caused by gas adsorption or desorption, phase transitions and decomposition etc.

Plotting the rate of mass change upon heating as a function of time or temperature is Derivative Thermogravimetry (DTG). It is commonly used to analyze more subtle effects, e.g., the point at which weight loss is most apparent, changes in the mechanism during a reaction.

The thermal behaviors of calcium hydroxide, calcium carbonate, GC, CNCs and oleic acid were studied using an SDT Q600 TA Instrument, operating between 30 and 500 °C at a heating rate of 10 °C/min under nitrogen flow (100 mL/min). For each measurement, about 30 mg of sample were placed inside an aluminum pan and analyzed. From the thermal curves, the pyrolysis temperature (Tp), defined as the maximum of the weight loss derivative, was

recorded and used to gain information about the composition of the sample. Tp experimental error is ± 1 °C.

3.1.4 Mastersizer 3000

The Mastersizer 3000 laser diffraction particle size analyzer delivers rapid, accurate particle size distributions for both wet and dry dispersions measuring over the nanometer to millimeter particle size ranges.

It uses the technique of laser diffraction to measure the size of particles by recording the intensity of light scattered as a laser beam passes through a dispersed particulate sample. This data is then analyzed to calculate the size of the particles that created the scattering pattern.

A typical measurement system is made up of optical bench, sample dispersion units. In the area of optical bench, a laser beam illuminates dispersed particles. A series of detectors then accurately measure the intensity of light scattered by the particles within the sample for both red and blue light wavelengths and over a wide range of angles. Sample dispersion is controlled by a range of wet and dry dispersion units which guarantee that the particles are delivered to the measurement area of the optical bench at the correct concentration and in a suitable, stable state of dispersion.

Measurements were carried out on diluted systems (1 g/L) with a laser obscuration of about 2-3%. The external control module of sample pumping/stirring was set at 1800 rpm. The “general purpose” analysis was used to obtain the volume-based size distributions of particles.

3.1.5 Small-Angle X-ray Scattering (SAXS)

A SAXS instrumentation includes the X-Ray source, a monochromator, a collimation system, a sample chamber and a detection system.

It is a non-destructive and highly versatile standard method to study at the nanoscale the structure of materials in solution, solid, gas phase or at the interface with specially designed sample holders. Samples can be measured under various conditions, such as different temperatures, humidity, pressures, even during chemical reaction.

Photons interact with electrons and intensities of X-rays scattered by a sample as a function of the scattering angle are measured. By means of appropriate model fittings and reconstructions, SAXS data deliver structural

parameters, such as average particle sizes, shapes and distributions, the materials' porosity as well as degree of crystallinity.

Small-angle X-ray scattering (SAXS) measurements were performed with a HECUS S3-MICRO SWAXS-camera, equipped with a Hecus System 3 2D-point collimator (min divergence 0.4 × 0.9 mrad²) and two position sensitive detectors (PSD-50M) consisting of 1024 channels with a width of 54μm. During the experiments, the K_α radiation (λ = 1.542 Å) emitted by a Cu anode from the Oxford 50 W microfocus source with customized FOX-3D single-bounce multilayer point focusing optics (Xenocs, Grenoble) was used, while the K_β line was removed by a multilayer filter. The voltage is generated by the GeniX system (Xenocs, Grenoble). The sample-to-detector distance was 26.9 cm. The volume between the sample and the detector was kept under vacuum during the measurements to minimize the scattering from the atmosphere. The camera was calibrated in the small-angle region using silver behenate (d = 58.38 Å). Scattering curves were obtained in the q-range between 0.01 and 0.6 Å^{-1}. The temperature control was set to 25 °C. Samples were contained in 1.5 mm thick quartz capillary tubes sealed with hot-melting glue. Scattering curves were corrected for the empty capillary contribution considering the relative transmission factors. Desmearing of the SAXS curves was not necessary thanks to the sophisticated focusing system.

In the present case, we adopted a parallelepiped model implemented in the SASView software to fit our systems. Here, the scattering intensity $I(q)$ of a rectangular solid particle, having $A < B < C$ as the three dimensions, is calculated as follows (Kline 2006):

$$I(q) = \frac{K}{V}(\Delta\rho V)^2 P(q,\sigma) + \text{bkg}$$

Where K is a scale factor, V is the volume of a single particle ($V = A \times B \times C$), and the contrast term is $\Delta\rho = \rho_{CNC} - \rho_{solvent}$. $P(q,\alpha)$ is the form factor corresponding to a parallelepiped oriented at an angle given by $\cos(\sigma)$ (being σ the angle between the direction of C and the scattering vector $\boldsymbol{q}$). The calculations are performed by using reduced lengths, instead of the actual dimensions, obtained by normalizing each length to the middle one, B, as follows:

$$a = \frac{A}{B}(< 1)$$

$$b = \frac{b}{B} (\equiv 1)$$

$$c = \frac{C}{B} (> 1)$$

The form factor, averaged over all possible orientations (spanning the whole range of $\cos(\sigma)$), is then given by the following double integral (Mittelbach and Porod 1961):

$$P(q,\sigma) = \int_0^1 \phi_Q(\mu\sqrt{1-\alpha^2}, a) \left[S\left(\frac{\mu c\sigma}{2}\right)\right]^2 d\sigma$$

with:

$$\phi_Q(\mu, a) = \int_0^1 \left\{S\left[\frac{\mu}{2}\cos\left(\frac{\pi}{2}u\right)\right] S\left[\frac{\mu a}{2}\cos\left(\frac{\pi}{2}u\right)\right]\right\}^2 du$$

$$S(x) = \frac{\sin x}{x}$$

$$\mu = qB$$

Where u is the cosine of the angle between B and the scattering vector.

3.1.6 Rheological analysis

Different materials display different types of response to an applied stress: viscous flow, elastic deformation and viscoelastic response. If the material deforms instantly under stress and the deformation is spontaneously reversed when the stress is removed, the material possesses an elastic response, accordingly to the Hooke's law (Ferry 1980a). The stress is directly proportional to strain in deformations and is independent of the rate of strain. If a material continues to deform as long as the stress is exerted and the energy put in to maintain the flow is dissipated as heat, the material possesses a viscous response, accordingly to the Newton's law (Ferry 1980a). The stress is directly proportional to rate of strain and is independent of the strain. Perfect viscous or elastic materials are much easier to measure. Unfortunately, they are not very common. Most materials are viscoelastic, meaning that they combine the

features of a so-called perfect elastic solid and a perfect fluid, representing apparent viscosities that depend entirely on the specific experimental conditions, such as stress, strain, timescale and temperature.

Rheology is the study of flow and deformation of materials under exerted forces, especially the establishing relationships between stress and deformation for materials where neither Newton's law nor Hooke's law suffice to explain their mechanical behaviors. The extent to which a material deforms under a certain force depends strongly on its properties and gives information about structure. In our study, the rheological characteristics of materials directly affect the way that they should be handled in conservation.

Oscillatory shear measurements were carried out with a TA Instrument Hybrid Rheometer DISCOVERY HR-3, using a plate-plate geometry (Flat Plate 40 mm diameter) and a Peltier for temperature control. The cell was closed by lowering the head to the measuring position in the z axis force-controlled mode. Each gel sample was gently loaded onto the plate and care was taken to minimize shearing during sample removal and sample loading. To minimize ethanol evaporation during tests, silicone oil was placed around the sample. Measurements were performed at 25 °C and at least twice on duplicate samples.

In the system of hybrids in water/ethanol blend, flow and frequency sweep curves and three interval thixotropy tests (3ITT) (Mewis and Wagner 2009; Said et al. 2015; Yilmaz and Vatansever 2016) were measured. For flow curves, viscosity is measured as a function of shear rate, were acquired between 10^{-3} and 10^{2} s^{-1}. Frequency sweep measurements were carried out over the frequency range 0.05-50 Hz, in the linear viscoelastic region (strain 1%), previously determined by amplitude sweep tests (strain 0.01-200%; 1Hz). Three interval thixotropy tests (3ITT) were performed as follows: a low-shear rate ($0.1s^{-1}$) was applied for 60 s; thereafter, a high-shear rate regime (60 s at 10 s^{-1}) was used to break the structure of the samples; the final stage at low-shear (0.1 s^{-1}) lasted 600 s, to favor the recovery of the internal structure.

In the system of hybrids in ethanol, amplitude sweep tests were performed to determine the linear viscoelastic (LVE) domain (strain 0.01-100%; 1Hz). Frequency sweep measurements were carried out over the frequency range 15-0.1Hz at a constant strain of 0.2% within LVE domain. Three-interval test (3ITT test) (Wollny and Huck 2002) were performed using a parallel−plate geometry (diameter 40 mm). In the first interval of oscillation, 600s soak time was applied to remove loading effects, then test was performed at constant frequency, 1Hz, and amplitude oscillatory strain, γ= 0.02%, within the linear

viscoelastic range for 90s. In the second interval, 60s soak time was applied and followed by a large amplitude oscillatory strain (80%) for 90s aiming to break down the structure of the gel. In the third interval, 600s soak time was applied to get sample in new equilibrium state, same conditions were applied as in the first interval.

3.2 Characterization of paper conditions

3.2.1 pH measurements

Paper pH is generally defined as the pH of its extractives soluble in distilled water. Several procedures can be adopted to test the pH of cellulose-based artifacts. The most commonly used procedure, defined by TAPPI (Technical Association of the Pulp and Paper Industries), implies the use of 1g of paper to be immersed in 70mL of cold (TAPPI. 2002) or hot (TAPPI. 2006) water. This approach is indeed destructive and, for that, is not always easily applied during conservation practice. Alternatively, surface pH measurements can be performed (TAPPI. 2004): a drop of water is placed on the surface of sample and, after a suitable amount of time, the pH is measured with a universal indicator.

Nowadays, paper pH is world widely accepted and considered a very useful tool to assess conservation conditions of cellulosic material. It is worth noting that the pH results can not represent the condition of the entire sample since a small portion of the sample was took during the measurement.

As above indicated, the determination of paper pH can be an useful tool to decide if a deacidification treatment is needed and the deacidification effects; but, in our opinion, 1g of sample required in the TAPPI procedures (TAPPI. 2002, 2006) is often inapplicable due to the limitation of cellulosic material. On the other hand, the measurement of surface paper pH(TAPPI. 2004) cannot obtain reliable results in this situation. Therefore, a modified TAPPI procedure was used: 125 mg of sample was weighed, cut in small pieces and placed inside screw top vials. 9 mL of distilled water was added inside each vial, subsequently sealed to avoid the solubilization of CO_2 from air into the extracting water. Vials were kept under stirring for one hour, before measuring the pH of the extraction by using a digital pH-meter (CrisonBasic 20, equipped with a combined electrode, model 52-21). Three measurements were performed

on each sample. The error associated to pH measurements on these samples is ± 0.2.

3.2.2 Colorimetry

A colorimeter consists of a light source, a sample holder, and a light intensity sensor to control the light source and integrate the transmitted light intensity.

It measures color quantitatively, replacing the subjective responses, such as 'dark red', 'light purple', 'bright gold', with an objective numerical system.

The Commission International de l'Eclairage (CIE) recommended a system of color specification based on the three tristimulus values X, Y and Z, which are obtained from the spectral measurement of the light reflected by the perfect reflecting diffuser, once an illuminant is chosen. CIE defined in 1976 two psychometric systems, termed CIELAB and CIELUV. The CIELAB colorimetric system is spanned by the coordinates (L*, a*, b*). L* is lightness. a* and b* are coordinates recalling the opponent unique hues.

Reflectance spectra were acquired using a Cary 100 UV-VIS spectrophotometer, working in a λ range of 400–700 nm (with 1 nm of resolution), equipped with an integrating sphere having a circular sampling spot (diameter = 1.5 cm). Colorimetric coordinates were extracted from reflectance spectra using standard illuminant D65 and a standard observer at 2°. The color difference between samples can be expressed in terms of the ΔE parameter, calculated from the colorimetric coordinates and L^*, a^*, and b^* as follows (Wyszecki and Stiles 2000):

$$\Delta E = \sqrt{(L_2^* - L_1^*)^2 + (a_2^* - a_1^*)^2 + (b_2^* - b_1^*)^2}$$

The experimental error of colorimetric measurements on paper is ± 0.5.

3.2.3 Tensile strength measurements

Tensile strength is the maximum tensile force per unit width of test specimen before rupture. It is a measure of the strength derived from factors such as fiber strength, fiber length and bonding.

Several standards are available to test the tensile strength of cellulose-based materials. The most common are those based on constant rates of elongation. As

is described in the standard method ASTM D828 (ASTM D828-97 2002; TAPPI T494 2006), the initial dimension of specimen require is 2.54 mm of width, 254 mm of length, 180 mm of gauge length (the distance between the clamping zones), and about 2.54 mm per minute of rate of grips separation. The time to break a single strip should be between 15 and 30 s. The speed of the instrument must be reported, along with the test data. However, samples of that size are not commonly available in the paper conservation field. In our case, test span and speed were changed proportionally as suggested in the standard test method.

Tensile strength measurements were conducted on paper stripes using a TA Instrument Hybrid Rheometer DISCOVERY HR-3, equipped with a Film Tension Dynamic Mechanical Analysis tool.

The used procedure was adapted from standards for tensile measurements on paper (ASTM D828-97 2002; TAPPI T494 2006). Each stripe measures 1 x 8 cm^2 and was clamped on two jaws, whose distance was fixed at 4 cm. The rate of separation of the two jaws was set at 94 μm/s or 47μm/s. This rate of grip separation generally results in sample rupture in 10-30 s. At least six measurements were performed for each series of samples. The mean value of the load at which sample rapture occurred was used to calculate the Ultimate Tensile Strength (UTS), given by:

$$\mathrm{UTS} = \mathrm{AF/W[kN/m]}$$

where AF is the axial force at rupture and W is the width of the sample, measured with a digital caliper.

Chapter 4 Strengthening and deacidification of paper with hybrids of alkaline nanoparticles and cellulose nanoparticles in water/ethanol blend

As deeply discussed in Chapter 1, the most important degradation mechanism of cellulose is the acid-catalyzed hydrolysis of β-1,4-glycosidic bonds, which results in the decrease of cellulose DP and, macroscopically, in the loss of the original mechanical properties. Therefore, both a deacidification and a reinforcement treatment are required.

A single-step treatment grants a reduction in terms of costs, time, risk and the stress for the artifact. Therefore, we devoted research efforts to the formulation of combined systems to neutralize acidity, hampering further degradation of the cellulose chains, and, at the same time, improve the mechanical resistance of the original material. As discussed in Chapter 2, our research group proposed the use of alkaline nanoparticles for deacidification in 2002 and have worked on the field since then. Therefore, for the combined deacidification and consolidation of cellulose-based artworks, we decided to use similar dispersions, i.e., calcium hydroxide and calcium carbonate nanoparticles. Calcium hydroxide nanoparticles were prepared according to a synthetic route involving ethanol and calcium metal (Poggi et al. 2014c, 2016a). On the other hand, calcium carbonate nanoparticles were obtained using an innovative procedure, which includes the usage of an alkyl carbonate for the conversion of the intermediate reaction products into carbonates that will be discussed in the following sections. For the reinforcement of cellulosic materials, nanocellulose was adopted. As is discussed in chapter 2, there is a growing interest in the use of nanocellulose, due to its unique properties. As a matter of fact, nanocelluloses are non-toxic, renewable and biodegradable. In addition to that, they have excellent mechanical properties, high surface area, and form almost transparent

films (Habibi et al. 2010; Moon et al. 2011; Lavoine et al. 2012; Abdul Khalil et al. 2014; Nechyporchuk et al. 2016b, a).

Hybrid systems for the simultaneous strengthening and deacidification of paper are presented in the following section, including the physico-chemical characterization by means of rheological and SAXS measurements. The efficacy of the proposed systems for strengthening and deacidification of acidic paper was evaluated with tensile testing and pH measurements.

4.1 Alkaline nanoparticles

4.1.1 Synthesis via solvothermal reaction

Calcium hydroxide nanoparticles were prepared using a solvothermal synthesis, starting from ethanol and calcium metal (Poggi et al. 2014c, 2016a). Calcium carbonate nanoparticles were obtained as follows: 10 g of granular calcium and 500 mL of ethanol were placed inside a high-pressure reactor (Parr-instruments). Before starting the reaction, vacuum/nitrogen cycles were performed to ensure an oxygen-free atmosphere inside the sealed reaction chamber. During the first step of the reaction, calcium alkoxide is obtained. To hydrolyze the alkoxide to calcium carbonate, 35 mL of water and 35 mL of diethyl carbonate was added inside the reaction chamber by means of steel pipette in a nitrogen atmosphere. The addition was carried out at 70 °C and the system was stirred for 60 min. Contrarily to calcium hydroxide nanoparticles, which were prepared according to a previously reported procedure, calcium carbonate nanoparticles were obtained using a new procedure, based on a solvothermal process. During the first step of the reaction, ethanol oxidizes metal calcium to the corresponding alkoxide (equation 4.1), i.e., calcium ethoxide, which is soluble in ethanol. To hydrolyze the alkoxide and favor its conversion to calcium carbonate, both water and diethyl carbonate were added inside the reaction chamber by means of steel pipette in an inert atmosphere. Water triggers the conversion of calcium ethoxide into calcium hydroxide, while diethyl carbonate releases carbonate ions (Faatz et al. 2004) that react with the calcium hydroxide formed after the addition of water (equation 4.2).

$$Ca + ethanol \rightarrow Ca(ethoxide)_2 + H_2 \qquad (4.1)$$

$$Ca(ethoxide)_2 + H_2O + DEC \rightarrow CaCO_3 + ethanol \quad (4.2)$$

4.1.2 Characterizations of synthesized nanoparticles

ATR-FTIR spectrum of the dried calcium carbonate nanoparticles (black line) only shows the peaks related to carbonate ions, such as the asymmetric stretching at 1485 cm^{-1}, the symmetric stretching at 1082 cm^{-1}, and the symmetric bending at 870 cm^{-1} (Andersen, Flemming A. Brečević 1991). Peaks due to the OCO bending (in-plane deformation) located between 750 cm^{-1} and 700 cm^{-1} provide interesting information about calcium carbonate polymorphs. Synthesized nanoparticles, in fact, are composed of both calcite ($\nu4$ = 713 cm^{-1}) and vaterite ($\nu4$ = 746 cm^{-1}), two of the most common crystalline polymorphs of $CaCO_3$ (Andersen, Flemming A. Brečević 1991). The ATR-FTIR spectrum of the dried calcium hydroxide nanoparticles (grey line in figure 4.1-A) shows a sharp peak located at 3640 cm^{-1}, which can be attributed to portlandite, i.e. the crystalline form of calcium hydroxide. The presence of a weak signals typical of carbonate are due to the incipient conversion of the hydroxide nanoparticles that, due to their high surface area, react readily with atmospheric CO_2.

The composition of nanoparticles was also assessed with DTG. The graph reported in figure 4.1-B shows the weight change of the dried samples during a thermal ramp. The DTG thermogram of calcium hydroxide nanoparticles (grey line) displays a peak between 350°C and 500°C, corresponding to the dehydration of calcium hydroxide (Halstead, P. E. 1957). On the other hand, the thermogram of calcium carbonate nanoparticles shows a broad peak between 500°C and 800°C that is the fingerprint of the decomposition of calcium carbonate into calcium oxide and carbon dioxide, with a yield of about 43% weight loss, in agreement with the theoretic weight loss of 44% (Halikia et al. 2001; Popescu et al. 2014).

Overall, ATR-FTIR and DTG clearly show that the conversion of calcium hydroxide into calcium carbonate during the second step of the reaction was complete. TEM images of synthesized calcium carbonate nanoparticles display two phases: one consisting of cubic crystals and the other consisting of globular shapes (see figure 4.1-C). This is in agreement with ATR-FTIR spectra, in which two polymorphs of calcium carbonate were detected, being the cubic crystals due to calcite and globular particles due to vaterite (Popescu et al. 2014). The TEM image of calcium hydroxide nanoparticles shows hexagonal platelets with

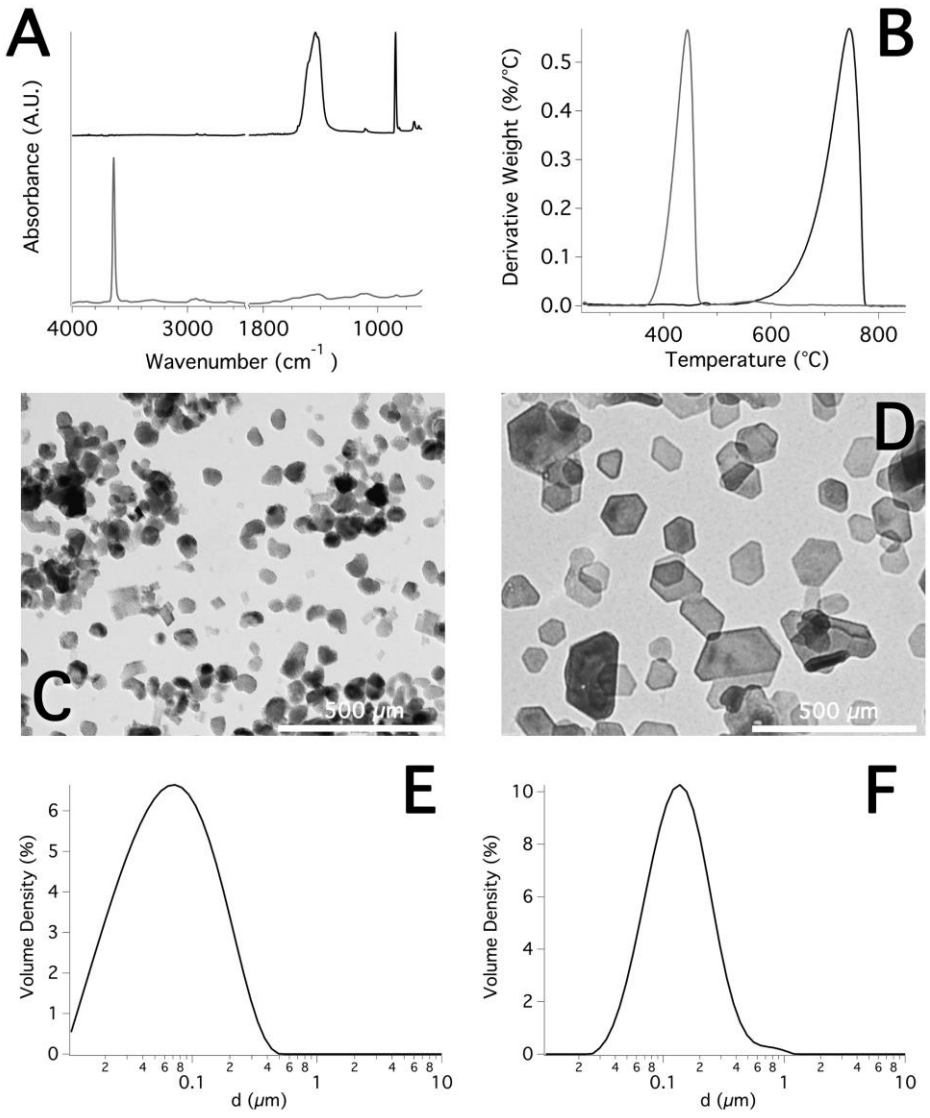

Figure 4.1. (A) ATR-FTIR spectrum of dried calcium hydroxide (grey line, bottom spectrum) and carbonate (black line, top spectrum) nanoparticles. (B) DTG curve of dried calcium hydroxide (grey line) and carbonate (black line) nanoparticles. (C) TEM picture of calcium carbonate nanoparticles. (D) TEM picture of calcium hydroxide nanoparticles. (E) Volume-based size distribution of calcium carbonate nanoparticles obtained with laser diffraction analysis. (F) Volume-based size distribution of calcium hydroxide nanoparticles obtained with laser diffraction analysis.

a high degree of ordering, having a thickness of about 20–30nm (see figure 4.1-D). In agreement with the TEM images, the volume-based size distribution of calcium carbonate nanoparticles, obtained by laser diffraction, is centered at about 70 nm (figure 4.1-E), while the average diameter of calcium hydroxide is about 140 nm (figure 4.1-F).

Overall, the physico-chemical characterization of calcium hydroxide and carbonate nanoparticles showed that the solvothermal reaction yields crystalline and relatively small nanoparticles. These features indicate that both calcium hydroxide and carbonate are good candidate for the cellulose-based artworks conservation. In addition to that, these nanoparticles are already dispersed in the appropriate solvent for the conservation treatment, i.e. the system can be directly employed without any further purification step.

4.2 CNCs dispersions and hybrid systems

4.2.1 Preparation

Cellulose nanocrystals powder was placed, as received, in a vial, together with highly pure water. The dispersion was then stirred for 6 hours at 800 rpm. Thereafter, the dispersion was sonicated for 5 minutes with a Branson S-450 (450W) equipped with a micro-tip, with an output power of 20%. Initially tested CNC concentration ranges from 0.5 wt% to 12 wt%.

For the preparation of CNC dispersion in water/ethanol mixture, ethanol was gradually added to a highly-concentrated aqueous CNC dispersion kept under stirring. After some preliminary tests, a concentration of 50 wt% of ethanol and a concentration of 3 wt% of CNC was selected for the preparation of final systems.

Hybrid systems were prepared by mixing an aqueous CNC dispersion with calcium hydroxide or calcium carbonate nanoparticles in ethanol. Alkaline nanoparticle dispersions were gradually added, keeping the hybrid systems under stirring. After some preliminary tests, a nanoparticles concentration in the hybrid systems of 0.3 wt% was selected for the preparation of final systems. Ethanol was added to these systems to obtain a concentration of 50 wt%. Name and composition of selected hybrid systems are indicated in Table 1.

Table 4.1. Name and composition of CNC dispersions and hybrid systems

CNCs dispersions and hybrid systems					
Name	**CNCs wt%**	**NanoP type**	**NanoP wt%**	**Solvent**	**Ethanol wt%**
CNC12W	1.2	-	-	Water	-
CNC120W	12	-	-	Water	-
CNC30W	3	-	-	Water	-
CNC30	3	-	-	Water/Ethanol	50
CNC30-OH3	3	$Ca(OH)_2$	0.3	Water/Ethanol	50
CNC30-CO3	3	$CaCO_3$	0.3	Water/Ethanol	50

4.2.2 Characterization

Preliminary tests were conducted on CNC dispersion over a wide range of CNC concentration (0.5-12 wt%). Flow curves were used to gain information about the viscosity of systems and its changes as a function of the shear rate. Viscosity is a fundamental property of a material, and it can shed light on some interesting features useful for applicative purpose.

Some of the recorded flow curves are reported in Figure 4.2. All these selected systems behave as non–Newtonian fluids. In general, the viscosity decreases with increasing shear rate, even if the particular behavior of each sample depends on the concentration of CNC. The flow curve of CNC12W exhibits three discrete regions, as already reported in the literature (Hamza 2017): at low shear rate, a pseudo-Newtonian plateau can be seen; at intermediate shear rate, a significant drop in the viscosity is related to a change in the structure, leading to an alignment of nanocrystals; consequently, at high shear rate, another pseudo-Newtonian plateau can be seen. The flow curve of a more concentrated systems, i.e. CNC30W, displays a similar behavior, even if the difference between the three regions is less clear. At higher concentration (CNC120W), the CNC aqueous dispersion behaves as a pure shear thinning material, where the viscosity significantly decreases with increasing shear rate.

This is due to the electrostatic interactions between particles, which leads to strong systems at high concentration of CNC (Lu et al. 2014). It is very interesting to note that the addition of ethanol in 3 wt% CNC aqueous dispersion leads to the change in the rheological behavior of the systems. In fact, the flow curve of CNC30 exhibit a pseudo-plateau at low shear rate, in which the viscosity is about 600 times higher than CNC30W. The viscosity then decreases with increasing shear rate, in a manner that is typical of a shear thinning material. The presence of ethanol in CNC dispersion results in the overall increase of the viscosity of the system. This behavior can be explained as follows: the Debye length, which is a measure of how far the electrostatic effect of charged particles persists, depends on the permittivity of the solvent. The lowest the permittivity of the solvent, the highest is the screening of the electrostatic repulsions between crystals. Permittivity of ethanol is lower than water (24.5 and 78, respectively), therefore, in presence of a hydroalcoholic mixture, the Debye length of nanocrystals decreases, allowing for stronger interactions between particles. As a result, the viscosity of the dispersion significantly increases.

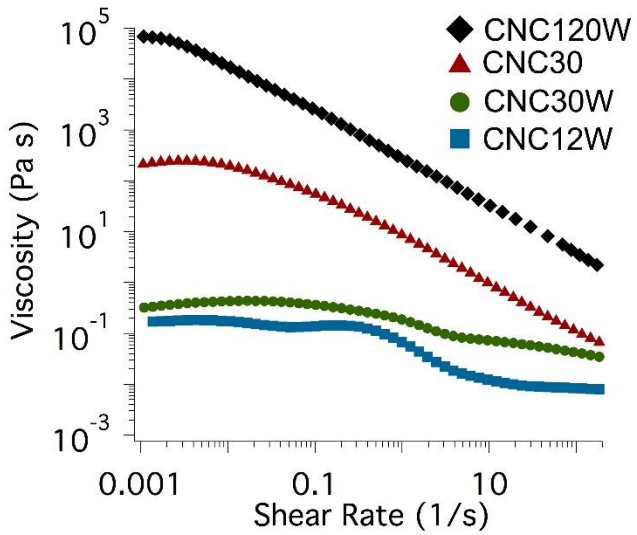

Figure 4.2. Flow curves of CNC featuring systems: CNC at 12 wt% in water (CNC120W, black diamonds); CNC at 3 wt% in water/ethanol (CNC30, red triangles); CNC at 3 wt% in water – (CNC30W, green circles); CNC at 1.2 wt% in water (CNC12W, blue squares).

On the basis of these preliminary tests, systems featuring 3% of CNC, which display the most interesting behavior in terms of viscosity, were selected to be used for the preparation of hybrid systems, following the procedure reported in 3.1.6. The mechanical response of hybrid systems was assessed using frequency sweep measurements and compared to the one of reference dispersions, i.e., CNC30W and CNC30. In a typical frequency sweep test, the frequency of the applied strain is increased, and the mechanical response is recorded in terms of G', the storage modulus, and G'', the loss modulus, which are, respectively, a measure of the stored energy, i.e. the elastic response, and of the dissipated energy, i.e. the viscous response at a given frequency of oscillation (Ferry 1980a). The mechanical dynamic response exhibited by CNC30W, reported in figure 4.3-A is typical of a viscoelastic liquid, i.e. of an entangled system where nanocrystals interactions are negligible: at low frequencies the system behaves as a diluted solution (predominant viscous behavior, G''>G'), while at high frequencies the response becomes more solid-like (G'≈G''), as the system cannot rearrange within the time of an oscillation (Ross-Murphy 1995). On the other hand, CNC30 displays a solid-like mechanical spectrum, being G'>>G'' over the entire range of investigated frequencies, with both moduli almost frequency-independent (see figure 4.3-B). Moreover, the values of both G' and G'' in CNC30 are more than 10 times higher than CNC30W. These results are in accordance with the flow curves reported in Figure 4.2, and they confirm that the addition of ethanol increases the interaction between cellulose nanocrystals, as a result of the decrease in the Debye length.

In Figure 4.3-C, the frequency sweep of the hybrid system with CNC (3 wt%) and calcium hydroxide nanoparticles (0.3 wt%), in a water/ethanol blend (ethanol 50 wt%), i.e. CNC30-OH3, is reported. The addition of calcium hydroxide nanoparticles leads to strong increase in G' and G'', which are two orders of magnitude higher than in CNC30 and are frequency-independent. This system exhibits a true gel-like behavior indeed. Cellulose nanocrystals produced by sulfuric acid hydrolysis of cellulose usually yield negatively charged CNC particles with sulfate surface groups (Phan-Xuan et al. 2016); it has been recently shown that the addition of divalent ions, such as Ca^{2+} to charged nanocelluloses can induce the gelation of aqueous dispersion by screening the repulsive forces generated by surface charges (Dong et al. 2013; Chau et al. 2015). The overall effect is similar to the effect of the addition of ethanol, already discussed. Indeed, the Debye length is also a function of the

concentration of ions in solution, i.e., the ionic strength. The highest the ionic strength, the lowest is the Debye length. Therefore, the addition of both ethanol and calcium hydroxide to a CNC dispersion in water results in a strong gelled system. In addition to that, as crystals distances are reduced during gelation, divalent ions may complex different crystals, increasing the mechanical strength of the system (Dong et al. 2013).

A different behavior is shown by the hybrid system CNC30-CO3, as reported in Figure 4.3-D. Here, the G′ and G″ values are only slightly higher than those of CNC30 system, even if both moduli are frequency independent. This behavior can be simply explained by the lower solubility of calcium carbonate nanoparticles in the water/ethanol blend with respect to calcium hydroxide, which leads to a less pronounced effect on the screening of the crystal repulsive forces.

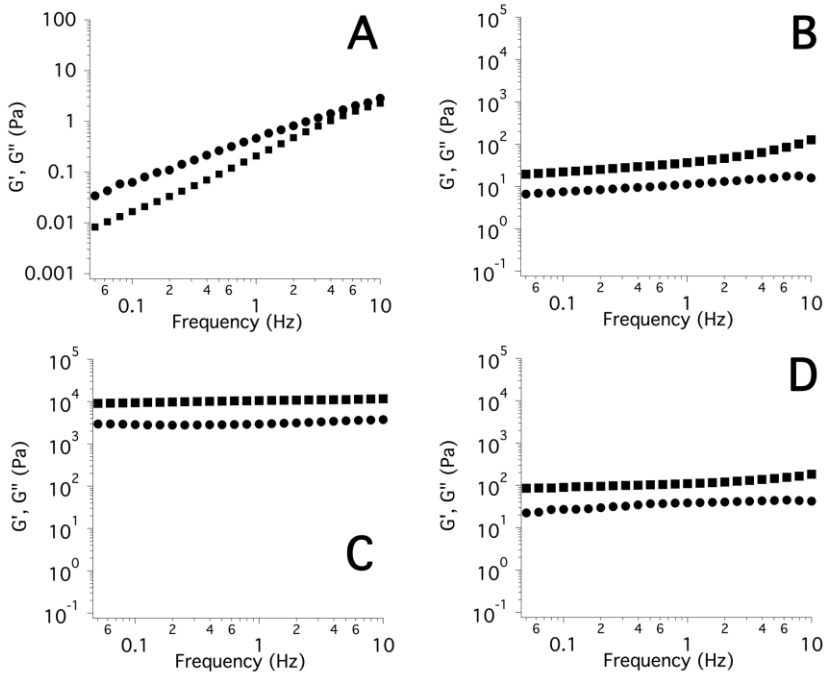

Figure 4.3. Frequency sweep measurements on CNCs featuring systems - G′(■), G″(●). (**A**) CNC30W: aqueous dispersion of CNC (3 wt%). (**B**) CNC30: dispersion of CNC (3 wt%) in water/ethanol blend (ethanol 50 wt%). (**C**) CNC30-OH3: hybrid system, with CNC (3 wt%) and calcium hydroxide nanoparticles (0.3 wt%), in water/ethanol blend (ethanol 50 wt%). (**D**) CNC30-CO3: hybrid system, with CNC (3 wt%) and calcium carbonate nanoparticles (0.3 wt%), in water/ethanol blend (ethanol 50 wt%).

The visual aspect of the samples, shown in Figure 4.4, confirms the rheological characterization of the systems; in fact, CNC30-OH3 (C) is more solid-like than CNC30 (A) and CNC30-CO3 (B). Interestingly, the latter two dispersions, if gently shaken, start to flow. This can potentially allow for their application by spraying, which is sometimes to be preferred in the case of very fragile artworks. On the contrary, a more solid-like system such as CNC30-OH3, should be selected when a more confined application is required. It is worth noting that, for the present study, all the systems were applied by brush to allow for a proper comparison of their effectiveness.

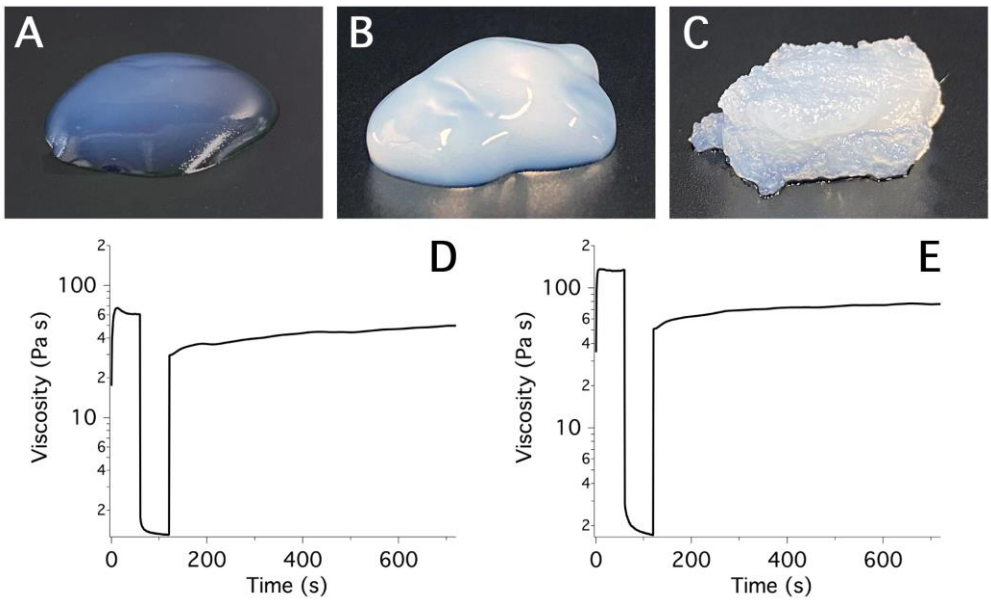

Figure 4.4. Upper row: (A) CNC30; (B) CNC30-CO3; (C) CNC30-OH3. Bottom row: three interval thixotropy test (3ITT) of CNC30 (D) and CNC30-CO3 (E). After the application of a high shear rate, the recovery in viscosity after 600 s is manifest (even if not complete).

After preparation 1 day, a three interval thixotropy test (3ITT) was used to perform instant shear stress/shear rate deformation. As the name suggests, the test is composed of three intervals: a low-shear interval, to be used as a reference of an undisturbed material; a high-shear interval, to break the internal structure; a final stage at low-shear conditions to favor the regeneration of the structure. As can be seen in Figure 4.4-D and 4.4-E, in the first interval, the viscosity of CNC30 and CNC30-CO3 is 60 and 130 Pa s, respectively; in response to a high-shear rate (10 s^{-1}), which induces the alignment of cellulose nanocrystals,

the viscosity drop to about 1 Pa s in both systems. In the third interval (0.1 s^{-1} shear rate), there is an immediate partial recovery of the viscosity, followed by a slower increase, which is typical of thixotropic systems. After 600 s, the viscosity of CNC30 and CNC30-CO3 is, respectively, 50 and 80 Pa s, corresponding to a recovery of about 80% and 60%.

SAXS measurements were used to deepen the interactions between cellulose nanocrystals in the presence of ethanol and alkaline nanoparticles. CNC have been the subject of several characterization studies, where scattering techniques such as quasi-elastic light scattering (QELS), small-angle neutron scattering (SANS) and SAXS measurements were performed, in order to gather information about size, shape and interparticle interactions of cellulose nanocrystals dispersions (Bonini et al. 2002; Su et al. 2014, 2015; Cherhal et al. 2015; Schütz et al. 2015; Uhlig et al. 2016; Mao et al. 2017). In particular, being the CNC elongated fibrillar particles, they are usually modeled as cylinders, ribbons, or parallelepipeds in the analysis of scattering data. Generally, ribbons and parallelepipeds provide the most reliable fitting results (Su et al. 2014). As is described in chapter 3, the systems were fitted by a parallelepiped model implemented in the SASView software.

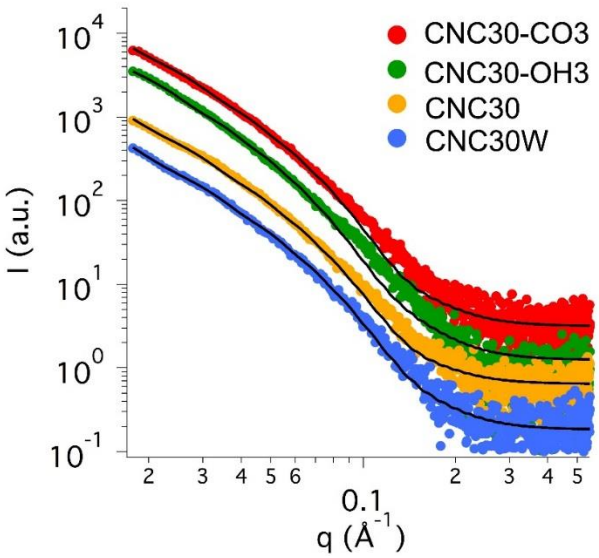

Figure 4.5. SAXS curves of the four samples: CNC30W, blue circles; CNC30, yellow circles; CNC30-OH3, green circles; CNC30-CO3, red circles. Fitting lines are represented as continuous black curves. The four curves, otherwise almost completely superimposed, have been arbitrarily stacked by shifting them along the y axis, for sake of clarity.

Figure 4.5 shows the scattering curves, together with their best fitting, of the four samples analyzed, i.e., CNC30W, CNC30, CNC30-OH3, and CNC30-CO3, while in Table 2 fitting results are reported.

By looking at Figure 4.5, scattering curves of all the systems can be noticed. CNC30 more in detail, CNC were found to have the major length, *C*, fixed around 150 nm, which is in agreement with the information available on the commercial product nanocrystals' length, even if this dimension is actually at the limit of the range that could be investigated with SAXS.

Thus, this value has rather a mathematical meaning than an actual physical one. The minor length, *A*, was found to be 3.5 – 4 nm, almost independently on the solvent, which CNC are dispersed in, or on the presence and kind of nanoparticles. A polydispersity index (PI) of about 0.35 was considered for the length of A, according to fitting results. It is worth noting that this value is in accordance with data reported in the literature (Cherhal et al. 2015). Finally, and most interestingly, *B*, the middle length dimension of the parallelepiped, is significantly bigger than *A*, and, moreover, it clearly changes from one sample to another.

The simplest explanation of the fact that *A* and *B* differ of about an order of magnitude is that we are actually observing dispersion of CNC clusters, rather than single particles. By hypothesizing that a single CNC has a square section (*A* x *A*), similarly to what done by Uhlig et al. (Uhlig et al. 2016), we can imagine that CNC aggregate side by side to form ribbons having a rectangular total section given by *A* x *B*. Therefore, the *B*/*A* ratio can be considered the aggregation number of CNC clusters. The last row of Table 2 reports the average aggregation number of CNC clusters; it can be noticed that goes from 9.4 CNC units for the CNC30W sample to the 11.8 units for the CNC30-OH3 sample, following this trend: CNC30W < CNC30 < CNC30-CO3 < CNC30-OH3 (see Figure 4.6). This trend is in good accordance with the results of rheology measurements that show the effect of ethanol and alkaline nanoparticles on the mechanical behavior of samples.

On the basis of the experimental data, we can hypothesize what follows: the addition of ethanol and alkaline nanoparticles results in the decrease of the Debye length, favoring the interaction between cellulose nanocrystals. This phenomenon is responsible for the increase in the size of clusters, as shown by SAXS measurements, and also for the formation of macrodomains, due to the interactions between different clusters. The changes in the mechanical behavior of the systems, assessed by rheological measurements, are probably due to the

these macrodomains, whose size or distance is too high to be investigated with small-angle scattering techniques.

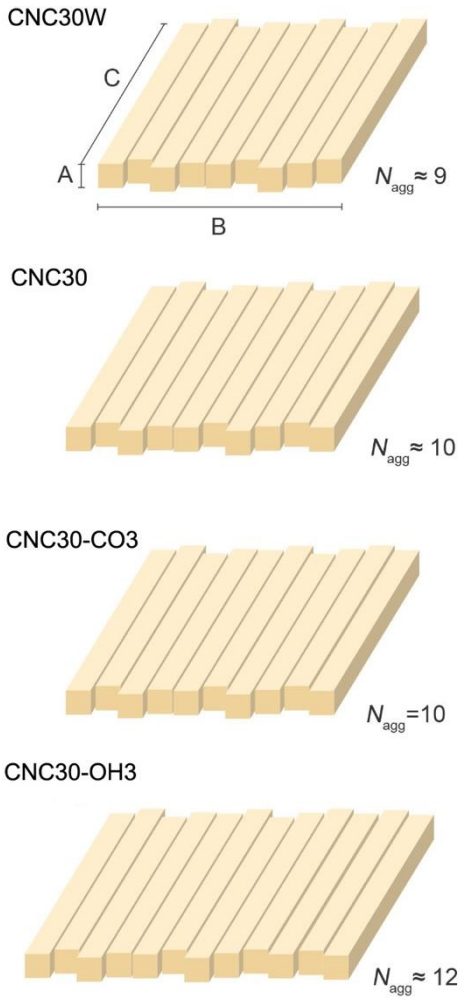

Figure 4.6. The cartoon shows the evolution of CNC clusters, as pictured from SAXS fitting results. The figure is in scale, though *C* is not; it should be about 7 times longer than represented in the figure. The actual *A* x *B* section of CNC clusters would be about 1.4 x 10^6 times smaller than its size in the image.

Table 4.2. Fitting parameters for the four samples analyzed.

Fitting parameter	CNC30W	CNC30	CNC30-OH3	CNC30-CO3
A (Å)	34.9 ± 2.1	36.1 ± 1.1	39.0 ± 1.0	38.1 ± 0.1
B (Å)	326.7 ± 1.4	355.8 ± 1.0	461.9 ± 1.2	382.8 ± 1.4
C (nm)	150 ± 2	150 ± 1	150 ± 1	152 ± 15
SLD_{CNC} (10^{-6} Å^{-2})	15.1	15.1	15.1	15.1
$SLD_{solvent}$ (10^{-6} Å^{-2})	9.4	8.4	8.4[a]	8.4[a]
PI_A	0.37 ± 0.1	0.34 ± 0.1	0.37 ± 0.1	0.33 ± 0.1
N_{agg} (B/A)	9.4	9.9	11.8	10.0

[a]The SLD of ethanol/water was used in this case, as $Ca(OH)_2$ and $CaCO_3$ nanoparticles were not present, being their volume at this concentration practically negligible.

4.3 Applicative tests

4.3.1 Application on paper

Filter paper (paper grammage: 75g/m^2) was used to test the efficacy of the hybrid systems. Paper sheets were immersed in a sulfuric acid solution (pH = 2.5) for 30 s and then aged at high temperature and relative humidity (80 °C and 75% RH) for 10 days, in order to have samples in need for both a deacidification and a strengthening treatment. These samples are labelled as AF, i.e., aged filter paper. Unaged filter paper was characterized and used as a reference system. This system is labelled as UF.

Three treatments were selected to be tested. Name and composition of paper samples are indicated in Table 4.3. All the treatments were applied by brush on both sides of paper samples measuring 6 x 8 cm^2. Samples were left to dry for at least two days before testing. Samples featuring calcium hydroxide nanoparticles were left at 50% RH for 14 days, time needed for calcium

hydroxide excess to turn into carbonate. Samples were weighed before and after the application. The weight change due to the application was about 10%.

Table 4.3. Name and composition of paper samples tested in the present study.

Paper samples					
Name	**CNC wt%**	**NanoP type**	**NanoP wt%**	**Solvent**	**Ethanol wt%**
UF	-	-	-	-	-
AF	-	-	-	-	-
AF-CNC30	3	-	-	Water/Ethanol	50
AF-CNC30-OH3	3	$Ca(OH)_2$	0.3	Water/Ethanol	50
AF-CNC30-CO3	3	$CaCO_3$	0.3	Water/Ethanol	50

4.3.2 Characterization of paper

Nanocelluloses have been recently used to modify the properties of paper pulp, before the formation of sheets or directly to form paper sheets (Kajanto and Kosonen 2012; Lee et al. 2012; González et al. 2014). To the best of our knowledge, this is the first time that hybrid systems, featuring both nanocellulose and a deacidification agent, have been used for the concomitant strengthening and deacidification of already formed paper sheets, which is of interested in the field of the conservation of documents, archival material and cellulose-based artworks.

Tensile tests are very useful to evaluate changes in the mechanical resistance of paper treated with strengthening agents. Paper sheets were immersed in a sulfuric acid solution and then aged at high temperature and relative humidity to prepare a set of samples in need for both a deacidification and a strengthening treatment. The immersion of filter paper in an acidic bath decreases the pH from 6.5 to 5, as shown in Figure 4.7. At high temperature and relative humidity, acids speed up the degradation of cellulose, resulting in a decrease of about 25% of the UTS (Ultimate Tensile Strength) after only ten days of aging (see Figure 4.7).

Acidity is usually interconnected with oxidation (Shanani and Harrison 2002). The yellowing of paper is mainly due to the formation of chromophores, such as conjugated carbonyl and carboxyl compounds (Bronzato et al. 2013), whose production is favored in an acidic environment. After 10 days of artificial aging, we measured a significant change in the visual aspect of samples, i.e., a ΔE (as is defined in part 4.2) of 7.9 units. It is worth noting that a ΔE higher than 2.3 units makes the color difference perceivable by the naked eye (Witzel et al. 1973).

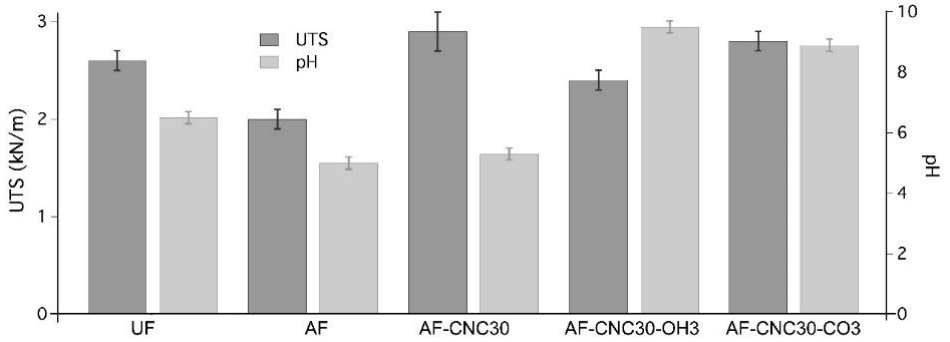

Figure 4.7. Ultimate tensile strength, dark bars, and pH, light bars, of paper samples. The beneficial effects due to the application of CNC, especially in combination with alkaline nanoparticles, are manifest.

The application of CNC30 on AF (sample AF-CNC30) increases the UTS to 2.9 kN/m. Tensile tests conducted on a control sample of paper treated with only the water/ethanol 1:1 (w/w) solvent mixture (AF-WE) confirm that the increase in UTS and E is only due to nanocellulose, being the two data 2.1 and 1.9, respectively. It is worth noting that the UTS of paper treated with CNC is even higher than the value of unaged paper. This is a confirmation that CNC act as an effective strengthening agent. On the other hand, pH values of AF-CNC30 and of AF are almost the same, because, as expected, nanocellulose cannot neutralize acidity (see Figure 4.7).

With the aim of providing conservator with a combined treatment to address the two main problem of cellulose-based materials conservation in a single application, hybrid systems were developed and applied on aged filter paper. Both formulations, containing calcium carbonate and calcium hydroxide nanoparticles, lead to an increase in the mechanical resistance of aged filter paper. In particular, the hybrid system featuring $CaCO_3$ nanoparticles was as

effective as the system featuring the sole CNC. Moreover, as expected, it neutralized the present acidity and increased the pH around 9. It is worth noting that a pH of 9 is quite high but is to be considered safe if paper is not heavily oxidized. However, the pH to be reached after application can be easily tuned by varying the amount of material applied during the treatment. The slightly less increase in term of mechanical resistance measured on AF-CNC30-OH3 is probably due to the quite high viscosity of the hybrid system, which probably lead to a less homogenous distribution of the material over the paper surface. However, when a confined application is needed, CNC30-OH3 can be used to provide an increase in the mechanical resistance and pH of cellulose-based materials, as clearly shown in Figure 4.7. The visual aspect of paper samples was not significantly altered after treatment. In fact, the ΔE of AF-CNC30, AF-CNC30-OH3 and AF-CNC30-CO3, calculated with respect to AF, is 0.6, 1.1 and 1.6, respectively. These values are lower than the threshold of a color difference perceivable by the naked eye (Witzel et al. 1973).

It can be therefore concluded that the proposed hybrid systems are effective in the strengthening and deacidification of acidic and mechanically-degraded paper, without significant alterations in the original visual aspect of samples, in a fully compatible way with the original material.

4.4 Conclusion

The acid-catalyzed hydrolysis of glycosidic bonds, that is the most important degradation pathway of cellulose-based materials, results in the decrease of cellulose DP and in the loss of the original mechanical properties. In the case of acidic and strongly mechanically-degraded cellulosic works of art, both a deacidification and a reinforcement treatment are required.

In this Chapter, hybrid systems for the concomitant neutralization of acidity and improvement of the mechanical resistance of the original material are presented. The advantages related to the use of a single-step treatment rely in the reduction of cost, treatment time, stress and risk for the artifact. Hybrid systems feature cellulose nanocrystals (CNC) and alkaline nanoparticles, alternatively calcium hydroxide or calcium carbonate, both obtained via a solvothermal process. The innovative synthetic route of $CaCO_3$ nanoparticles, which is based on the usage of an alkyl carbonate for the conversion of the intermediate reaction products into carbonates, yielded small and highly

crystalline nanoparticles already dispersed in an appropriate solvent for applicative purposes.

The mechanical response of CNCs dispersions was studied with rheological measurements. The presence of ethanol in CNC dispersion resulted in the overall increase in the viscosity of the system. This behavior is probably due to a decrease in the Debye length, triggered by the lowest permittivity of ethanol with respect to water that allows for stronger interactions between particles. A similar effect, even more pronounced, was obtained after the addition of calcium hydroxide nanoparticles. Indeed, the Debye length is also a function of the ionic strength and divalent ions screen the superficial charges of cellulose nanocrystals, favoring their interactions and resulting in the formation of a strong gelled system. A less pronounced effect on the screening of the crystal repulsive forces was displayed after the addition of calcium carbonate, which is significantly less soluble than $Ca(OH)_2$. CNC dispersion and hybrid with $CaCO_3$ are thixotropic, which is quite applicative.

SAXS measurements confirmed the increase in cellulose interactions after the addition of ethanol and alkaline nanoparticles. In fact, the changes in the aggregation number of CNC clusters follow the same trend displayed by the mechanical response, i.e., bigger clusters were found in the more gelled system.

After characterization, hybrid systems were applied on aged paper. Mechanical tests, pH and colorimetric measurements were used to evaluate their efficacy. Hybrid systems resulted highly effective in the strengthening and deacidification of acidic and mechanically-degraded cellulosic material, without significant alterations in the visual aspect of samples. It can be therefore concluded that these systems may represent a useful tool, fully compatible with the original material, to help the preservation of degraded cellulose-based artworks.

Chapter 5 Strengthening and deacidification of paper with hybrids of alkaline nanoparticles and cellulose nanocrystals in ethanol

Even if water is commonly used in conservation practice, it can solubilize original compounds, such as sizing agents, writing fluids, inks or dyes. In addition to that, it can swell cellulose fibers, leading to a decrease in the mechanical properties and changes in the paper sheet texture. Therefore, the use of water-based treatments for cellulose-based materials, is usually discouraged. Usually, the addition to water of solvent having a lower polarity, such as alcohols, reduces the possible detrimental effect of water. Indeed, as discussed in Chapter 4, we managed to obtain a good consolidating action using cellulose nanocrystals dispersed in a water/ethanol blend. Nevertheless, the use of such mixture may not be compatible with original materials that are sensitive even to less polar blends. Therefore, we have devoted research efforts to the modification of cellulose nanocrystals with the aim of increasing their dispersibility in pure ethanol, which offer good wetting properties without altering cellulose fibers. In the following paragraphs, different preparation procedures for the hydrophobization of cellulose nanocrystals are presented, together with the characterization of the synthetic products. The preparation and characterization of hybrid systems featuring alkaline nanoparticles for the concomitant deacidification and strengthening of cellulose-based materials are also reported. The final section will be devoted to the applicative tests on artificially and naturally aged paper.

5.1 Alkaline nanoparticles for deacidification

As already discussed in Chapter 4, calcium hydroxide and calcium carbonate nanoparticles were selected to be used for the preparation of hybrid

systems for the concomitant deacidification and strengthening of cellulose-based materials. Both nanoparticles dispersions were prepared using a solvothermal process, starting from ethanol and calcium metal. In particular, as describe in section 4.1, calcium carbonate nanoparticles were obtained as follows: 10 g of granular calcium and 500 mL of ethanol were placed inside a high-pressure reactor (Parr-instruments). Before starting the reaction, vacuum/nitrogen cycles were performed to ensure an oxygen-free atmosphere inside the sealed reaction chamber. During the first step of the reaction, calcium alkoxide is obtained. To hydrolyze the alkoxide to calcium carbonate, 35 mL of water and 35 mL of diethyl carbonate was added inside the reaction chamber by means of steel pipette in a nitrogen atmosphere. The addition was carried out at 70 °C and the system was stirred for 60 min.

The physico-chemical characterization of calcium hydroxide and calcium carbonate nanoparticles showed that the solvothermal reaction yields small and highly crystalline nanoparticles. These are desired features for systems to be used in the conservation of cellulose-based artworks. In addition to that, these nanoparticles are already dispersed in the appropriate solvent, and the system can thus be directly applied for conservation purposes without any further refinement.

5.2 Grafted cellulose nanocrystals

In Chapter 4, it was shown that CNC in water/ethanol blends can provide a good strengthening effect on cellulose-based materials. However, the highest amount of ethanol that can be added to the system without triggering precipitation is about 50 wt%. This is probably due to the high surface area and hydrophilic nature of CNC. Therefore, to allow the dispersion of CNC in less polar than water solvents, hydrophobization must be carried out. It is worth noting that different strategies have been proposed over the years for the surface modification of cellulose nanocrystals. In the following section, a brief introduction about this subject is given.

The strategies can be classified into physical and chemical methods. The use of surfactants to stabilize cellulose nanocrystals dispersions is the main physical method (Kim et al. 2009; Padalkar et al. 2010; Salajková et al. 2012). Chemical method are based on the substitution of some of the hydroxyl groups in

cellulose so to obtain products that can interact with less polar materials (Galina et al. 2011; Uschanov et al. 2011; Shang et al. 2013).

Among diverse chemical modifications, the esterification represents one of the most interesting procedure. It was first adopted to synthesize cellulose derivatives in 1998 (Klemm et al. 1998). Thereafter, several procedures have been tested. Both inorganic and organic acid can be grafted on cellulose. The grafted inorganic acids are usually short chain acids, such as nitric, sulfuric and phosphoric acid (Heinze et al. 2006). Organic acids, such as carboxylic acids, act as acylating agents, and the reaction requires the presence of strong-acids, anhydride, acyl chloride, or Lewis acid (Heinze et al. 2006). Carboxylic acid anhydrides or acyl chlorides are mostly used in the traditional acylation of cellulose. Over the past years, activators for the in-situ conversion of cellulose with more complex carboxylic acids have been developed (Heinze et al. 2006), and these include p-toluenesulfonyl chloride (TosCl) (Heinze and Liebert 2001), N,N′-dicyclohexylcarbodiimide in combination with 4-pyrrolidinopyridine or 4-dimethylaminopyridine (Fujisawa et al. 2011), 4-(4,6-dimethoxy-1,3,5-triazin-2-yl)-4-methyl-morpholinium chloride (DMT-MM) (Merima Mehmedovic Hasani 2007) and N,N′-carbonyldiimidazole (CDI) (Boufi et al. 2008).

For our study, the main challenge is to conduct esterification in such a way that the modified CNC can disperse well in ethanol, and, at the same time, can strengthen mechanically-degraded cellulosic artworks. In the following sections, three CNCs modification strategies will be presented and discussed.

5.2.1 Acetylation of cellulose nanocrystals with acetic anhydride and pyridine

5.2.1.1 Materials

Acetic anhydride (99.5%, Fluka) and anhydrous pyridine (99.8%, sigma-Aldrich) were used for the surface modification of cellulose nanocrystals produced by CelluForce (Canada). All the reagents were used as received without further purification. Highly pure water (having a resistivity of 18 MΩ cm) produced by a Millipore Milli-Q UV system and ethanol (absolute, Fluka) were used during purification and dilution of acetylated CNC.

5.2.1.2 Acetylated CNC synthesis

Acetylated CNC synthesis was based on a pyridine catalyzed method (Lin et al. 2011). When required, reaction operations were carried out under inert atmosphere, according to the standard Schlenk technique, employing dried and purified nitrogen.

At first, a cellulose nanocrystals dispersion was prepared: a mixture of CNC (0.50 g) and 10 mL of anhydrous pyridine was magnetically stirred for 15 min, until an almost completely transparent dispersion was obtained. Then, 5ml of acetic anhydride was added dropwise to the prepared CNC dispersion. The reaction temperature was then raised up to 80 °C. Different reaction times were tested, i.e., 5 h as reported in the literature (Lin et al. 2011) and 10h. After the selected amount of time, the mixture was allowed to cool down to room temperature and the product was isolated by precipitation in 0.5 L of water. The reaction product was then recovered by centrifugation and washed 4 times with water (around 100 mL in total). The washed acetylated cellulose nanocrystals, collected by centrifugation and labelled as ACNC, were oven-dried under vacuum at 60 °C for 12 h.

5.2.1.3 Characterizations of acetylated CNC

ATR-FTIR analysis and dispersion

After acetylation, ACNC was characterized by ATR-FTIR. Even if different reaction times were performed, the FTIR spectra were very similar. In Figure 5.1, the ATR-FTIR spectra of ACNC (a), CNC (b), acetic anhydride (c) and pyridine (d) are shown. The spectrum of ACNC shows a clear evidence that esterification reactions occurred. Indeed, a new peak in the carbonyl area around 1752 cm^{-1} is visible and it was associated to the formation of the ester group. As expected, the carbonyl C–O stretching in ACNC is located at 1246 cm^{-1}, shifted from the signal in acetic anhydride (1120 cm^{-1}). Finally, no signals due to pyridine can be found in the ACNC spectrum. These results indicated successful acetylation of ACNC and that no reactants and side compounds were present in the final product.

The dried ACNC was dispersed in ethanol as concentration of 10 g/L by stirring for 4 hours at 800 rpm and then sonicated for 5 minutes with a Branson S-450 (450W) equipped with a micro-tip, with an output power of 20%. Even if

the ATR-FTIR spectra showed that the acetylation reaction was successful, ACNC precipitated within 30 min, as is shown in figure 5.1-B. On the basis of these evidence, it was concluded that the tested preparation was not able to modify the surface of the nanocrystals so to stabilize their dispersion in ethanol.

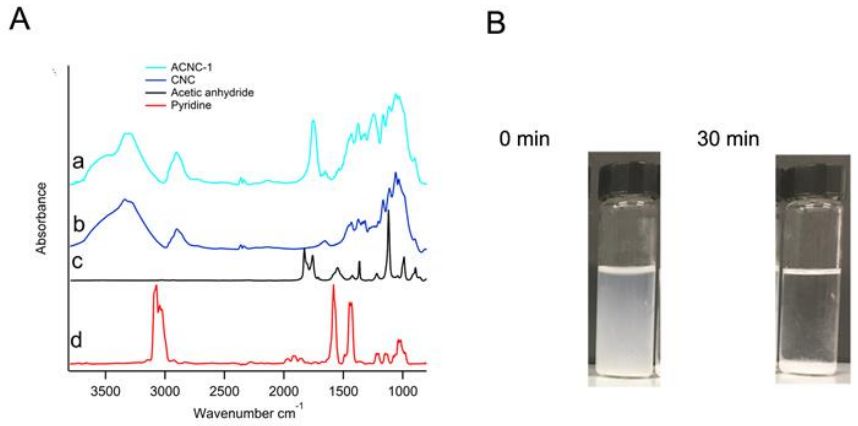

Figure 5.1 A: ATR-FTIR spectra of ACNC (a), CNC (b), acetic anhydride (c) and pyridine (d); B: dispersion of ACNC in ethanol (10g/L), right after preparation and after 30 minutes.

5.2.2 Acetylation of cellulose nanocrystals with acetic anhydride and iodine

5.2.2.1 Materials

Acetic anhydride (99.5%, Fluka) and iodine (reagent grade, sigma-Aldrich) were used for the surface modification of cellulose nanocrystals (CNC) produced by CelluForce (Canada). All the reagents were used as received without further purification. Acetone (absolute, Carlo Erba) and ethanol (absolute, Fluka) were used during purification and dilution of acetylated CNC.

5.2.2.2 Acetylated CNC synthesis

Acetylated CNC synthesis was based on an iodine-catalyzed method (Eldho Abraham et al. 2016). The method is advantageous over the alternative approaches, because, in its procedure, the solvent acts also as a reactant.

When required, reaction operations were carried out under inert atmosphere, according to the standard Schlenk technique, employing dried and purified nitrogen. At first, a mixture of CNC (0.50 g) and 25 mL of Ac_2O was magnetically stirred at 800 rpm and heated to a temperature of 100−105 °C for 1 h. Then, the catalyst (0.025g I_2) was added. The reaction chamber was maintained at this temperature for different reaction times, i.e., 25 minutes, as reported in the literature, (Eldho Abraham et al. 2016), 50, 75 and 100 minutes. After the selected amount of time, the functionalization reaction was terminated by adding acetone to the brown-colored reactant. The reaction product was then recovered by centrifugation and washed 4 times with ethanol (around 100 mL in total) to remove traces of iodine and unreacted Ac_2O. The washed acetylated cellulose nanocrystals, collected by centrifugation and labelled as ACNC, were oven-dried under vacuum at 60 °C for 12 h.

5.2.2.3 Characterizations of acetylated CNC

ATR-FTIR analysis and dispersion

After acetylation, ACNC was characterized by ATR-FTIR. Even if different reaction times were tested, similar ATR-FTIR spectra were obtained. One of the ATR-FTIR spectra of ACNC (a) is reported in figure 5.2, together with CNC (b), and acetic anhydride (c). The spectrum of ACNC shows that the acetylation reaction occurred evidently. Indeed, after the reaction, a peak appeared at 1755 cm^{-1}, which is due to the presence of an ester group. Moreover, in ACNC, the carbonyl C–O stretching can be found at 1240 cm^{-1}, while is located at 1120cm^{-1} in the acetic anhydride. These results revealed that CNC was acetylated successful and no remaining reactants were left.

The dried ACNC was dispersed in ethanol as concentration of 10 g/L by stirring for 4 hours at 800 rpm and then sonicated for 5 minutes with a Branson S-450 (450W) equipped with a micro-tip, with an output power of 20%. Even if the ATR-FTIR spectra showed that the acetylation reaction was successful, ACNC precipitated within 30 min, as is shown in figure 5.2-B. On the basis of these evidences, it was concluded that the tested preparation was not able to modify the surface of the nanocrystals so to stabilize their dispersion in ethanol.

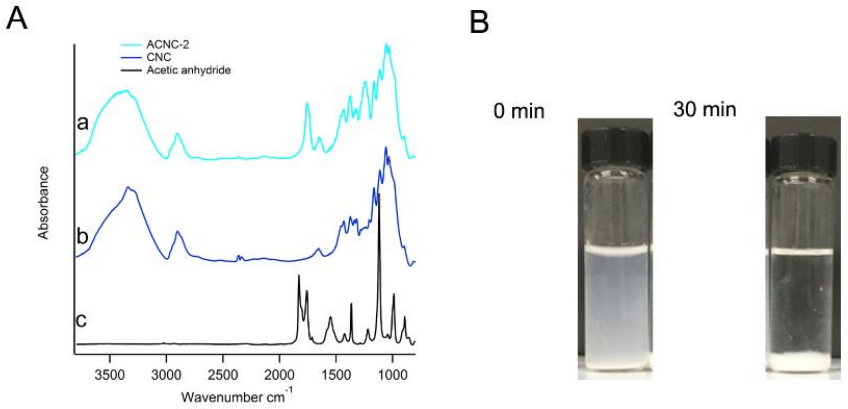

Figure 5.2. A: ATR-FTIR spectra of ACNC (a), CNC (b) and acetic anhydride (c); B: dispersion of ACNC in ethanol (10g/L), right after preparation and after 30 minutes.

5.2.3 Esterification of cellulose nanocrystals with oleic acid

As shown in the previous sections, two different acetylation procedures based on the use of acetic anhydride were tested; unfortunately, the reaction products cannot be stably dispersed in ethanol. Therefore, oleic acid, which is a carboxylic acid having a long alkyl chain, was selected as a grafting agent for the hydrophobization of cellulose nanocrystals, with the aim of obtaining a modified product that can be stably dispersed in short-chain alcohols.

5.2.3.1 Materials

Dimethyl sulfoxide (DMSO, anhydrous 99.9%), 1'1-carbonyldiimidazole (CDI, reagent grade) and oleic acid (90%) were purchased from Sigma-Aldrich. These reagents were used for the surface modification of cellulose nanocrystals produced by CelluForce (Canada). Sulfuric acid (96 %, Carlo Erba) was used for the acidification of paper. All reagents were used as received without further purification. Alkaline nanoparticles, namely $CaCO_3$ and $Ca(OH)_2$ were synthesized using a solvothermal reaction described in Chapter 4. Highly pure water (having a resistivity of 18 MΩ cm) produced by a Millipore Milli-Q UV system and ethanol (absolute, Fluka) were used during purification and dilution of grafted CNC.

5.2.3.2 Grafted CNC synthesis

Grafted CNC (GC) synthesis was based on a CDI-mediated method developed by Heinze and Peng (Heinze 2004; Peng et al. 2016). When required, reaction operations were carried out under inert atmosphere, according to the standard Schlenk technique, employing dried and purified nitrogen. The reaction was carried out in the mild reaction conditions, which avoids the common side reactions including pericyclic reactions, hydrolysis, and oxidation (Heinze et al. 2006). At first, a cellulose nanocrystals dispersion was prepared: a mixture of CNC (0.50 g) and 12 mL of DMSO was magnetically stirred for 30 min and then sonicated for 2 min with a Branson S-450 equipped with a micro-tip and an output power of 20%, until an almost completely transparent dispersion was obtained.

Meanwhile, CDI (0.67 g, 4 mmol) was dissolved in 12 mL of dry DMSO and treated with 1.16 g (4 mmol, 1 eq.) of oleic acid. The obtained solution was stirred for 1 h at 60 °C and then the previously prepared dispersion of CNC in DMSO was added. The reaction temperature was raised up to 80 °C and the system kept under stirring for 24 h. The mixture was then allowed to cool down to room temperature and the particles were then precipitated by addition of water (about 150 mL), recovered by centrifugation and washed twice with ethanol (around 100 mL in total). The product was collected by centrifugation and stored as ethanol suspension (35g/L concentration).

5.2.3.3 Characterizations of grafted CNC

Figure 5.3-A shows the ATR-FTIR spectra of GC (black), CNCs (green), oleic acid (red) and DMSO (blue). The spectra of GC and CNC were normalized using the C–C vibration at 1060 cm^{-1}. The spectrum of GC showed clear evidence that esterification reactions occurred. In the range of 2850 and 2950 cm^{-1}, the two sharp bands at 2921 and 2856 cm^{-1} appeared, while only one broad, less defined, band can be found in the same range in CNC spectrum. These two bands were attributed to the asymmetric and symmetric CH_2 stretch, arising from the aliphatic chain of the oleic acid (Jandura et al. 2000). The C=O stretch band was shifted from 1711 cm^{-1} in the oleic acid, to 1735 cm^{-1}, indicating the formation of an ester group (Freire et al. 2006). It is worth noting that no peaks of DMSO, which is the solvent of the reaction, can be found in the ATR spectrum of GC. These results show that oleic acid was successfully grafted

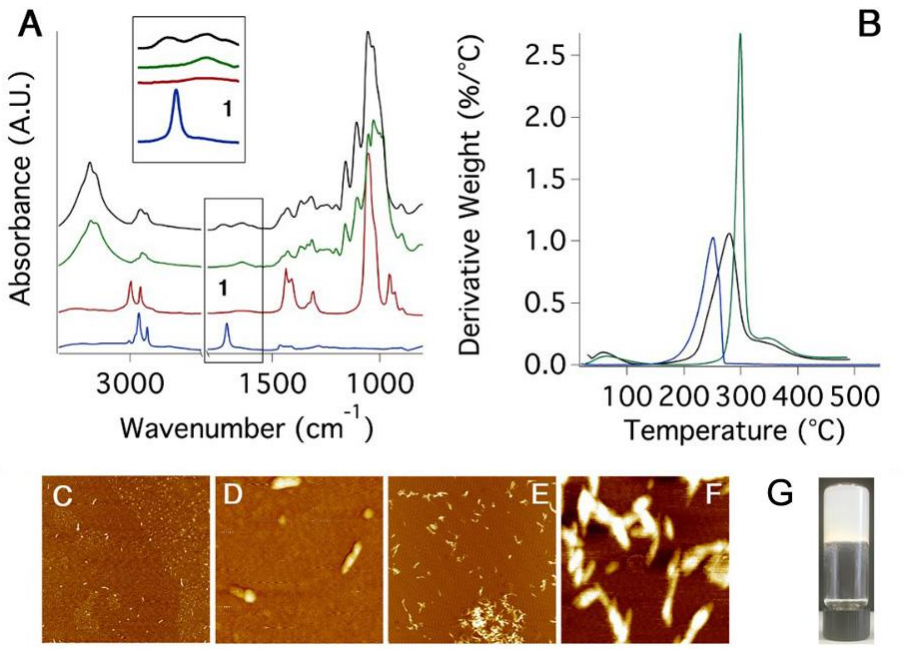

Figure 5.3. (A) ATR-FTIR spectrum of oleic acid (blue), DMSO (red), CNCs (green) and GC (black). (B) DTG curves of oleic acid (blue), CNCs (green) and GC (black). (C-D) AFM pictures of CNCs over a fleshly cleaved mica sheet (10 x 10 μm2 and 1 x 1 μm2, respectively). (E-F) AFM picture of GC over a fleshly cleaved mica sheet (10 x 10 μm2 and 1 x 1 μm2, respectively). (G) concentrated GC, showing a gel-like behavior.

on CNC, and no reactants and side compounds are found in the reaction product.

Thermal analysis of GC, CNC and oleic acid revealed different degradation profiles (Fig.5.3-B). The initial small weight loss of both unmodified CNC and GC in the temperature range 50–100 °C can be ascribed to the evaporation of physically bound moisture. In thermal curve of CNC, the sharp peak corresponding to the degradation of cellulose nanocrystals is located at about 300 °C, similarly to what has been reported by Johar (Johar et al. 2012). On the contrary, the main degradation peak of GC sample is a broad signal located in the 200-400 °C range having a maximum at 280 °C. The lower thermal stability of GC can be ascribed to the surface grafting. In fact, as clearly shown in Figure 5.3-B, oleic acid degrades at about 250 °C and the presence of oleate moieties on the surface of nanocrystals is probably responsible for both the decrease in the pyrolysis temperature and in the broadening of the degradation peak, due to the variable amount of oleic acid-grafted on each nanocellulose crystals.

The effective surface modification of cellulose nanocrystals is also confirmed by the AFM pictures reported in figure 5.3-C/F. In fact, thanks to the increased hydrophobicity induced by the grafting, GC deposit on the fleshly cleaved mica sheet more easily than CNCs, even if the concentration of the dispersions used for the preparation of the samples was the same (see chapter 3.1.3 for further information). It is also worth noting that, despite the aggregation of GC, the size and shape of nanocellulose crystals is not altered by the CDI mediated oleic acid grafting.

As is mentioned in 5.2.3.2, GC was stored as ethanol suspension after purification. After 24 hours, the system displays a gel-like behavior, as shown in figure 5.3-G. Therefore, on the basis of the ATR-FTIR, DTG, AFM and of the behavior shown by the suspension, GC were deemed a suitable starting material to prepare hybrid systems featuring alkaline nanoparticles, for the concomitant strengthening and deacidification of cellulose-based materials. In the following paragraph, the characte5rization of these systems and the results of their application on artificially and naturally aged paper are reported.

Hybrid systems preparation

GC dispersion was prepared by diluting wet GC with ethanol, which was stirred for 4 hours at 800 rpm and then sonicated for 5 minutes with a Branson S-450 (450W) equipped with a micro-tip, with an output power of 20%. GC at different concentrations, i.e., 3.5, 6, 9 and 30 g/L were mixed with alkaline nanoparticles, i.e. calcium hydroxide or calcium carbonate nanoparticles in ethanol. Name and composition of the prepared systems are reported in Table 5.1. For example, in the GC9-OH3 system, the concentration of OCNCs is 9 g/L and the concentration of $Ca(OH)_2$ is 3 g/L.

Characterization of systems at low concentration of GC

Freshly prepared samples were left undisturbed. It was noted that systems with low amount of GC displayed a different behavior depending on the concentration of the ingredients. Indeed, as shown in the phase diagrams reported in figure 5.4, the systems are liquid or gel. For instance, GC dispersions (without alkaline nanoparticles) are liquid at low concentrations (3.5 and 6 g/L), while they behave as gels at higher concentrations (9 g/L). In some cases, the addition of alkaline nanoparticles triggered the liquid−gel transitions. For example, higher concentration of $CaCO_3$ was required to induce gelation in

comparison with $Ca(OH)_2$. It is also worth noting that the gelation of the systems is time-dependent. Indeed, the phase diagrams reported in figure 5.4, were prepared after 7 or 14 days from the preparation of the systems. Even after that amount of time, the less concentrated dispersions cannot gel, even if in the presence of $CaCO_3$ nanoparticles.

Table 5.1 Name and composition of GC dispersions and hybrid systems.

Name		GC g/L	NanoP g/L
GC3.5		3.5	-
GC3.5-CO0.7	GC3.5-OH0.7		0.7
GC3.5-CO2	GC3.5-OH2		2
GC3.5-CO3	GC3.5-OH3		3
GC6		6	-
GC6-CO0.7	GC6-OH0.7		0.7
GC6-CO2	GC6-OH2		2
GC6-CO3	GC6-OH3		3
GC9		9	-
GC9-CO0.7	GC9-OH0.7		0.7
GC9-CO2	GC9-OH2		2
GC9-CO3	GC9-OH3		3
GC30		30	-
GC30-CO0.7	GC30-OH0.7		0.7
GC30-CO3	GC30-OH3		3

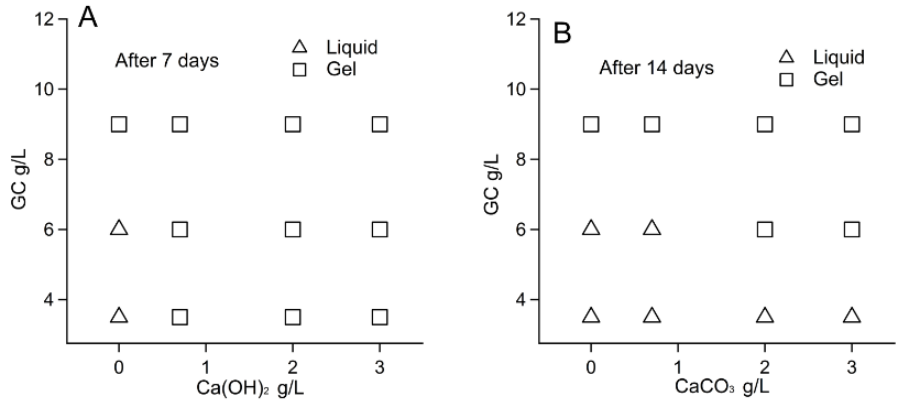

Figure 5.4 Phase diagrams of hybrids featuring $Ca(OH)_2$ (A) and $CaCO_3$ (B). Liquid phase (triangles), gel phase (squares).

Pure GC dispersion at 9 g/L and different hybrids were also characterized by rheological tests. The mechanical response of all the systems was firstly assessed with amplitude sweeps measurements, to determine the linear-viscoelastic (LVE) region. Thereafter, frequency sweep measurements at 0.2% strain were carried out. In a typical frequency sweep test, the frequency of the applied strain is increased, and the mechanical response is recorded in terms of G', the storage modulus, and G", the loss modulus, which are, respectively, a measure of the stored energy, i.e. the elastic response, and of the dissipated energy, i.e. the viscous response at a given frequency of oscillation (Ferry 1980b).

In figure 5.5-A, the frequency sweeps of GC9 and hybrid systems of GC9 and calcium hydroxide nanoparticles at 0.7, 2 and 3 g/L respectively, i.e. GC9-OH0.7, GC9-OH2 and GC9-OH3, are reported. GC9 display a true gel like behavior, with G' higher than G" over the entire investigated range of frequency. The addition of 0.7 g/L calcium hydroxide nanoparticles leads to a strong increase in G' and G", which are about three orders of magnitude higher than in GC9 and are frequency-independent. A similar behavior is shown by GC9-OH2, featuring an higher amount of $Ca(OH)_2$ nanoparticles. The addition of 3g/L calcium hydroxide nanoparticles leads to about four orders of magnitude increase in G' and G" compared with sole GC9. This behavior was explained as follows: during the washing process, water was used with the aim of removing the DMSO from the reaction product. The subsequent washing steps were carried out in ethanol, which has been also used as a dispersing agent. Therefore, the presence of traces of water in the final systems are highly probable. As discussed in Chapter 4, the addition of alkaline nanoparticles to CNC in water/ethanol blends, lead to the gelation of the systems, due to the decrease in the Debye length that favors the interaction between particles. The Debye length, in fact, is a function of the concentration of the ions in solution, i.e., the ionic strength of the dispersing media. The highest the ionic strength, the lowest is the Debye length. In addition to that, as crystals distances are reduced during gelation, divalent ions from the alkaline nanoparticles may complex different crystals, increasing the mechanical strength of the system (Dong et al. 2013).

A different behavior is shown by the hybrid system featuring $CaCO_3$, as reported in figure 5.5-B. Here, the G' and G" values increases due to the 3g/L $CaCO_3$ dispersion are even lower than those induced by the addition of the 0.7g/L $Ca(OH)_2$. This behavior, already shown by the CNC systems discussed in Chapter 4, can be simply explained by the lower solubility of calcium carbonate

nanoparticles with respect to calcium hydroxide, which leads to a less pronounced effect on the screening of the crystal repulsive forces.

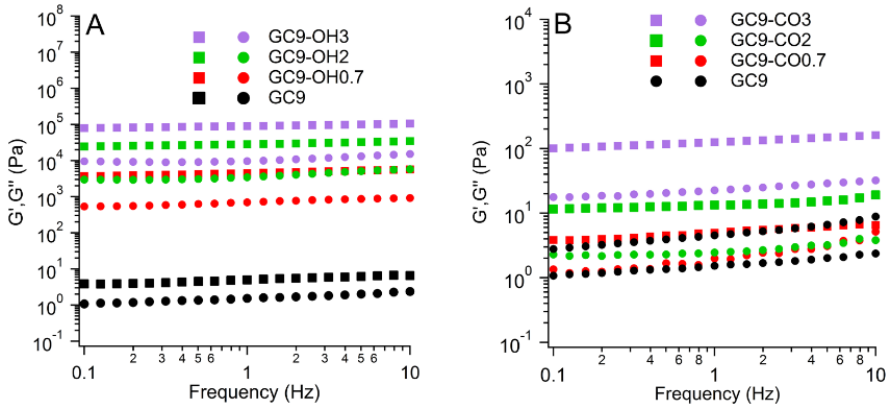

Figure 5.5. Frequency sweep measurements on hybrids featuring $Ca(OH)_2$ (A) and $CaCO_3$ (B), G′ (square), G″ (circle).

Thixotropy is a time-dependent shear thinning property. In other terms, a thixotropic material is a gel or a thick fluid that starts flowing when shaken or stressed. When left still for a fixed amount of time, this material becomes a gel or a thick fluid again (Whelan A 1994). This property is usually associated to systems containing aligned particles or spatial distribution of entanglement density (Barnes 1997). CNC are known to be thixotropic. In order to check if the same behavior was shown also by the hybrid samples, GC9-CO3 and GC9-OH3 were tested with a three interval thixotropy tests (3ITT), performed following the procedure reported in section 3.1.6. As illustrated in figure 5.6, in the first interval, the flow-stress introduced by 0.2% strain at 1Hz was not strong enough to change the microstructure of hybrids. In fact, hybrids systems displayed a gel-like behavior, with G′ higher than G′′. At higher flow-stress, the microstructure was deformed and reached a new equilibrium between inflow stress, Brownian motion and flow-stress. As a result of an increased stress, the hybrids displayed a liquid-like behavior, being G′ smaller than G′′. In the third interval the same regime applied during the first step of the test, the initial configuration was reverted back, i.e., systems displayed a gel-like behavior (Barnes 1997). Finally, it is worth noting that the values of G′ and G″ in the hybrids are consistent with FS results reported in figure 5.5.

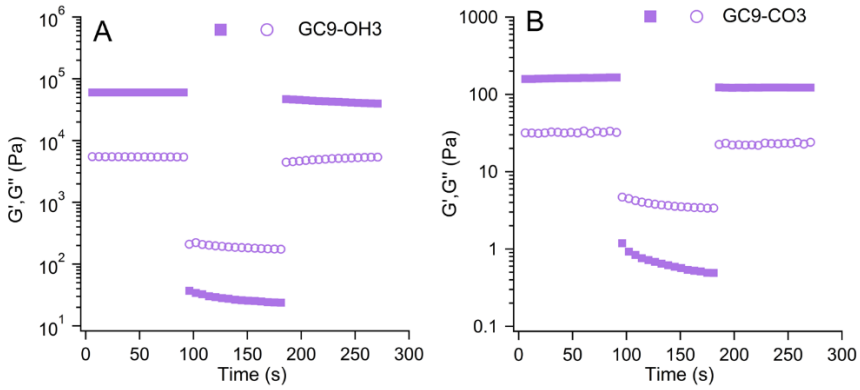

Figure 5.6. Three interval thixotropy tests (3ITT) on GC9-OH3 (A) and GC9-CO3 (B), G′ (square), G″ (circle).

Characterization of systems at 30 g/L of GC

All the systems at 30 g/L of GC displayed a gel-like behavior after 24 hours from the preparation. Therefore, in this case, no phase diagrams were prepared. However, in order to see if the gel-like behavior changes with time, systems were left still for variable amount of time (1, 7 and 14 days) before characterization. The mechanical response of all the systems was firstly assessed with amplitude sweeps measurements, to determine the linear-viscoelastic (LVE) region. Thereafter, frequency sweep measurements at 0.2% strain were carried out. In figure 5.7-A, a comparison between the frequency sweeps of GC dispersions at different concentration, namely 9 g/L and 30 g/L is reported. As expected, in GC30, both G′ and G′′ are more than two orders of magnitude higher than in GC9. This is probably due to the increased electrostatic interactions between particles (Lu et al. 2014), which leads to strong systems at high concentration of GC.

As is discussed in Chapter 4, 3wt% CNC were successfully dispersed in a water/ethanol blend. In figure 5.7-B, the frequency sweep curves of GC30 and CNC30 are reported. Even if the concentration of nanocrystals is almost the same in the two systems, both G′ and G″ of GC30 are about two orders of magnitude higher than CNC30; moreover, the two moduli in GC30 are frequent-independent. This behavior can be explained as follows: the Debye length, which is a measure of how far the electrostatic effect of charged particles persists, depends on the permittivity of the solvent. The lowest the permittivity, the highest is the screening of the electrostatic repulsions between crystals.

Permittivity of ethanol is lower than water (24.5 and 78, respectively), therefore, the Debye length of nanocrystals in ethanol decreases, allowing for stronger interactions between particles. As a result, GC30 behaves as strong gels. The frequency sweeps of hybrids of CNC and GC, having almost the same concentrations of alkaline particles, are displayed in figure 5.7-C and D. The values of both G′ and G″ in GC hybrids are more than 10 times higher than those of hybrids in the ethanol/water blend, confirming the increase in the interaction between cellulose nanocrystals, above described.

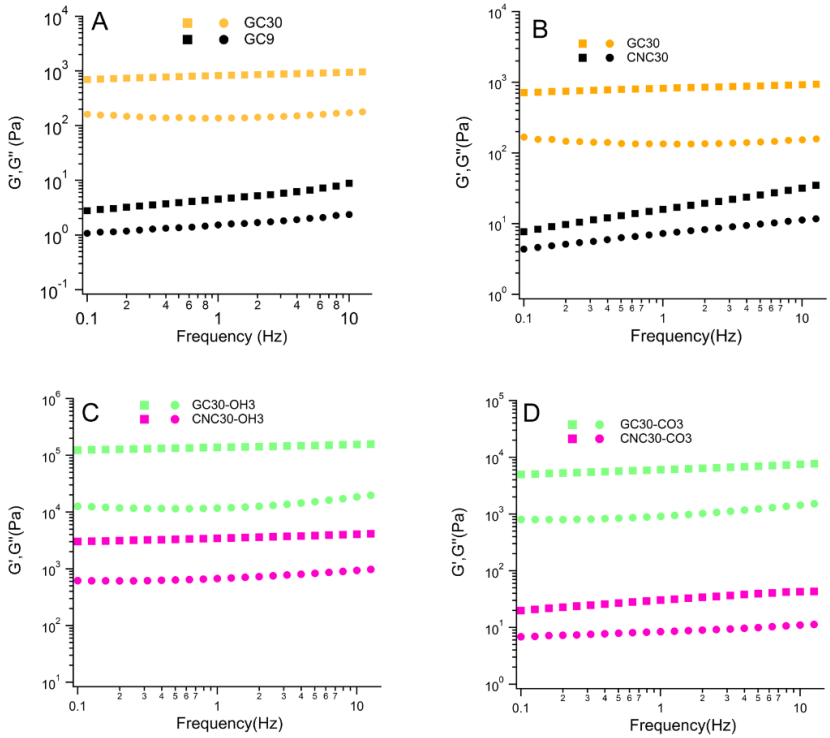

Figure 5.7. Frequency sweep measurements of GC9 and GC30 (A), GC30 and CNC30 (B), GC30-OH3 and CNC30-OH3 (C), GC30-CO3 and CNC30-CO3 (D). G′ (square), G″ (circle).

Rheological measurements were also carried out on GC systems having different concentration of alkaline nanoparticles. These are reported in figure 5.8-A and B. The addition of calcium hydroxide nanoparticles leads to a strong increase in G′ and G′′, which are more than 100 times higher than in GC30. As expected, the increase in alkaline nanoparticles concentration leads to an increase in the gel-like character (higher G′ and G″) of the systems. These results are in accordance with the frequency sweeps reported in figure 5.5, and confirm

that the addition of alkaline nanoparticles induce the gelation of dispersion, as a result of the screening of the repulsive forces generated by surface charges due to the presence of calcium ions. The introduction of calcium carbonate in GC30 leads to a lower change in the mechanical spectrum of the systems. As already stated, this phenomenon can be explained by the lower solubility of calcium carbonate, which leads to a less pronounced effect on the screening of the crystal repulsive forces.

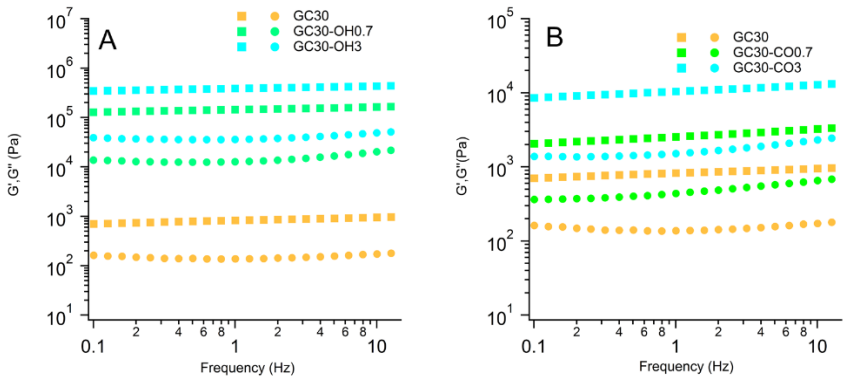

Figure 5.8. Frequency sweep measurements on hybrids featuring 30 g/L GC and $Ca(OH)_2$ (A), $CaCO_3$ (B) at different concentrations. G′ (square), G″ (circle).

Figure 5.9 showed the changes in the mechanical spectrum of systems with GC at 30 g/L as a function of time (1, 7 and 14 days). As shown in figure 5.9-A, after 1 day and 7 days, the G′ and G′′ curves of GC30 are almost superimposed, while both moduli values are doubled after 14 days. A similar behavior is shown by the hybrid systems, as reported in figure 5.9-B and C. It is worth noting that the moduli values of GC30-OH3 decreased after 14 days. This can be explained as follows: at increasing still time, a small amount of the solvent, i.e. ethanol, is probably expelled out from the surface, due to the increasing interactions between particles (Sabet et al. 2013). The expelled liquid, which is not retained in the systems, is probably located on the surface of the sample, and this may have induced a slight slippering of the rheometer head during the rheological tests.

For all the systems, the tan δ, which is the averaged G″/G′ over the frequency range investigated, was calculated; the obtained values are reported in table 5.2. Tan δ has been used to differentiate gel-like systems in two categories, namely, “weak” and “strong”. Systems having a tan δ>0.1 are

considered weak gels. On the contrary, a tan $\delta<0.1$ is typical of strong gels (Ross-Murphy 1995; Chronakis et al. 1996; Ikeda and Nishinari 2001). Interestingly, after 1 day from the preparation, all the dispersions are weak gels, expect for GC30-OH3. Even more interestingly, all the systems featuring $Ca(OH)_2$ nanoparticles, even at lower concentration, became strong gels at increasing still time.

After 7 days from the preparation, three-interval thixotropy tests (3ITT), which can be used to evaluate the deformation and recovery of the structure (Mewis and Wagner 2009; Said et al. 2015; Yilmaz and Vatansever 2016) were perform on GC30, GC30-CO3 and GC30-OH3 (see figure 10). As the name suggests, the test is composed of three intervals: a low-strain interval, to be used as a reference of an undisturbed material; a high-strain interval, to break the internal structure; a final stage at low-strain conditions to favor the regeneration of the structure. In the first interval, all the systems maintained their original structure under a 0.2% strain. During the second step of the measurement, an 80% strain was applied, leading to a significant change in the systems that, consequently, behave as liquids ($G''>G'$). In the third interval, the same conditions of the first interval were applied resulting in an almost complete recovery of the initial gel-like character (Barnes 1997). For the applicative standpoint, as already discussed in Chapter 4, this behavior represents an interesting feature: in fact, these systems can be applied at the liquid state, after being energetically shaken. Or, when a more confined application is required, systems can be applied with a gentle action, in gel-like state, as the one shown in figure 5.10-D/F. It is worth noting that, for the present study, all the systems were applied by brush to allow for a proper comparison of their effectiveness.

SAXS measurements were performed, in order to investigate the grafted cellulose nanocrystals at 30 g/L and alkaline nanoparticles interactions. Non-modified CNCs have been the subject of several characterization studies, where scattering techniques such as quasi-elastic light scattering (QELS), small-angle neutron scattering (SANS) and SAXS measurements were performed, in order to gather information about size, shape and interparticle interactions of cellulose nanocrystals dispersions (Bonini et al. 2002; Su et al. 2014, 2015; Cherhal et al. 2015; Schütz et al. 2015; Uhlig et al. 2016; Mao et al. 2017). In particular, being the CNC elongated fibrillar particles, they are usually modeled as cylinders, ribbons, or parallelepipeds in the analysis of scattering data. Generally, ribbons and parallelepipeds provide the most reliable fitting

results (Su et al. 2014). Similarly, OCNC hybrids were also fitted by parallelepiped model.

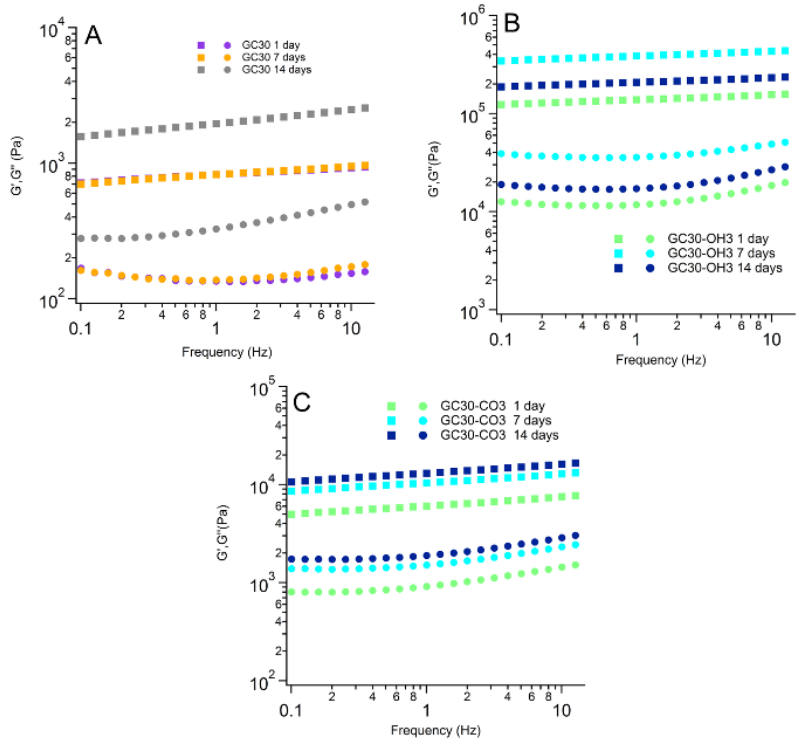

Figure 5.9. Frequency sweep measurements on GC30 (A), GC30-OH3 (B), GC30-CO3 (C) after preparation 1, 7 and 14 days. G′ (square), G″ (circle).

Table 5.2. Tan δ (G′/G′) values of GC systems with or without alkaline nanoparticles.

System	Tan δ 1 day	Tan δ 7 days	Tan δ 14 days
GC30	0.17 ± 0.01	0.19 ± 0.04	0.18 ± 0.01
GC30-CO0.7	0.20 ± 0.04	0.18 ± 0.01	0.16 ± 0.01
GC30-CO3	0.17 ± 0.02	0.16 ± 0.01	0.16 ± 0.01
GC30-OH0.7	0.16 ± 0.01	0.09 ± 0.01	0.10 ± 0.01
GC30-OH3	0.10 ± 0.01	0.10 ± 0.01	0.10 ± 0.01

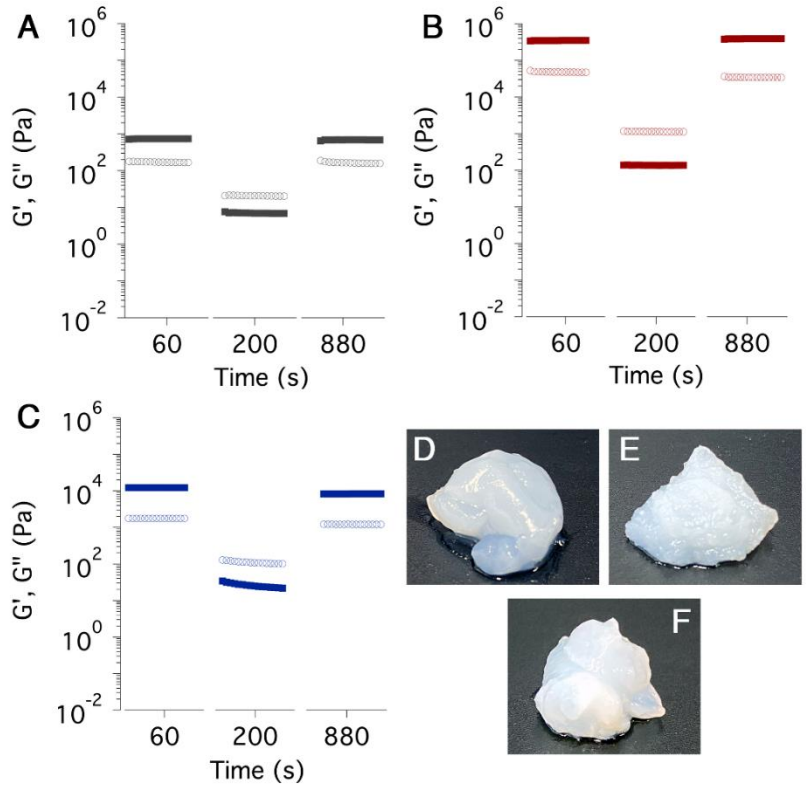

Figure 5.10. Top row (right and left panels) and bottom row (left panel): three interval thixotropy tests (3ITT) of GC30 (A), GC30-OH3 (B) and GC30-CO3 (C) - G′(■), G″(○). Bottom row, right panel: visual aspect of the samples: GC30 (D), GC30-OH3 (E) and GC30-CO3 (F).

Figure 5.11 shows the scattering curves, together with their best fitting, of the three samples analyzed, i.e., GC30, GC30-CO3 and GC30-OH3, while in Table 5.3 fitting results are reported.

By looking at Figure 5.11, it can be noticed that the three scattering curves are well fitted by our model. It is worth noting, then, that the curves of samples GC30-CO3 and GC30-OH3 are almost perfectly superimposed and at a slightly higher intensity with respect to the one of grafted CNC alone. This can be ascribed to an increase in the volume fraction of the systems due to the addition of nanoparticles. The grafted CNC were found to have the major length, *C*, comprised between 130 and 140 nm, which is in good agreement with the information available on the commercial products, even if it is worth saying that this dimension is actually at the limit of the range that could be investigated

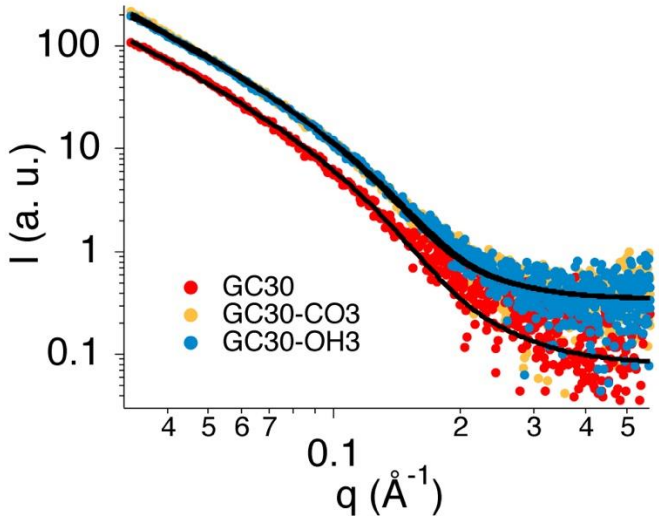

Figure 5.11. SAXS curves of the three samples: GC30, red circles; GC30-CO3, yellow circles; GC30-OH3, blue circles. Fitting lines are represented as continuous black curves.

Table 5.3. Fitting parameters for the three samples analyzed.

Fitting parameter	**GC30**	**GC30-OH3**	**GC30-CO3**
A (Å)	23.7 ± 0.1	22.5 ± 0.1	23.9 ± 0.1
B (Å)	386.25 ± 6.7	423.9 ± 5.7	467.0 ± 6.3
C (nm)	136 ± 5	140 ± 4	138 ± 4
SLD_{CNC} (10^{-6} Å^{-2})	15.1	15.1	15.1
$SLD_{solvent}$ (10^{-6} Å^{-2})	7.6	7.6[a]	7.6[a]
PI_A	0.40 ± 0.05	0.40 ± 0.05	0.40 ± 0.05
N_{agg} (*B*/*A*)	16.3	18.9	19.5

[a]The SLD of ethanol was used in this case, as $Ca(OH)_2$ and $CaCO_3$ nanoparticles were not present, being their volume at this concentration practically negligible.

with SAXS. The minor length, *A*, was found to be 2.3 – 2.4 nm (Uhlig et al. 2016; Mao et al. 2017). Also, this value is in agreement with previously published data on similar systems. Similar systems dispersed in water or in water/ethanol 1:1 mixture and previously characterized gave a slightly higher value for the length of A, as reported in Chapter 4; however this difference can be explained by the different solvent used in this case. In fact, it is likely that CNC in neat ethanol may tend to shrink a little (of a 35% of their size in water), in view of their lesser affinity with this solvent with respect to water. However, it is worth saying that a polydispersity index (PI) of about 0.4 was used to fit the length of *A*. Thus, even if this value is perfectly in accordance with previous works reported in the literature (Cherhal et al. 2015), the size distribution of the minor length of grafted CNC in ethanol is quite broad. Interestingly, it is slightly broader than the one of non-grafted CNC in water or water/ethanol mixtures, indicating that the grafting reactions might have affect the size distribution of nanocrystals. Finally, and as previously reported by some authors (Uhlig et al. 2016), the middle dimension of the parallelepiped, *B*, is highly longer than *A*, and it is not the same for the three samples analyzed. We observed something similar in Chapter 4 on CNC dispersions and we interpreted that result as if we were actually observing a dispersion of nanocrystals clusters, rather than single particles. Therefore, by hypothesizing that a single particle has a square section (*A* x *A*), in a similar way to what done by Uhlig et al. (Uhlig et al. 2016), we assumed that the interactions between grafted-CNC led to the formation of plate-like ribbons having a rectangular total cross section given by *A* x *B*. Therefore, the *B*/*A* ratio can be considered the aggregation number of CNC clusters. The last row of Table 5.3 reports the average aggregation number of grafted-CNC clusters. The trend is clear; the addition of nanoparticles increases the grafted nanocrystals' aggregation number from about 16 to about 19. Interestingly, the average aggregation number of GC30 is sensibly higher than that of CNC in water or water/ethanol 1:1 at the same concentration, which is reported in Chapter 4 and it was found to be 9-10. This big difference can be due to the combined effect of replacing all the water with ethanol and of the grafting. It is likely that grafted nanocrystals tend to create stronger interparticles interactions, due to the presence of grafting residues, which are boosted by the non-aqueous environment. Indeed, it is reasonable that the CNC in ethanol tend to create bigger aggregates aiming to minimize the area of the surface exposed towards the alcohol. The addition of alkaline nanoparticles further increases the aggregation number.

5.3 Application

After characterization, applicative tests of GC systems were performed. As shown in Chapter 4, CNC system at 3 wt% display excellent strengthening and deacidification effects. Considering the increased gel character of systems featuring 9 g/L of GC with respect to CNC at 3 wt%, we decided to firstly test these materials, on artificially and naturally aged paper. As it will be shown later, systems at 30 g/L were also applied on the same cellulosic supports. The effectiveness of these innovative materials in the strengthening and deacidification was assessed with tensile tests and pH measurements, following the procedures reported in Chapter 3.

5.3.1 Application of GC9 system

Filter paper (paper grammage: 75g/m^2), made of cellulose fibers without any sizing and fillers, was selected as standard paper to test the efficacy of the hybrid systems. Paper sheets were immersed in a sulfuric acid solution (pH = 2.5) for 30 s and then aged at high temperature and relative humidity (80 °C and 75% RH) for 10 days or 20 days, in order to have samples in need for both a deacidification and a strengthening treatment. These samples are labelled as AF, i.e., aged filter paper. Unaged filter paper was characterized and used as a reference system. This system is labelled as UF.

Tests were also carried out on an acidic paper (PT1), which is composed of 70% hardwood bleached pulp, 30% softwood bleached pulp and 20% pulp-filling agent kaolin OT80. Acidity is due to the presence of an acidic resinous sizing (Sacocell 309 aluminum sulphate). This paper was produced about 15 years ago within the EU Papertreat project. Since this paper is already acidic, it was directly aged at high temperature and relative humidity (80 °C and 75% RH) for 20 days. The aged samples are labelled as AP, i.e., aged PT1. Unaged PT1 was characterized and used as a reference system. This system is labelled as UP.

Table 5.4. Name and composition of paper samples treated with GC9 system.

Name	GC g/L	NanoP type	NanoP g/L	Weight increment
UF1/UP1	-	-	-	-
AF1/AP1/B1	-	-	-	-
AF1-GC9-CO3-1	9	$CaCO_3$	3	4 wt%
AF1-GC9-CO3-2	9	$CaCO_3$	3	9 wt%
AP1-GC9	9	-	-	2 wt%
B1-E	-	-	-	-
B1-GC9-1	9	-	-	5 wt%
B1-GC9-2	9	-	-	9 wt%

As stated in Chapter 1, due to the growing demand of paper, wood was started to be used as raw material for paper-making in the second half of the 19th century. The extraction of cellulose fibers from wood, i.e., which mainly consists in the removal of lignin, is carried out with strong mechanical or chemical treatments, which usually result in a partial degradation of the fibers. Even after that, lignin is not completely removed, and may trigger further degradation because it generates radicals and acid groups upon natural aging. In other terms, paper sheets produced in the last two centuries usually display lower resistance to aging with respect to older paper. Here we selected a book from the 1970s, which has a pH of 5.3, therefore is in need of deacidification treatment. Due to the marked discoloring of the paper and its low pH, we hypothesized that this object was in need also of a strengthening treatment. The untreated book samples, labelled as B, were characterized and used as a reference system. Book samples treated with ethanol are labelled as B-E.

All the name and composition of paper samples treated with GC9 system are indicated in Table 5.4.

5.3.1.1 Application on standard filter paper

The pH of filter paper decreased from 6.9 to 5.4 as a result of ten days of artificial aging. The UTS, i.e., the tensile strength at break, decreased from 2.6 to 2.2, as shown in figure 5.12.

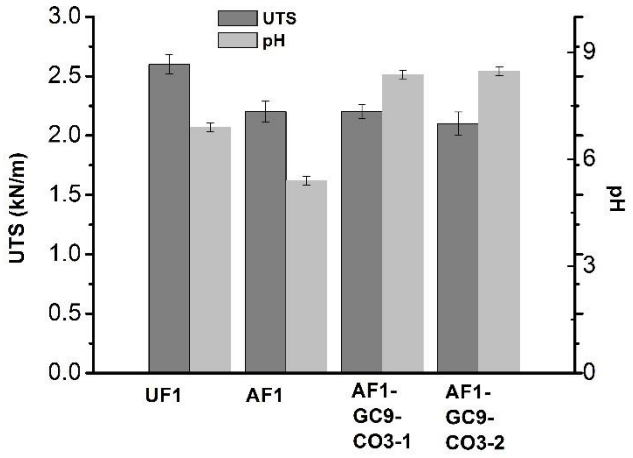

Figure 5.12. Effects of GC9 system on standard paper FP.

The application of the hybrid system featuring calcium carbonate nanoparticles on aged filter paper (4% weight increment) did not increased the UTS, even if, as expected, it resulted in a stabilization of the pH around the optimal value of 8.5. The UTS of filter paper treated with the same material but in higher amount (9% weight increment) is even lower. This was explained as follows: even if to a different extent than water, ethanol can slightly swell cellulose fibers, especially if it is applied on non-sized paper, i.e., filter paper. In this case, the tested concentration of GC was probably too low to improve the mechanical strength of the paper. At the same time, ethanol, i.e., the dispersing medium provoked a decrease in the tensile resistance. It was thus decided to test the same material at the same concentration on sized paper, such as PT1 and the book from the 1970s.

5.3.1.2 Application on real paper

The UTS of aged PT1 is 8% lower than that of the unaged samples (see figure 5.13). On this set of samples, the application of GC9 increased the weight only by 2%. This is probably due to the low porosity of the paper, which hampers the penetration of the treatment. Higher amount of treatment had no effect or a slight decrease in the UTS.

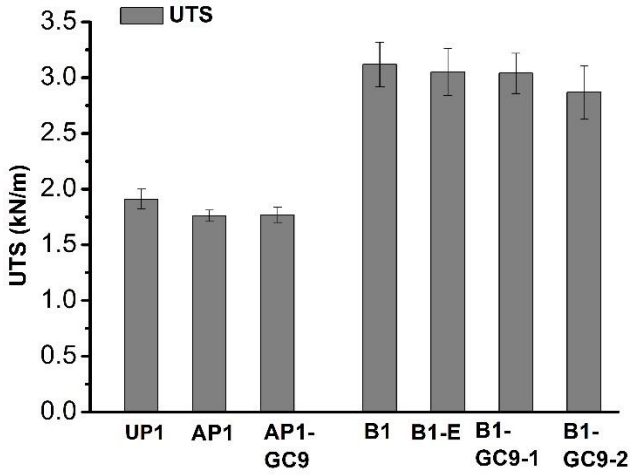

Figure 5.13. Effects of GC9 system on real samples, i.e., PT1 and Book from 1970s.

Paper sheets from the 1970s book were treated with ethanol and GC9 in different amounts. As is shown in figure 5.13, only slight changes in the UTS were induced by the application of the sole dispersing medium. This corroborates our hypothesis on the role of the sizing on the sensitiveness of paper to the solvent, discussed in the previous section. Nevertheless, samples treated with GC9 (5% weight increment) display the same UTS of B1-E. The increase of the applied amount of the treatment (9% weight increment) resulted in a slight decrease in the UTS. It is worth noting that all these data are close to the experimental errors. It was thus concluded that the concentration of nanocrystals was not enough to compensate the effect of the solvent on cellulose fibers. Therefore, further testing was conducted using systems at 30 g/L of GC.

Table 5.5. Name and composition of paper samples treated with GC30 systems.

Name	GC g/L	NanoP type	NanoP g/L	Weight increment
UF2/ UF3/	-	-	-	-
UP2	-	-	-	-
AF2/AF3	-	-	-	-
AP2	-	-	-	-
B2/B3/B4	-	-	-	-
AF2-GC30	30	-	-	10 wt%
AF2-GC30-CO3	30	$CaCO_3$	3	12 wt%
AF2-GC30-OH3	30	$Ca(OH)_2$	3	12 wt%
AF3-GC30	30	-	-	10 wt%
AF3-GC30-CO3	30	$CaCO_3$	3	10 wt%
AF3-GC30-OH3	30	$Ca(OH)_2$	3	12 wt%
AP2-GC30	30	-	-	4 wt%
B2-GC30	30	-	-	5 wt%
B3-GC30-CO3	30	$CaCO_3$	3	8 wt%
B4-GC30	30	-	-	7 wt%
B4-GC30-CO3	30	$CaCO_3$	3	9 wt%

5.3.2 Application of GC30 system

All the name and composition of paper samples treated with GC30 systems are reported in table 5.5.

5.3.2.1 Application on standard filter paper

As a result of the aging, the pH of filter paper decreased from 7 to 5.4, while the UTS of about 10% (see figure 5.14). The application of GC30 on AF2 (sample AF2-GC30) increased the UTS from 2.4 to 2.6 kN/m, which is a positive, still slight change, if compared to the experimental error.

Both hybrids, containing calcium carbonate or calcium hydroxide nanoparticles, lead to slight increase in the mechanical resistance of aged filter paper. Moreover, as expected, hybrids neutralized the acidity of aged samples and increased the pH to 8.5 and 9.5, respectively. It is worth noting that pH at

9.5 is quite high, but yet still acceptable as long as paper is not heavily oxidized. However, it is worth noting that the pH of the treated samples can be easily tuned during application. Here, to ease the comparison between different GC-based systems in terms of tensile strength, we decided to apply the same amount of dispersion on each series of samples.

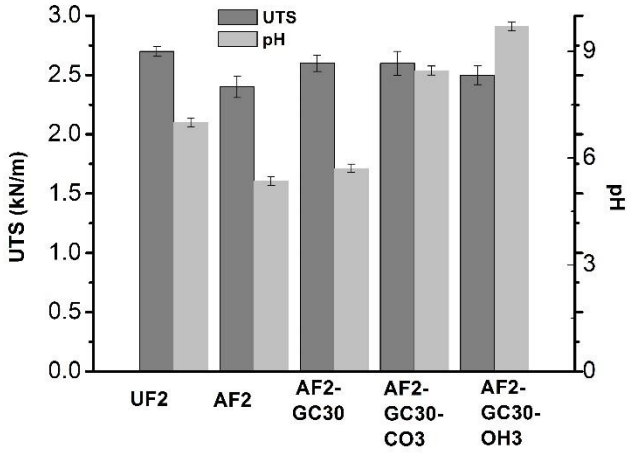

Figure 5.14. Effects of GC30 system on standard paper FP aged with 10 days.

On the basis of these experimental results, it was thus decided to prolong the aging of filter paper to 20 days, so to have a more degraded starting material. As expected, the UTS decrement induced by the prolonged aging was of about 17%, as shown in figure 5.15.

Interestingly, the application of GC30 to the aged filter paper resulted in an increase of about 15% in the UTS. In other terms, grafted cellulose nanocrystals almost revert back the tensile strength of unaged filter paper. As expected, the pH values of AF3-GC30 and AP3 are similar, as is shown in figure 5.15, and clearly show the importance of using hybrid systems on acidic and mechanically degraded paper samples.

Both hybrids, featuring calcium carbonate or calcium hydroxide nanoparticles, lead to an increase in the mechanical resistance of filter paper, as shown in figure 5.15. However, it is worth noting that hybrid systems lead to slightly less increase in term of mechanical resistance if compared to GC30. This is probably due to the relatively higher viscosity of hybrids, which probably lead to a less homogenous distribution of the material over the paper surface. In terms of the deacidification effects, both hybrids neutralized the present acidity and increased the pH to a safe value, i.e., 8.5.

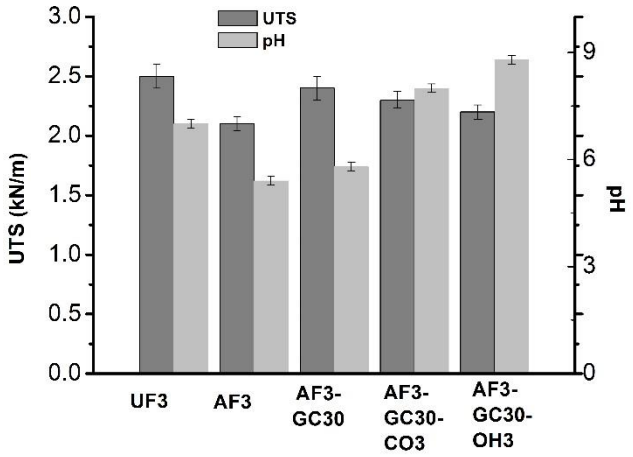

Figure 5.15. Effects of GC30 system on standard paper FP aged with 20 days.

On these samples, colorimetric measurements, following the procedure reported in Chapter 3, were performed. Acidity is usually interconnected with oxidation (Shanani and Harrison 2002). The yellowing of paper is mainly due to the formation of chromophores, such as conjugated carbonyl and carboxyl compounds (Bronzato et al. 2013), whose production is favored in an acidic environment. After 20 days of artificial aging, we measured a significant change in the visual aspect of samples, i.e., a ΔE of 10.3 units. It is worth noting that a ΔE higher than 2.3 units makes the color difference perceivable by the naked eye (Witzel et al. 1973).

The visual aspect of paper samples was not significantly affected by the applied treatments. In fact, the ΔE of AF3-GC30, AF3-GC30-CO3 and AF3-GC30-OH3, calculated with respect to AF3, is 1.7, 1.9 and 2.0, respectively.

5.3.2.2 Application on real paper

The application of GC30 on aged PT1 slightly decreased the UTS of the paper, and it resulted in a small weight increase of about 4%. It was thus concluded that this paper, which contains about 20% of fillers, it is not a good candidate for testing our system because it has a low porosity that hampers the penetration of nanocrystals. If the treatment cannot penetrate, we cannot expect any improvement in the mechanical resistance.

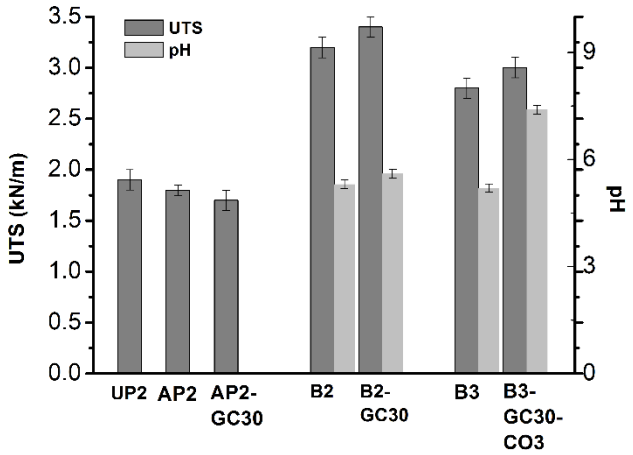

Figure 5.16. Effects of GC30 system on real samples, i.e., PT1 and Book from 1970s.

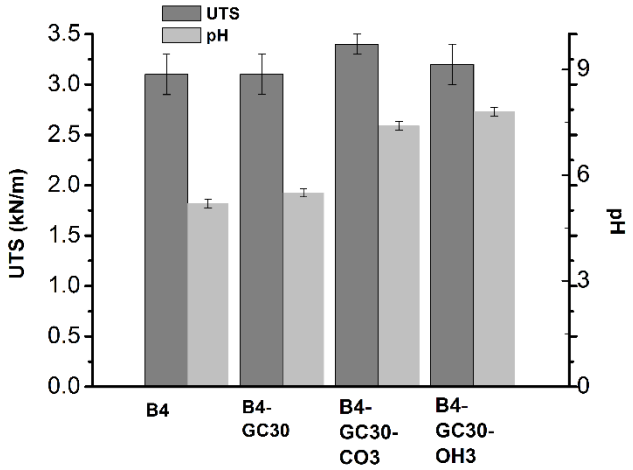

Figure 5.17. Effects of GC30 system on real samples, i.e., Book from 1970s.

Samples from different pages of the 1970s book were treated with GC30 and GC30-CO3. B2-GC30 and B3-GC30-CO3 samples show a slight strength increment of about 5% and 6%, respectively, as shown in Figure 5.16. It is worth noting that GC30-CO3 increase pH from 5.2 to 7.2. It seems that hybrid featuring $CaCO_3$ is effective on both strengthening and deacidification. The application of GC30-CO3 on samples from a different page lead to a similar increment in the UTS (6%), as shown in figure 5.17. However, no or slight effects were obtained on the same set of samples treated with GC30 and GC30-OH3 (see figure 5.17). Overall, we can conclude that the effectiveness of our systems on this paper is probably affected by the initial conservation status of real objects, which is not

easily controlled. In other terms, the inhomogeneity of book's paper doesn't permit to obtain reproducible results, but that is a widely known problem affecting real cellulosic systems. Even if the limited set of data does not allow us to obtain a statistically sound evaluation, it can be concluded that our systems work on filter paper, which is a reference material, and that an overall positive effect was also obtained on paper samples from the 1970s book.

5.4 Conclusion

The most important degradation mechanism of cellulose-based materials is the acid-catalyzed hydrolysis of β-1,4-glycosidic bonds, which results in the decrease of cellulose degree of polymerization and, macroscopically, in the loss of the original mechanical properties. In the case of acidic and strongly mechanically-degraded cellulosic works of art, both a deacidification and a reinforcement treatment are required.

In this Chapter, hybrid systems in ethanol for the concomitant neutralization of acidity and improvement of the mechanical resistance of the original material are presented. The dispersing use of a single-step treatment rely in the reduction of cost, treatment time, stress and risk for the artifact. Hybrid systems feature modified cellulose nanocrystals and alkaline nanoparticles, alternatively calcium hydroxide or calcium carbonate, both obtained via a solvothermal process. The innovative synthetic route of $CaCO_3$ nanoparticles, which is based on the usage of an alkyl carbonate for the conversion of the intermediate reaction products into carbonates, yielded small and highly crystalline nanoparticles already dispersed in an appropriate solvent for applicative purposes. Modified cellulose nanocrystals act as strengthening agents. In order to allow the dispersion of CNC in ethanol, three CNC modification strategies were discussed. The two different acetylation procedures based on the use of acetic anhydride that were tested, were not able to modify the surface of the nanocrystals so to stabilize their dispersion in ethanol. On the contrary, the grafting of oleic acid on CNC using a CDI-activated method allow us to obtain a modified product that can be stably dispersed in short-chain alcohols.

Hybrids were therefore prepared by mixing oleic-acid grafted CNC (GC) and alkaline nanoparticles, i.e. calcium hydroxide or calcium carbonate nanoparticles in ethanol, at different concentrations. Systems with low

concentration of GC (<9 g/L) displayed a liquid-like or a gel-like behavior depending on the concentration of nanocrystals and of alkaline nanoparticles and on the still time. On the contrary, all the systems at 30 g/L of GC displayed a gel-like behavior after 24 hours from the preparation.

The mechanical response of GC dispersions was studied with rheological measurements. GC dispersions display an increased mechanical response with increasing concentration, due to the electrostatic interactions between particles. More interestingly, GC and CNC dispersions, having a similar concentration, display a different mechanical response: in fact, both G′ and G″ of GC30 are about two orders of magnitude higher than those of CNC30; moreover, the two moduli in GC30 are frequent-independent. This behavior is probably due to a decrease in the Debye length triggered by the lower permittivity of ethanol with respect to water that allows for stronger interactions between particles. A strong increase in G′ and G″ was also displayed after the addition of calcium hydroxide to the GC dispersion. Here, calcium ions lead to the gelation of the systems mainly because the Debye length depends also on the concentration of the ions in solution. It is worth noting that water was used during the purification step of the reaction and some traces are probably present in the final dispersing medium. The introduction of calcium carbonate for the hybrid preparation led to a less pronounced effect on the screening of the crystal repulsive forces due to the lower solubility of calcium carbonate. At higher concentration of GC (30 g/L), the different behavior of the systems was also confirmed by the tan δ, which is the averaged G″/G′ over the investigated frequency range. Interestingly, all the prepared systems are weak gel, except for those featuring calcium hydroxide nanoparticles.

Other interesting features were investigated, such as thixotropy showed in the three interval thixotropy tests (3ITT). This is particularly interesting for the application of these materials to cellulose-based objects: in fact, these systems can be applied at the liquid state, after being energetically shake. Or, when a more confined application is required, both systems can be applied with a gentle action, in a more gelled state.

SAXS measurements confirmed the increase in cellulose interactions after the surface modification and the addition of alkaline nanoparticles. In fact, the changes in the aggregation number of GC clusters follow a similar trend displayed by the mechanical response, i.e., bigger clusters were found in the more gelled system.

After characterization, hybrid systems featuring 9 g/L and 30 g/L GC were applied on artificially and naturally aged paper. Mechanical tests, pH and colorimetric measurements were used to evaluate their effect.

Systems with low concentration of GC (9 g/L) were not able to significantly increase the mechanical resistance of artificially and naturally aged paper samples. It is also worth noting that an increase in the amount of treatment applied on some samples, resulted in a lower UTS values. It was thus concluded that the concentration of nanocrystals was not enough to compensate the swelling of the cellulose fibers due to the solvent.

Systems with higher concentration of GC (30 g/L) led to an increase in the mechanical resistance, and, in the case of hybrids, also neutralized the present acidity of filter paper, without significant alterations in the visual aspect of samples. The strengthening and deacidification effects were even more significant on highly degraded filter paper. An overall positive effect was also obtained on paper samples from the 1970s book, even if the effectiveness of our systems on this material is probably affected by the initial conservation status of the real object, which is not easily controlled.

Part IV – Final conclusions

Concluding remarks

Cellulose-based materials constitute a large part of the global patrimony of mankind. Their preservation and protection must be granted to transfer this heritage to future generations. The acid-catalyzed hydrolysis of glycosidic bonds, that is the most important degradation pathway of cellulose-based materials, results in the decrease of cellulose DP and in the loss of the original mechanical properties. Therefore, two are the classes in which conservation interventions for cellulosic material can be divided: deacidification and strengthening treatments.

Deacidification treatments are based on the usage of alkaline compounds that neutralize paper acidity. The neutralizing agents can be dispersed in water, short chain alcohol and low-polar and inert solvents. The most interesting systems are those based nanoparticles stably dispersed in organic solvents.

On the other hand, the compounds that can be used for the reinforcement treatments include natural and synthetic polymer and, more recently, nanocellulose. Nanocellulose is newly developed and it is probably the most interesting material due to the unique mechanical properties and high compatibility with cellulosic material.

For the preservation of acidic and strongly mechanically-degraded cellulosic works of art, both a deacidification and a reinforcement treatment should be carried out. In this regard, a single-step method can reduce risk and stress for the artifact and, at the same time, grant a reduction in terms of costs and time.

Alkaline nanoparticles, i.e., calcium or magnesium hydroxide, in short-chain alcohols were proposed for the deacidification of paper and canvas about 15 years ago. Since then, several synthetic strategies and formulations of nanoparticles in different carrier solvents have been developed and excellent results in neutralizing acidity and creating an alkaline buffer have been achieved.

In the present dissertation, hybrid systems for the simultaneous strengthening and deacidification of paper were prepared, characterized and applied on paper samples; these materials have been prepared using cellulose nanocrystals and alkaline nanoparticles. Nanocelluloses are non-toxic,

renewable and biodegradable. Moreover, they have excellent mechanical properties, high surface area, and form almost transparent films.

Alkaline nanoparticles allow for fast neutralization and carbonation processes. In addition to that, nanoparticles dispersed in alcohols easily penetrate the cellulosic material without altering the composition or damaging water-sensitive components and grant a homogenous distribution within the fibers. The alkaline nanoparticles used for the preparation of hybrids were obtained using a novel synthetic route based on a solvothermal process, which yields small and highly crystalline nanoparticles already dispersed in an appropriate solvent for applicative purposes. In particular, an innovative synthetic route of $CaCO_3$ nanoparticles, which is based on the usage of an alkyl carbonate for the conversion of the intermediate reaction products into carbonates, was developed.

Considering water sensitive and non-water sensitive artifacts, two types of hybrid systems were developed. One is hybrid of pristine cellulose nanocrystals and alkaline nanoparticles dispersed in water/ethanol. The other is hybrid featuring grafted cellulose nanocrystals dispersed in pure ethanol.

In this regard, three CNC modification strategies were tested. The two different acetylation procedures based on the use of acetic anhydride were not able to modify the surface of the nanocrystals so to stabilize their dispersion in ethanol. On the contrary, the grafting of oleic acid on CNC using a CDI-activated method allowed us to obtain a modified product that can be stably dispersed in short-chain alcohols.

Hybrids systems were prepared by mixing CNC or oleic-acid grafted CNC (GC) and alkaline nanoparticles, i.e. calcium hydroxide or calcium carbonate nanoparticles in ethanol, at different concentrations.

Systems with low concentration of GC displayed a liquid-like or a gel-like behavior depending on the concentration of nanocrystals and of alkaline nanoparticles and on the still time. On the contrary, all the systems at higher concentration of GC displayed a gel-like behavior after 24 hours from the preparation.

The mechanical responses of both CNC and oleic-acid grafted CNC (GC) dispersions were studied with rheological measurements. The presence of ethanol in CNC dispersion resulted in the overall increase in the viscosity of the systems than that of CNC in water dispersion. GC in ethanol and CNC in water/ethanol dispersions, having a similar concentration, showed a different mechanical response: in fact, both G′ and G″ of GC30 are about two orders of

magnitude higher than those of CNC30; moreover, the two moduli in GC30 are frequent-independent. This behavior is probably due to a decrease in the Debye length, triggered by the lowest permittivity of ethanol with respect to water that allows for stronger interactions between particles.

A strong increase in G' and G" was also displayed after the addition of calcium hydroxide to the CNC and GC dispersion. In fact, the Debye length is also a function of the ionic strength and divalent ions screen the superficial charges of cellulose nanocrystals, favoring their interactions and resulting in the formation of a strong gelled system. A less pronounced effect on the screening of the crystal repulsive forces was displayed after the addition of calcium carbonate, which is significantly less soluble than $Ca(OH)_2$.

At higher concentration of GC, the different behavior of the systems was also confirmed by the tan δ, which is the averaged G"/G' over the investigated frequency range. Interestingly, all the prepared systems are weak gel, expect for those featuring calcium hydroxide nanoparticles.

Thixotropy were investigated by three interval thixotropy tests (3ITT). This property is particularly interesting for the application of these materials to cellulose-based objects: in fact, these systems can be applied at the liquid state, after being energetically shake. Or, when a more confined application is required, both systems can be applied with a gentle action, in a more gelled state.

SAXS measurements confirmed the increase in cellulose interactions after the addition of ethanol, alkaline nanoparticles and grafting alkyl chains. In fact, the changes in the aggregation numbers of CNC and GC clusters follow a similar trend displayed by the mechanical response, i.e., bigger clusters were found in the more gelled system.

After characterization, hybrid systems were applied on artificially aged filter paper. Mechanical tests, pH and colorimetric measurements were used to evaluate their efficacy.

Systems featuring pristine CNC resulted highly effective in the strengthening and deacidification of acidic and mechanically-degraded cellulosic material, without significant alterations in the visual aspect of samples. Even if the pH, around 9, of samples applied by hybrids with $Ca(OH)_2$ is quite high, it is safe if the paper is not oxidized. In addition, the pH can be easily decreased by applying less amount of material.

Hybrids systems in ethanol with low concentration of GC were not able to significantly increase the mechanical resistance of artificially and naturally aged paper samples. It is also worth noting that an increase in the amount of treatment applied on some samples, resulted in a lower UTS values. It was thus concluded that the concentration of nanocrystals was not enough to compensate the swelling of the cellulose fibers due to the solvent.

Systems with higher concentration of GC led to an increase in the mechanical resistance, and, in the case of hybrids, also neutralized the present acidity of filter paper, without significant alterations in the visual aspect of samples. The strengthening and deacidification effects were even more significant on highly degraded filter paper. An overall positive effect was also obtained on paper samples from the 1970s book, even if the effectiveness of our systems on this material is probably affected by the initial conservation status of the real object, which is not easily controlled.

In conclusion, hybrid systems based on unmodified or oleic-acid grafted cellulose nanocrystals and alkaline nanoparticles for the simultaneous strengthening and deacidification may represent a powerful tool to extend the useful life of several cellulosic artifacts, including valuable and historical objects whose preservation and protection must be granted to transfer this heritage to future generations.

Part V - Annex

Bibliography

Abdul Khalil HPS, Davoudpour Y, Islam MN, et al (2014) Production and modification of nanofibrillated cellulose using various mechanical processes: A review. Carbohydr Polym 99:649–665. doi: 10.1016/j.carbpol.2013.08.069

Agnes Timar-Balazsy DE (1998) Chemical principles of textile conservation. Routledge, London

Ahn K, Banik G, Antje P (2012) Sustainability of Mass-Deacidification. Part II: Evaluation of Alkaline Reserve. Restaurator 33:48–75. doi: 10.1515/rest.2011.010

Ambrosi M, Dei L, Giorgi R, et al (2001) Colloidal Particles of Ca (OH) 2 : Properties and Applications to Restoration of Frescoes. Langmuir 17:4251–4255. doi: 10.1021/la010269b

Andersen, Flemming A. Brečević L (1991) Infrared Spectra of Amorphous and Crystalline Calcium Carbonate. Acta Chem Scand 45:1018–1024. doi: 10.3891/acta.chem.scand.45-1018

Ardelean E, Bobu E, Niculescu G, Groza C (2011) Effects of different consolidation additives on ageing behaviour of archived document paper. Cellul Chem Technol 45:97

ASTM D828-97 (2002) Standard Test Method for Tensile Properties of Paper and Paperboard Using Constant-Rate-of-Elongation Apparatus

Baer, Norbert S., Norman Indictor and AJ (1972) j _. Restaurator 1:5–23

Baglioni P, Chelazzi D (2013) Nanoscience for the Conservation of Works of Art

Barnes HA (1997) Thixotropy - A review. J Nonnewton Fluid Mech 70:1–33. doi: 10.1016/S0377-0257(97)00004-9

Basta AH (2003) The Role of Chitosan in Improving the Ageing Resistance of Rosin Sized Paper. Restaurator 106–117

Bastone S, Chillura Martino DF, Renda V, et al (2017) Alcoholic nanolime dispersion obtained by the insolubilisation-precipitation method and its application for the deacidification of ancient paper. Colloids Surfaces A Physicochem Eng Asp 513:241–249. doi: 10.1016/j.colsurfa.2016.10.049

Baty JW, Sinnott ML (2005) The kinetics of the spontaneous, proton- and AlIII-catalysed hydrolysis of 1,5-anhydrocellobiitol — Models for cellulose depolymerization in paper aging and alkaline pulping, and a benchmark for cellulase efficiency. Can J Chem 83:1516–1524. doi: 10.1139/V05-168

Begin P, Deschätelets S, Grattan D, et al (1998) The Impact of lignin on paper permanence. A comprehensive study of the ageing behaviour of handsheets and commercial paper samples. Restaurator 19:135–154

Bluher A, Vogelsanger B, Bern C-, Ag HN (2001) Mass Deacidification of Paper. Chim Int J Chem 55:981–989

Bodin A, Ba¨ckdahl H, Fink H, et al (2007) Influence of Cultivation Conditions on Mechanical and Morphological Properties of Bacterial Cellulose Tubes. Biotechnol Bioeng 97:425–434. doi: 10.1002/bit

Bonini C, Heux L, Cavaillé J-Y, et al (2002) Rodlike Cellulose Whiskers Coated with Surfactant: A Small-Angle Neutron Scattering Characterization. Langmuir 18:3311–3314. doi: 10.1021/la015511t

Boufi S, Vilar MR, Parra V, et al (2008) Grafting of Porphyrins on Cellulose Nanometric Films. Langmuir 24:7309–7315

Bronzato M, Calvini P, Federici C, et al (2013) Degradation products from naturally aged paper leaves of a 16th-century-printed book: a spectrochemical study. Chemistry 19:9569–77. doi: 10.1002/chem.201300756

Brückle I, Dambrogio J (2000) Paper Splitting : History and Modern Technology. J Am Inst Conserv 295–325. doi: 10.1179/019713600806113211

Buchanan S, M.L.S., Bennett W, et al (1994) An evaluation of the bookkeeper mass deacidification process

Castro C, Robin Z, Jean-luc P, et al (2011) Structural characterization of bacterial cellulose produced by Gluconacetobacter swingsii sp . from Colombian agroindustrial wastes. Carbohydr Polym 84:96–102. doi: 10.1016/j.carbpol.2010.10.072

Chamberlain D (2007) Anion mediation of aluminium-catalysed degradation of paper. Polym Degrad Stab 92:1417–1420. doi: 10.1016/j.polymdegradstab.2007.04.006

Chau M, Sriskandha SE, Pichugin D, et al (2015) Ion-Mediated Gelation of Aqueous Suspensions of Cellulose Nanocrystals. Biomacromolecules 16:2455–2462. doi: 10.1021/acs.biomac.5b00701

Cheradame H, Ipert S, Rousset E (2003) Mass Deacidification of Paper and Books I : Study of the Limitations of the Gas Phase Processes. Restaurator 24:227–239

Cherhal F, Cousin F, Capron I (2015) Influence of Charge Density and Ionic Strength on the Aggregation Process of Cellulose Nanocrystals in Aqueous Suspension, as Revealed by Small-Angle Neutron Scattering. Langmuir 31:5596–5602. doi: 10.1021/acs.langmuir.5b00851

Chronakis IS, Piculell L, Borgstriim J (1996) Rheology of kappa-carrageenan in mixtures of sodium and cesium iodide : two types of gels. Carbohydr Polym 31:215–225

Dong H, Snyder JF, Williams KS, Andzelm JW (2013) Cation-induced hydrogels of cellulose nanofibrils with tunable moduli. Biomacromolecules 14:3338–3345. doi: 10.1021/bm400993f

Ek M, Gellerstedt G, Henriksson G (2009) Pulping chemistry and technology. Walter de Gruyter

Eldho Abraham, Kam D, Nevo Y, et al (2016) Highly Modi fi ed Cellulose Nanocrystals and Formation of Epoxy- Nanocrystalline Cellulose (CNC) Nanocomposites. ACS Appl Mater Interfaces 8:28086–28095. doi: 10.1021/acsami.6b09852

Faatz M, Gröhn F, Wegner G (2004) Amorphous Calcium Carbonate: Synthesis and Potential Intermediate in Biomineralization. Adv Mater 16:996–1000. doi: 10.1002/adma.200306565

Ferry JD (1980a) Viscoelastic Properties of Polymers. John Wiley & Sons

Ferry JD (1980b) Viscoelastic properties of polymers. Sons, John Wiley &

Freire CSR, Silvestre AJD, Neto CP, et al (2006) Controlled heterogeneous modification of cellulose fibers with fatty acids: Effect of reaction conditions on the extent of esterification and fiber properties. J Appl Polym Sci 100:1093–1102. doi: 10.1002/app.23454

Fujisawa S, Okita Y, Saito T, et al (2011) Formation of N-acylureas on the surface of TEMPO- oxidized cellulose nanofibril with carbodiimide in DMF. Cellulose 18:1191–1199. doi: 10.1007/s10570-011-9578-z

Galina R, Marianne L, Øyvind E, Øyvind G (2011) Surface chemical modification of microfibrillated cellulose : improvement of barrier properties for packaging applications. Cellulose 18:127–134. doi: 10.1007/s10570-010-9474-y

Galinsky EVA, Haberditzl A (2004) Paper splitting: Systematisation, quality control and risk minimisation. Restaurator 25:171–198

Gicquel E, Martin C, Garrido Yanez J, Bras J (2017) Cellulose nanocrystals as new bio-based coating layer for improving fiber-based mechanical and barrier properties. J Mater Sci 52:3048–3061. doi: 10.1007/s10853-016-0589-x

Giorgi R, Ambrosi M, Toccafondi N, Baglioni P (2010) Nanoparticles for Cultural Heritage Conservation: Calcium and Barium Hydroxide Nanoparticles for Wall Painting Consolidation. Chem - A Eur J 16:9374–9382. doi: 10.1002/chem.201001443

Giorgi R, Bozzi C, Dei L, et al (2005a) Nanoparticles of $Mg(OH)_2$: Synthesis and Application to Paper Conservation. Langmuir 21:8495–8501. doi: 10.1021/la050564m

Giorgi R, Bozzi C, Dei L, et al (2005b) Nanoparticles of Mg(OH)2: Synthesis and application to paper conservation. Langmuir 21:8495–8501. doi: 10.1021/la050564m

Giorgi R, Chelazzi D, Baglioni P (2006) Conservation of acid waterlogged shipwrecks: Nanotechnologies for de-acidification. Appl Phys A Mater Sci Process 83:567–571. doi: 10.1007/s00339-006-3542-z

Giorgi R, Chelazzi D, Baglioni P (2005c) Nanoparticles of calcium hydroxide for wood conservation. The deacidification of the Vasa warship. Langmuir 21:10743–10748. doi: 10.1021/la0506731

Giorgi R, Chelazzi D, Fratini E, et al (2009) Nanoparticles of calcium hydroxide for wood deacidification: Decreasing the emissions of organic acid vapors in church organ environments. J Cult Herit 10:206–213. doi: 10.1016/j.culher.2008.06.012

Giorgi R, Dei L, Baglioni P (2000) A New Method for Consolidating Wall Paintings Based on Dispersions of Lime in Alcohol. Stud Conserv 45:154–161. doi: 10.1179/sic.2000.45.3.154

Giorgi R, Dei L, Ceccato M, et al (2002a) Nanotechnologies for Conservation of Cultural Heritage: Paper and Canvas Deacidification. Langmuir 18:8198–8203. doi: 10.1021/la025964d

Giorgi R, Dei L, Schettino C, Baglioni P (2002b) a New Method for Paper Deacidification Based on Calcium Hydroxide Dispersed in Nonaqueous Media. Stud Conserv 47:69–73. doi: 10.1179/sic.2002.47.s3.014

Giummarella N, Pu Y, Ragauskas AJ, Lawoko M (2019) A critical review on the analysis of lignin carbohydrate bonds. Green Chem 21:1573–1595. doi: 10.1039/c8gc03606c

González I, Alcalà M, Chinga-Carrasco G, et al (2014) From paper to nanopaper: Evolution of mechanical and physical properties. Cellulose 21:2599–2609. doi: 10.1007/s10570-014-0341-0

Guerra RA, Vtves G, Garrido JF (1995) Procedure for Simultaneous Deacidification and Sizing of Paper. Restaur 16:175–193

Habibi Y, Lucia LA, Rojas OJ (2010) Cellulose nanocrystals: chemistry, self-assembly, and applications. Chem Rev 110:3479–3500

Halikia I, Zoumpoulakis L, Christodoulou E, Prattis D (2001) Kinetic study of the thermal decomposition of calcium carbonate by isothermal methods of analysis. Eur J Miner Process Environ Prot 1:89–102. doi: 10.1016/S1011-1344(02)00277-4

Halstead, P. E. and AEM (1957) The Thermal Dissociation of Calcium Hydroxide. J Chem Soc 3873–3875

Hamza SE (2017) MHD Flow of Cellulose Derivatives and Dilute Suspensions Rheology of Its Nanocrystals. Am J Fluid Dyn 7:23–40. doi: 10.5923/j.ajfd.20170701.03

Harris J (1975) Acid hydrolysis and dehydration reactions for utilizing plant carbohydrates

Hasan S (2015) A Review on Nanoparticles : Their Synthesis and Types. Int J Mater Sci Appl 4:325–332

Hassan PA, Rana S, Verma G (2015) Making sense of Brownian motion: Colloid characterization by dynamic light scattering. Langmuir 31:3–12. doi: 10.1021/la501789z

Heinze MAHTLT (2004) Acylation of Cellulose withN,N′-Carbonyldiimidazole-Activated Acids in the Novel Solvent Dimethyl Sulfoxide/Tetrabutylammonium Fluoride. Macromol Rapid Commun 25:916–920. doi: 10.1002/marc.200300308

Heinze T, Liebert T (2001) Unconventional methods in cellulose functionalization. Prog Polym Sci 26:

Heinze T, Liebert T, Koschella A (2006) Esterification of Polysaccharides. Springer Science & Business Media

Horie CV (2010) Materials for conservation: organic consolidants, adhesives and coatings

Hosoya T, Bacher M, Potthast A, et al (2018) Insights into degradation pathways of oxidized anhydroglucose units in cellulose by b -alkoxy-elimination : a combined theoretical and experimental approach. Cellulose 25:3797–3814. doi: 10.1007/s10570-018-1835-y

Humphrey BJ (2015) Maney Publishing THE APPLICATION OF PARYLENE CONFORMAL COATING TECHNOLOGY TO ARCHIVAL AND ARTIFACT CONSERVATION. Stud Conserv 29:117–123

Ikeda S, Nishinari K (2001) " Weak Gel " -Type Rheological Properties of Aqueous Dispersions of Nonaggregated K -Carrageenan Helices. J Agric Food Chem 49:4436–4441. doi: 10.1021/jf0103065

IPERT S, ROUSSET E, CHERADAME H (2005) Mass Deacidification of Papers and Books III : Study of a Paper Strengthening and Deacidification Process. Restaurator 26:250–264

Jančovičová V, Havlínová B, Mináriková J, Hanus J (2012) Impact of Stabilizing Procedures on Acidic Paper. Restaurator 33:170–198. doi: 10.1515/res-2012-0008

Jandura P, Kokta B V., Riedl B (2000) Fibrous long-chain organic acid cellulose esters and their characterization by diffuse reflectance FTIR spectroscopy, solid-state CP/MAS 13C-NMR, and X-ray diffraction. J Appl Polym Sci 78:1354–1365. doi: 10.1002/1097-4628(20001114)78:7<1354::AID-APP60>3.0.CO;2-V

Johar N, Ahmad I, Dufresne A (2012) Extraction , preparation and characterization of cellulose fibres and nanocrystals from rice husk. Ind Crop Prod 37:93–99. doi: 10.1016/j.indcrop.2011.12.016

Kajanto I, Kosonen M (2012) The potential use of micro-and nanofibrillated cellulose as a reinforcing element in paper. J-FOR 2:42–48

Kargarzadeh H, Mariano M, Huang J, et al (2017) Recent developments on nanocellulose reinforced polymer nanocomposites : A review. Polymer (Guildf) 132:368–393. doi: 10.1016/j.polymer.2017.09.043

Kharissova O V, Dias HVR, Kharisov BI, et al (2013) The greener synthesis of nanoparticles. Trends Biotechnol 31:240–248. doi: 10.1016/j.tibtech.2013.01.003

Kim J, Montero G, Habibi Y, et al (2009) Dispersion of cellulose crystallites by nonionic surfactants in a hydrophobic polymer matrix. Polym Eng Sci 49:2054–2061. doi: 10.1002/pen.21417

Klemm D, Heublein B, Fink H, Bohn A (2005) Cellulose : Fascinating Biopolymer and Sustainable Raw Material. Angew chemie Int Ed 44:3358–3393. doi: 10.1002/anie.200460587

Klemm D, Philipp B, Heinze T, et al (1998) WILEY-VCH Comprehensive Cellulose Chemistry Volume 2 Functionalization of Cellulose

Kline SR (2006) Reduction and analysis of SANS and USANS data using IGOR Pro. J Appl Crystallogr 39:895–900. doi: 10.1107/S0021889806035059

Kolar J (1997) Mechanism of Autoxidative Degradation of Cellulose. Restaurator 18:163–176

Kolar J, ˇStolfa A, Strliˇ M, et al (2006) Historical iron gall ink containing documents — Properties affecting their condition. Anal Chim Acta 555:167–174. doi: 10.1016/j.aca.2005.08.073

Kolar J, Strlič M, Budnar M, et al (2003) Stabilisation of corrosive iron gall inks. Acta Chim Slov 50:763–770

Kolbe G (2004) Gelatine in Historical Paper Production and as Inhibiting Agent for Iron-Gall Ink Corrosion on Paper. Restaurator 25:26–39

Kolman K, Nechyporchuk O, Persson M, et al (2018) Combined Nanocellulose/Nanosilica Approach for Multiscale Consolidation of Painting Canvases. ACS Appl Nano Mater acsanm.8b00262. doi: 10.1021/acsanm.8b00262

Lavoine N, Desloges I, Dufresne A, Bras J (2012) Microfibrillated cellulose – Its barrier properties and applications in cellulosic materials: A review. Carbohydr Polym 90:735–764. doi: 10.1016/j.carbpol.2012.05.026

Lee KY, Tammelin T, Schulfter K, et al (2012) High performance cellulose nanocomposites: Comparing the reinforcing ability of bacterial cellulose and nanofibrillated cellulose. ACS Appl Mater Interfaces 4:4078–4086. doi: 10.1021/am300852a

Letnar MČ, Vodopivec J (2004) Optimizing the Leafcasting Technique. Restaurator 25:1–14

Lin J, Chang Y, Hsu Y (2009) Degradation of cotton cellulose treated with hydrochloric acid either in water or in ethanol. Food Hydrocoll 23:1548–1553. doi: 10.1016/j.foodhyd.2008.10.005

Lin N, Huang J, Chang PR, et al (2011) Surface acetylation of cellulose nanocrystal and its reinforcing function in poly (lactic acid). Carbohydr Polym 83:1834–1842. doi: 10.1016/j.carbpol.2010.10.047

Lindon J, Tranter G, Koppenaal D (2010) Encyclopedia of spectroscopy and spectrometry. Academic Press

Lu A, Hemraz U, Khalili Z, Boluk Y (2014) Unique viscoelastic behaviors of colloidal nanocrystalline cellulose aqueous suspensions. Cellulose 21:1239–1250. doi: 10.1007/s10570-014-0173-y

Lunjakorn A, Mattea-Coco M, Thirvengadam P, et al (2018) Nano-Structures & Nano-Objects Strengthening of paper by treatment with a suspension of alkaline nanoparticles stabilized by trimethylsilyl cellulose. Nano-Structures & Nano-Objects 16:363–370. doi: 10.1016/j.nanoso.2018.09.009

Lunjakorn A, Tamilselvan M, Silvo H, et al (2015) RSC Advances deacidi fi cation and strengthening of paper †. RSC Adv 5:32950–32961. doi: 10.1039/c4ra15153d

M CL, J V (1997) Protection and conservation of materials on paper; evaluation of permanence and durability of the laminated material on paper. Restaurator 18:177–190

Malesic J, Kolar J, Strlic M (2002) Effect of pH and Carbonyls on the Degradation of Alkaline Paper. Restaurator 23:145–153

Mao Y, Liu K, Zhan C, et al (2017) Characterization of Nanocellulose Using Small-Angle Neutron, X-ray, and Dynamic Light Scattering Techniques. J Phys Chem B 121:1340–1351. doi: 10.1021/acs.jpcb.6b11425

Marina B, Barbara M (1996) Hydroxypropyl Cellulose and Polyvinyl Alcohol on Paper as Fixatives for Pigments and Dyes. RESTAURATOR-COPENHAGEN 17:238–251

Mcmurry J, Castellion M, Ballantine DS, et al (2010) Fundamentals of General , Organic , and Biological Chemistry. Pearson Education

Merima Mehmedovic Hasani GW (2007) New coupling reagents for homogeneous esterification of cellulose. Cellulose 14:347–356. doi: 10.1007/s10570-007-9107-2

Mewis J, Wagner NJ (2009) Thixotropy. Adv Colloid Interface Sci 147:214–227. doi: 10.1016/j.cis.2008.09.005

Mittelbach P, Porod G (1961) Small-Angle X-Ray Scattering by Dilute Colloid Sytems. The Calculation of Scattering Curves for Parallelepipeds. Acta Phys Austriaca 14:185–211

Moon RJ, Martini A, Nairn J, et al (2011) Cellulose nanomaterials review: structure, properties and nanocomposites

Nada A-AM, Kamel S, Mohamed E-S (2000) Physicomechanical Properties of Paper Treated With Polymers. Restaurator 21:238–247

Nanni A, Luigi D (2003) $Ca(OH)_2$ Nanoparticles from W/O Microemulsions. Langmuir 19:933–938. doi: 10.1021/la026428o

Nathalie LavoineIsabelle DeslogesBertine KhelifiJulien Bras (2014) Impact of different coating processes of microfibrillated cellulose on the mechanical and barrier properties of paper. J Mater Sci 49:2879–2893. doi: 10.1007/s10853-013-7995-0

Nechyporchuk O, Belgacem MN, Bras J (2016a) Production of cellulose nanofibrils: A review of recent advances. Ind. Crops Prod. 93:2–25

Nechyporchuk O, Belgacem MN, Pignon F (2016b) Current Progress in Rheology of Cellulose Nanofibril Suspensions. Biomacromolecules 17:2311–2320

Nechyporchuk O, Kolman K, Bridarolli A, et al (2018) On the potential of using nanocellulose for consolidation of painting canvases. Carbohydr Polym 194:161–169. doi: 10.1016/j.carbpol.2018.04.020

Neevel JG (1995) Phytate : a Potential Conservation Agent for the Treatment of Ink Corrosion Caused by Irongall Inks. Restaurator 16:143–160

Olsson C, Westman G (2013) Direct Dissolution of Cellulose: Background, Means and Applications. Cellul Asp 10:

Padalkar S, Capadona JR, Rowan SJ, et al (2010) Natural biopolymers: Novel templates for the synthesis of nanostructures. Langmuir 26:8497–8502. doi: 10.1021/la904439p

Peng SX, Chang H, Kumar S, et al (2016) A comparative guide to controlled hydrophobization of cellulose nanocrystals via surface esterification. Cellulose 23:1825–1846. doi: 10.1007/s10570-016-0912-3

Phan-Xuan T, Thuresson A, Skepö M, et al (2016) Aggregation behavior of aqueous cellulose nanocrystals: the effect of inorganic salts. Cellulose 23:3653–3663. doi: 10.1007/s10570-016-1080-1

Poggi G, Baglioni P, Giorgi R (2011) Alkaline earth hydroxide nanoparticles for the inhibition of metal gall ink corrosion. Restaurator 32:247–273. doi: 10.1515/rest.2011.012

Poggi G, Giorgi R, Mirabile A, et al (2017) A stabilizer-free non-polar dispersion for the deacidification of contemporary art on paper. J Cult Herit 26:44–52. doi: 10.1016/j.culher.2017.02.006

Poggi G, Giorgi R, Toccafondi N, et al (2010) Hydroxide nanoparticles for deacidification and concomitant inhibition of iron-gall ink corrosion of paper. Langmuir 26:19084–19090. doi: 10.1021/la1030944

Poggi G, Toccafondi N, Chelazzi D, et al (2016a) Calcium hydroxide nanoparticles from solvothermal reaction for the deacidification of degraded waterlogged wood. J Colloid Interface Sci 473:1–8. doi: 10.1016/j.jcis.2016.03.038

Poggi G, Toccafondi N, Chelazzi D, et al (2016b) Calcium hydroxide nanoparticles from solvothermal reaction for the deacidification of degraded waterlogged wood. 473:1–8. doi: 10.1016/j.jcis.2016.03.038

Poggi G, Toccafondi N, Melita LN, et al (2014a) Calcium hydroxide nanoparticles for the conservation of cultural heritage: New formulations for the deacidification of cellulose-based artifacts. Appl Phys A Mater Sci Process 114:685–693. doi: 10.1007/s00339-013-8172-7

Poggi G, Toccafondi N, Melita LN, et al (2014b) Calcium hydroxide nanoparticles for the conservation of cultural heritage: new formulations for the deacidification of cellulose-based artifacts. Appl Phys A 114:685–693. doi: 10.1007/s00339-013-8172-7

Poggi G, Toccafondi N, Melita LN, et al (2014c) Calcium hydroxide nanoparticles for the conservation of cultural heritage: new formulations for the deacidification of cellulose-based artifacts. Appl Phys A 114:685–693. doi: 10.1007/s00339-013-8172-7

Popescu M-A, Isopescu R, Matei C, et al (2014) Thermal decomposition of calcium carbonate polymorphs precipitated in the presence of ammonia and alkylamines. Adv Powder Technol 25:500–507. doi: 10.1016/j.apt.2013.08.003

Ross-Murphy SB (1995) Structure–property relationships in food biopolymer gels and solutions. J Rheol (N Y N Y) 39:1451–1463. doi: 10.1122/1.550610

Rousset E, Ipert S, Cheradame H (2004) Mass Deacidification of Paper and Books II : Deacidification in the Liquid Phase Using Aminosilanes. Restaurator 25:104–118

Sabet SS, Submitted AT, Partial IN, et al (2013) Shear Rheology of Cellulose Nanocrystal (CNC) Aqueous Suspensions A THESIS SUBMITTED IN PARTIAL FULFILLMENT OF

Said O, Karasu S, Tahsin M, Karaman S (2015) Three interval thixotropy test (3ITT) in food applications : A novel technique to determine structural regeneration of mayonnaise under different shear conditions. FRIN 70:125–133. doi: 10.1016/j.foodres.2015.02.002

Salajková M, Berglund LA, Zhou. Q (2012) Hydrophobic cellulose nanocrystals modified with quaternary ammonium salts. J Mater Chem 22:19798. doi: 10.1039/c2jm34355j

Salvadori B, Dei L (2001) Synthesis of Ca (OH) 2 Nanoparticles from Diols. 17:2371–2374. doi: 10.1021/la0015967

Santos SM, Carbajo JM, Go´mez N, et al (2016a) Use of bacterial cellulose in degraded paper restoration. Part I: application on model papers. J Mater Sci 51:1541–1552. doi: 10.1007/s10853-015-9476-0

Santos SM, Carbajo JM, Go´mez N, et al (2016b) Use of bacterial cellulose in degraded paper restoration. Part II: application on real samples. J Mater Sci 51:1553–1561. doi: 10.1007/s10853-015-9477-z

Santos SM, Carbajo JM, Quintana E, et al (2015) Characterization of purified bacterial cellulose focused on its use on paper restoration. Carbohydr Polym 116:173–181. doi: 10.1016/j.carbpol.2014.03.064

Sarip H, Hossain MS, N. MAM, Allaf K (2016) A Review of the Thermal Pretreatment of Lignocellulosic Biomass towards Glucose Production : Autohydrolysis with DIC Technology. BioResources 11:10625–10653

Schofield EJ, Sarangi R, Mehta A, et al (2011) Nanoparticle deacidification of the Mary Rose. Mater Today 14:354–358. doi: 10.1016/S1369-7021(11)70166-3

Schütz C, Agthe M, Fall AB, et al (2015) Rod Packing in Chiral Nematic Cellulose Nanocrystal Dispersions Studied by Small-Angle X-ray Scattering and Laser Diffraction. Langmuir 31:6507–6513. doi: 10.1021/acs.langmuir.5b00924

Seki M, Naoko S, Shingo H, et al (2010) A New Technique for Strengthening Book Papers with Cellulose Derivatives . Part 2 : Effect of Cellulose Derivatives on Different (1) A homogeneous suspension can be prepared using a cellulose derivative as a strengthening agent . In practice , cellulose. Restaurator 31:126–141. doi: 10.1515/rest.2010.008

Seki M, Sonoda N, Morita T, Okayama T (2005) A New Technique for Strengthening Book Papers Using Cellulose Derivatives. Restaurator 26:239–249. doi: 10.1515/REST.2005.239

Sequeira S, Casanova C, Cabrita EJ (2006) Deacidification of paper using dispersions of $Ca(OH)_2$ nanoparticles in isopropanol. Study of efficiency. J Cult Herit 7:264–272. doi: 10.1016/j.culher.2006.04.004

Shahani CJ, Harrison G (2002) Spontaneous formation of acids in the natural aging of paper. Stud Conserv 47:189–192. doi: 10.1179/sic.2002.47.s3.039

Shanani CJ, Harrison G (2002) Spontaneous formation of acids in the natural aging of paper. In: Daniels V, Donnithorne A, Smith P (eds) Works of Art on Paper: Books, Documents and Photographs. International Institute for Conservation of Historic and Artistic Works, London, UK, pp 189–192

Shang W, Huang J, Luo H, et al (2013) Hydrophobic modification of cellulose nanocrystal via covalently grafting of castor oil. Cellulose 20:179–190. doi: 10.1007/s10570-012-9795-0

Sharples A (1954a) The Hydrolysis of Cellulose Part I . The Fine Structure of Egyptian Cotton. J Polym Sci 13:393–401

Sharples A (1954b) The Hydrolysis of Cellulose Part 11 . Acid Sensitive Linkages in Egyptian Cotton. J Polym Sci 14:95–104

Sjöström E (1993) Wood chemistry: fundamentals and applications. Gulf professional publishing

Souguir Z, Dupont A, Lacaillerie JE De (2011) Chemical and Physicochemical Investigation of an Aminoalkylalkoxysilane As Strengthening Agent for Cellulosic Materials. Biomacromolecules 12:2082–2091. doi: 10.1021/bm200371u

Stefanis E, Panayiotou C (2007) Protection of Lignocellulosic and Cellulosic Paper by Deacidification with Dispersions of Micro- and Nano-particles of $Ca(OH)_2$ and $Mg(OH)_2$ in Alcohols. Restaurator 28:185–200. doi: 10.1515/REST.2007.185

Stefanis E, Panayiotou C (2008) Study of the Photochemical Stability of Paper Deacidified with Dispersions of $Ca(OH)_2$ and $Mg(OH)_2$ Nanoparticles in Alcohols. Restaurator 29:125–138. doi: 10.1515/rest.2008.007

Sternitzke M (1997) Structural ceramic nanocomposites. J Eur Ceram Soc 17:1061–1082

Strnadova J, Durovic M (1994) The Cellulose Ethers in Paper Conservation. Restaurator 15:. doi: 10.1515/rest.1994.15.4.220

Su Y, Burger C, Hsiao BS, Chu B (2014) Characterization of TEMPO-oxidized cellulose nanofibers in aqueous suspension by small-angle X-ray scattering. J Appl Crystallogr 47:788–798. doi: 10.1107/S1600576714005020

Su Y, Burger C, Ma H, et al (2015) Exploring the Nature of Cellulose Microfibrils. Biomacromolecules 16:1201–1209. doi: 10.1021/bm501897z

Sun B, Hou Q, Liu Z, Ni Y (2015) Sodium periodate oxidation of cellulose nanocrystal and its application as a paper wet strength additive. Cellulose 22:1135–1146. doi: 10.1007/s10570-015-0575-5

Sun D-W (2009) Infrared Spectroscopy for Food Quality Analysis and Control. Academic Press

Sundholm F, Tahvanainen M (2003) Paper Conservation Using Aqueous Solutions of Calcium Hydroxide / Methyl Cellulose 1 . Preparation of the solution. Restaurator 24:1–17

Sundholm F, Tahvanainen M (2004) Paper Conservation Using Aqueous Solutions of Calcium Hydroxide / Methyl Cellulose 3 . The influence on the degradation of papers. Restaurator 25:15–25

TAPPI. (2002) Hydrogen ion concentration(pH) of paper extracts (cold extraction method)

TAPPI. (2006) Hydrogen ion concentration (pH) of paper extracts (hot extraction method)

TAPPI. (2004) Surface pH measurement of paper

TAPPI T494 (2006) Tensile properties of paper and paperboard (using constant rate of elongation apparatus)

Timell TE (1964) The acid hydrolysis of glycosides: I. General conditions and the effect of the nature of the aglycone. Can J Chem 42:1456–1472

Tse S, Bégin P, Kaminska E (2014) HIGHLIGHTS OF PAPER RESEARCH AT THE CANADIAN CONSERVATION INSTITUTE. Stud Conserv 47:193–198. doi: 10.1179/sic.2002.47.s3.040

Uhlig M, Fall A, Wellert S, et al (2016) Two-Dimensional Aggregation and Semidilute Ordering in Cellulose Nanocrystals. Langmuir 32:442–450. doi: 10.1021/acs.langmuir.5b04008

Uschanov P, Johansson L-S, Maunu SL, Janne L (2011) Heterogeneous modification of various celluloses with fatty acids. Cellulose 18:393–404. doi: 10.1007/s10570-010-9478-7

Vallejos ME, Felissia FE, Area MC, et al (2016) Nanofibrillated cellulose (CNF) from eucalyptus sawdust as a dry strength agent of unrefined eucalyptus handsheets. Carbohydr Polym 139:99–105. doi: 10.1016/j.carbpol.2015.12.004

Whelan A WT (1994) Polymer Technology Dictionary

Whitmore PM, Bogaard J (1994) Determination of the Cellulose Scission Route in the Hydrolytic and Oxidative Degradation of Paper. Restaurator 15:26–45

Wilson WK, Parks EJ (1983) Historical Survey of Research at the National Bureau of Standards on Materials for Archival records. Restaurator 5:191–241

Wittekind J (1994) The Battelle mass deacidification process: a new method for deacidifying books and archival materials. Restaurator 15:189–207

Witzel RF, Burnham RW, Onley JW (1973) Threshold and suprathreshold perceptual color differences. J Opt Soc Am 63:615. doi: 10.1364/JOSA.63.000615

Wollny K, Huck S (2002) Direct Strain Oscillation : a new oscillatory method enabling measurements at very small shear stresses and strains. Rheol acta 41:356–361. doi: 10.1007/s00397-002-0231-5

Wyszecki G, Stiles WS (2000) Color Science: Concepts and Methods, Quantitative Data and Formulae, 2nd edn. John Wiley & Sons, New York, NY

Yilmaz MT, Vatansever C (2016) Food Hydrocolloids Three interval thixotropy test to determine structural regeneration of a glucomannan based hydrocolloid fi lm at air / water interface : Interfacial , molecular , thermal and surface characterization. Food Hydrocoll 61:458–468. doi: 10.1016/j.foodhyd.2016.06.004

ZAPPALÄ MP (1997) Conservation of Acid Paper : Studies Carried out in the Chemistry Laboratory. Restaurator 18:12–24

Zhu H, Fang Z, Preston C, et al (2014) Environmental Science device applications. Energy Environ Sci 7:269–287. doi: 10.1039/c3ee43024c

List of Publications

Q. Xu, G. Poggi, C. Resta, M. Baglioni, P. Baglioni, Hybrid systems for the strengthening and deacidification of paper featuring modified cellulose nanocrystals and alkaline nanoparticles, submitted to ELSEVIER Journal of Colloid and Interface Science, 2019.

G. Poggi, M. Baglioni, Q. Xu, P. Baglioni, Strengthening and deacidification of paper: development and assessment of a single-step treatment based on nanoparticles and cellulose nanocrystals, submitted to ACS Applied Materials & Interfaces, 2019.

N. Palladino, M. Hacke, G. Poggi, O. Nechyporchuk, K. Kolman, Q. Xu, M. Persson, R. Giorgi, K. Holmberg, P Baglioni, R. Bordes, Nanomaterials for the strengthening and deacidification of fibrous materials– the case of iron-tannate dyed cotton, submitted to Heritage Science, 2019.

Acknowledgments

The experimental work presented in this dissertation has been performed at the laboratories of CSGI and Chemistry Department of the University of Florence. The President and the Director of CSGI, along with the secretariat, as well as the Head and the secretariat of the Chemistry Department are acknowledged.

Giovanna Poggi is gratefully thanked for the guiding and inspiring discussion during my whole PhD, and for always being encouraging when I was struck in the research. I have been so lucky to work with her. Her attitude to life and work will affect the rest of my life. Many thanks are given to Claudio Resta for the useful discussion during the modification of CNC. Michele Baglioni is acknowledged for the help with the SAXS measurements and fitting. Thanks to Emiliano Carretti for his support during rheological measurements. I'd like also to thank David Chelazzi for his help during ATR-FTIR measurement.

A grateful thank is due to my friends, Xueru Zhao, Yiming Jia and Felicia who comfort me when I'm sad and pick me up when I'm down.

Finally, I wish to thank all the people at CSGI, in particular Diego, Rita, Harshal, Marco, Marianna, Costantina， Marta, Teresa, Nicole, and my officemates, Jorge and Rosangela, for the support that they always gave me during these years.

This work was supported by China Scholarship Council（CSC）and by the European Union's Horizon 2020 research and innovation programme under grant agreement No 646063 [Nanorestart Project]. SasView, which has been used for the fitting of SAXS data, contains code developed with funding from the European Union's Horizon 2020 research and innovation programme under the SINE2020 project, grant agreement No 654000.